Adaptive MMSE Multiuser Receivers in MIMO OFDM Wireless Communication Systems

by

Titus Ikechukwu ENEH

Thesis

Submitted to the University of Greenwich

in partial fulfilment of the requirements

for admission to the degree of

Doctor of Philosophy

Medway School of Engineering

June 2011

DECLARATION

I certify that this work has not been accepted in substance for any degree, and is not concurrently being submitted for any degree other than that of Doctor of Philosophy (PhD) being studied at the University of Greenwich. I also declare that this work is the result of my own investigations except where otherwise identified by references and that I have not plagiarized the work of others.

Signed ...., *Date* ....

Titus Ikechukwu Eneh

(Student)

Signed ...., *Date* ....

Prof. Predrag Rapajic

(Ist supervisor)

Signed ...., *Date* ....

Dr Re-wu

(2nd supervisor).

ACKNOWLEDGMENTS

This project over the last four years is by far, the most significant accomplishment of my life and it would be impossible without people who supported and believed in me.

My utmost gratitude goes to the ancient of days, the Almighty God, the author of life who has enabled and provided me with the opportunity to embark on this journey of acquisition of knowledge. May His name be forever praised.

My heartfelt appreciations and deepest thanks goes to my amiable supervisor, Professor Predrag Rapajic for his expert guidance. His approach to research work is professional and his support throughout my PhD was phenomenal and tremendous. His vast knowledge in Engineering, especially wireless communications, and his skills in research paper writing is overwhelming. His belief in me and the various privileges he had given to me have helped to bring me to this end. He found time to proffer invaluable suggestions and advice towards the realization of this research work. It will be an understatement to say I have gained immensely from his pool of knowledge and persistent encouragement during the course of my PhD work.

I would like to express my heartfelt gratitude to the only love of my life, my angel, sweet Uzomaka Goretti ENEH for her understanding and total support at every stage of this PhD work. You are more than a wife to me. Thank you very much. Special appreciation to my lovely twins (Terry and Bliss) whom have continued to shower their love and disturbances throughout my PhD work.

I wish to express my special thanks to Mr Emeka Eneh (Akwaeke), Mr Obi Chime and Prof. Ezeugwu of University of Southbank Uk for their candid support from the start to the finish of this work.

My Special thanks goes to Prof. ND Ekere, Head of school, Medway School of Engineering, UoG , Dr Steve Woodhead, Director of Research, Medway School of Engineering and Dr Raj Bhatti for their support and assistance over the years.

I must also acknowledge my fellow PhD students: Dr Raam Balasub-ramanyam , Dr.Trianthafylos. Kanakis (Aldo), Kwashie Amartei Anang, Athar Qureshi, Yogesh Nijsure, Lawal Bello, Grace Oletu, Kojo Peter Banasko, Emeka Amalu, Kenny Otiaba, Mathias Ekpu, Joy Adeyemi, Shangtong Yang and Andrew Adekunle for their help, friendship and encouragement during the course of my PhD work.

A very special thanks to my sick mother (Mrs Christiana Ekpeluchi ENEH) for her prayers and understanding. My brothers Dozie.P, John. C, James. I and Herbert. E (ENEH) and their families. My sisters J. N. Jideofor and Eugenia. I Iloh and their families, for all the support they have provided for me through out my entire life. My in-laws Mr and Mrs .C. Izueke and family for their prayers and understanding.

I would also like to thank all the friends I made in United Kingdom, from around the world, for supporting me and giving me the strength to carry on with this research.

This report writing will not be complete, if I fail to express my gratitude to Medway School of Engineering, University of Greenwich, as without their assistance this research would not have been possible, if not the financial assistance and the scholarship provided.

Mobile and Wireless Communication Engineering
School of Engineering, University of Greenwich
Chatham Dockyard, Medway City, Kent
London, United Kingdom
ME4 4TB

May 2011

Titus. I. ENEH

ABSTRACT

In a bid to cope with challenges of increasing demand for higher data rate, better quality of service, and higher network capacity, there is a migration from Single Input Single Output (SISO) antenna technology to a more promising Multiple Input Multiple Output (MIMO) antenna technology. On the other hand, Orthogonal Frequency Division Multiplexing (OFDM) technique has emerged as a very popular multi-carrier modulation technique, thus it is considered as a promising solution to enhance the data rate of future broadband wireless communication systems.

The first contribution of this thesis is the development of a low complexity adaptive algorithm that is robust against slow and fast fading channel scenarios, in comparison to the conventional individual parameter estimation by E. Teletar in his famous paper of 1999. Implementing the Adaptive MMSE Receivers in MIMO OFDM systems which I refer to (AMUD MIMO OFDM), combines the adaptive minimum mean square error multiuser receiver's scheme with prior information of the channel and interference cancelation in the spatial domain, achieves enhanced joint channel estimation and signal detection which makes the new technique effectively mobile.

A mathematical analysis and simulation results to estimate the Information Capacity of Mobile Communication system with MMSE DFE and OFDM receivers were investigated. The capacity of a stationary channel with ISI is achievable by both the single carrier MMSE DFE and multicarrier modulation over narrow sub channels with OFDM receivers. The achieved capacity result shows that in both techniques single carrier and multicarrier, apart from different implementations are

essentially identical when it comes to achievable criteria for information channel capacity.

Lastly, AMUD MIMO OFDM were compared with both adaptive vector precoding and iterative system and their performance were fantastic, results shows that it will assure transmission over a high channel capacity.

ABBREVIATIONS

ADSL	Asynchronous Digital Subscriber Line
AMUD	Adaptive Multiuser Detection
AWGN	Additive White Gaussian Noise
BER	Bit Error Rate
BPSK	Binary Phase Shift Keying
CDMA	Code Division Multiple Access
CP	Cyclic Prefix
CSI	Channel State Information
DAB	Digital Audio broadcast
DFE	Decision Feedback Equalization
DMT	Discrete Multitone
DVB	Digital Video broadcast
ETSI	European Telecommunication Standards Institute
FEC	Forward Error Correction
FIR	Finite Impulse Responds
HIPERLAN	High Performance Radio Local Area Networks
ICI	Intercarrier Interference
IEEE	Institute of Electrical and Electronics Engineers
IIR	Infinite Impulse Response
iid	Independent Identically Distributed
ISI	Inter Symbol Interference

LS	Least Square
LAN	Local Area Network
LMS	Least Mean Square
MAC	Medium Access Control
MAI	Multiple Access Interference
MAP	Maximum a Posteriori
MBPS	Megabite per Second
MC	Multicarrier
MCM	Multi-carrier Modulation
MF	Matched Filter
MIMO	Multiple Input Multiple Output
MISO	Multiple Input Single Output
MLSE	Maximum Likelihood Sequence Estimator
MMSE	Minimum Mean Square Error
MMSE DFE	Minimum Mean Square Decision Feedback Equalization
MRC	Maximum Ratio Combiner
MSE	Mean Square Error
MUD	Multiuser Detector
MUI	Multi-User Interference
OFDM	Orthogonal Frequency Division Multiplexing
PIC	Picture Interference Cancellation
QAM	Quadrature Amplitude Modulation
RF	Radio Frequency
RLS	Recursive Least Square
SIC	Successive Interference Cancellation
SIMO	Single Input Multiple Output
SINR	Signal to Interference Noise Ratio
SISO	Single Input Single Output

SNR	Signal to Noise Ratio
STBC	Space Time Block Code
SVD	Singular Value Decomposition
VLSI	Very Large Scale Integration
WLAN	Wireless Local Area Networks
WSS	Wide Sense Stationary
ZF	Zeroforcing
ZMCSCG	Zero Mean Circular Symmetric Complex Gaussian

NOTATIONS

$\mathbf{A}^H$	Complex Conjugate transpose (Hermitian transpose) of a matrix $\mathbf{A}$
$\mathbf{a}^H$	Complex Conjugate transpose (Hermitian transpose) of a vector $\mathbf{a}$
$\mid \mathbf{A} \mid$	Determinant of a matrix $\mathbf{A}$
$\mathcal{E}[\mathbf{A}]$	Probabilistic expectation of a Matrix $\mathbf{A}$
λ_{min}(A)	Smallest eigen value of Matrix A
λ_{max}(A)	Largest eigen value of matrix A
$tr\{\mathbf{A}\}$	trace of a Matrix $\mathbf{A}$
$\mathbf{A} \otimes \mathbf{B}$	Kronecker product of Matrices $\mathbf{A}$, $\mathbf{B}$
$\mathbf{I}_n$	n x n identity matrix
σ_1^2	Unit Variance
μ	Threshold level
$\mathbf{H}_{ij}$	Channel Frequency response
$\mathbf{R}$	Correlation Matrix
$\triangle_n$	Gradient
ε_{opt}	Optimum (Wiener solution) Linear and DFE
$\mathbf{H}$	Toeplitz Matrix
$\mathbf{H}(a/\beta)$	Entropy
$(\hat{a} - a)$	Mutually Independent and gaussian
σ^2	Average Noise Power
$(.)^\star$	Conjugate
$(.;.)$	Mutual Information
$(.)^H$	Hermittian Transpose

CONTENTS

FIGURES

TABLES

LIST OF PUBLICATIONS

1. T. Eneh, Grace Oletu ,Predrag Rapajic, Kwashie Anang and Bello Lawal," Adaptive multiuser receivers scheme for MIMO OFDM over Iterative-Equalization for Single-Carrier Transmission. Scholar link Research Journal March 2011.
2. T. Eneh, P. Rapajic and K. Anang & Predrag Rapajic, "Adaptive MMSE Multiuser Receivers in MIMO OFDM Wireless Communication System", IEEE International Conference on communication Technology", IEEE ICCT 2010, Nanjing, China 11-14 Nov. 2010.
3. T. Eneh, P. Rapajic, K. Anang, B. Lawal and A. Qureshi, "Information Capacity limits of the communication system with Adaptive MMSE Receivers", IEEE International Conference on Future Information Technology, IEEE(ICFIT 2010), Changsha, China. 14-15 Dec. 2010.
4. T. Eneh, P. Rapajic and K. Anang , "Adaptive MIMO OFDM for Wireless Communication Systems", 10th University of Greenwich Engineering Conference September 2010.
5. T. Eneh, P. Rapajic and K. Anang and B. Lawal, "Adaptive MMSE Multiuser Detection in MIMO OFDM Wireless Communication System", 3rd International Conference on Engineering Research and Development,(icerd2010), Benin City, Nigeria, 7th - 9th September 2010.

6. S. Manam, P. Bakalis, B. Lawal, T. Eneh, and P Rapajic, " Performance Optimization of Mobile AD-HOC Reactive Routing Protocols", 63rd International Conference on Engineering Research and Development (icerd2010), Benin City, Nigeria, 7th - 9th September 2010.

7. K. A. Anang, P. B. Rapajic, T. I. Eneh and G. Oletu, "Sensitivity of Information Capacity of Land Mobile Cellular System to the Base Station Antenna Height at Higher Microwave Frequencies", IEEE - ICCRD 2011 - March 11th - 13th, 2011, Shanghai, China.

8. T. Eneh, Grace Oletu, K. Anang, P. Rapajic and Justina Eze, "Adaptive Vector Precoding for MIMO-OFDM Systems", International conference ICT for Africa Covenant University Canaan Land Nigeria, March 2011.

9. Bello Lawal, S. Manam, P. Bakalis, T. Eneh, and Kwashie Anang, "Power Control and Performance Comparison of AODV and DSR Ad Hoc Routing Protocols" Cambridge University United Kingdom, UKSim2011 March 2011.

10. T. Eneh, P. Rapajic, K. Anang and B. Lawal, "Information Capacity of Mobile Communication Systems with MMSE DFE and OFDM Receivers", 2011 IEEE 73rd Vehicle Technology conference VTC2011-Spring. Budapest, Hungary - Acceptance: Jan 9th 2011.

11. K. A. Anang, P. B. Rapajic, T. I. Eneh and Y. Nijsure, "Minimum Cell Size for Information Capacity Increase in Cellular Wireless Network", VTC- 2011 - May 15th-18th, 2011, Budapest, Hungary.

12. T. Eneh, Grace Oletu, P. Rapajic, K. Anang and B. Lawal," Adaptive MMSE Multiuser Detection for MIMO OFDM over Turbo-Equalization for Single-

Carrier Transmission Wireless Channel", 7th International conference on Wireless Communication and Computing Conference IWCMC 2011, 5-8 July 2011 Istanbul, Turkey. March 15th 2011.

13. K. Anang, P. Rapajic, T. Eneh and B. Lawal," Sensitivity of Information Capacity of Land Mobile Cellular System to Propagation Loss Parameters at Higher Microwave Frequencies", 7th International conference on Wireless Communication and Computing Conference IWCMC 2011, 5-8 July 2011 Istanbul, Turkey. March 15th 2011.

14. Grace Oletu, Predrag Rapajic Titus Eneh, and Kwashie Anang," Iterative Equalization Enhanced High Data Rate in Wireless Communication Networks", 9th Intl. Symposium on Modeling and Optimization in Mobile, Ad Hoc, and Wireless Networks May 9-13, 2011, Princeton, NJ, USA, WiOpt'11

15. K. A. Anang, L. Bello, T. I. Eneh, Panos Bakalis and P. B. Rapajic, "The Performance of Dynamic Source Routing Protocol to Path Loss Models At Carrier Frequency Above 2GHz", IEEE - ICCT 2011 - Sept 25th - 28th, 2011, Jinan, China.

16. Bello Lawal, P. Bakalis, Predrag Rapajic, Kwashie A. Anang and Titus I. Eneh, "Adaptive Receiver Power Routing Protocol for Mobile Ad Hoc Wireless Network" JOURNAL OF COMMUNICATIONS, VOL. 6, NO. 7, OCTOBER 2011.

17. Grace Oletu, P. Rapajic, T. Eneh, and K. Anang, "Enhanced Equalization for Mobile Communication Systems" IEEE 5th European Modelling Symposium (EMS2011) on mathematical modelling and computer simulation, Madrid 16 - 18 November 2011.To be presented.

18. Grace Oletu, P. Rapajic, T. Eneh, and K. Anang, "The Performance of It-

erative decoding with Imperfect MMSE DFE". The 4th IFIP Wireless Days conference WD'11, in Niagara Falls, Ontario, Canada, October 10-12, 2011.

19. T. Eneh, P. Rapajic, K. Anang, P.Bakalis and L.Bello, "Information Capacity of Adaptive MIMO OFDM Wireless Communication Systems" IIEEE 3rd International Conference on Adaptive Science Technology. IEEE (ICAST 2011), Abuja Nigeria 24-26 November 2011.To be presented.

20. K. A. Anang, L. Bello, T. Eneh, P. Bakalis and P. Rapajic, "The performance of dynamic source routing protocol to path loss models at carrier frequencies above 2 GHz". 13th IEEE International Conference on communication Technology (IEEE-ICCT 2011), Jinan, China, pp. 151 - 155, Sept. 2011.

21. K. A. Anang, P. B. Rapajic, T. I. Eneh, Lawal Bello and G. Oletu., "Impact of Vehicular Traffic on Information Capacity of Cellular Wireless Network at Carrier Frequencies Greater Than 3 GHz" IEEE UKsim 5th European Modelling Symposium on Mathematical modelling and Computer Simulation (5th IEEE EMS 2011), Madrid, Spain, Nov. 16-18. November 2011.To be presented.

To my dear wife Uzoamaka and my twins (Bliss and Terrence)

You will never do anything in this world without courage.

It is the greatest quality of the mind next to honor

Aristotle

Chapter 1

Introduction

1.0.1 Digital Wireless Communication

Wireless communication is the transfer of information signals through the air space by means of electromagnetic waves. To create electromagnetic waves, an electrical signal that continuously varies in power level and polarity is applied to the antenna. As the level varies, the energy contained in the electrical signal is converted to electromagnetic waves that propagate away from the antenna. The electromagnetic waves are characterized by their energy radio frequency power (RF Power) and frequency (cycles per second or Hz named after the German physicist Henrich Rudoph Hertz in (1888)).

Mobile Communication in the past, present and possible future will be discussed briefly in this paragraph before we proceed to the novel fundamentals of this research work, Adaptive Multiuser Receivers for Multiple input and Multiple Output, Orthogonal Frequency Division Multiplexing (AMUD MIMO OFDM). In 1820 Andre Ampere and Hans Osted discovered the magnetic field. It was then followed by the discovery of the first telegram by Joseph Henry in 1830. In 1831 Michael Faraday and Joseph Henry discovered induction and the telegraph was patented by Samuel Morse in 1837. James Maxwell in 1864 predicted Radio waves and Graham Bell developed the telephone in 1876. Henrich Hertz discovered Radio waves in 1888 while in 1906 the first radio broadcast was developed by Reginald Fessenden and was used for small scale voice and music broadcasts up until World War 1. In 1933, Edwin Armstrong patented Frequency Modulation, and in 1948, Channel Capacity was discovered by Claude Shannon. OFDM and MIMO came into existence in the late 1960's and in the 1970's respectively. Adaptive Multiuser Detection approach to Time Variable MIMO system, which this research falls into, is the state of the art research area in mobile and wireless communication System..

Communication systems have had a significant impact on the modern life of people in today's society. Demand for faster and easier ways to communicate and transfer information worldwide in real time processing is the basic requirement for current communication systems. Adaptive multiuser receivers in MIMO OFDM will provide a higher data rate, higher mobility, and higher carrier frequencies to enable reliable transmission over mobile or broadband wireless communication systems. Researchers in their various research areas in communication proved that multiuser systems information capacity was significantly improved on the conventional second generation (2G) and third generation (3G) mobile and wireless systems. They have a capacity of 0.3 bits/Hz/s while the forth generation (4G+) has 300 bits/Hz/s indicating 1000 bits/Hz/s capacity improvement factor to 2G and 3G.

IEEE 802.11 wireless local area network (LAN) standards employing OFDM offers high spectral efficiency and superior tolerance to multi-path fading. In OFDM, the computationally-efficient Fast Fourier Transform is used to transmit data in parallel over a large number of orthogonal subcarrier which are maintained in frequency selective fading environment [9][10][11][12][13]. Improvements in throughput and capacity can be achieved when multiple antennas are applied at both the transmitter and receiver side, especially in a rich scattering environment [14][15][16][17] as well as frequency-selective fading environment.

System capacity will be significantly improved by MIMO channels [1][18]. In OFDM, the entire channel is divided into many narrow parallel sub channels and diversity thereby increases the symbol duration and reduces the Intersymbol interference (ISI) caused by the multipath [9][10][11][19].

Adaptive multiuser detection (AMUD) is used for demodulation of digitally modulated signals with multiple access interferences (MAI). This scheme was proposed for total elimination of MAI in the system. In a single user environment, each bank of match filter plays the role of maximum likelihood receiver [4][20]. In this research work, fractionally space linear transversal bank of filters is used for the implementation of Adaptive Minimum Mean Square Error Multiuser Detection (A MMSE MUD).

MIMO-OFDM is a scheme which mitigates multiple access interference and increases capacity as presented in [21][22][3][23][24][25][26]. Adaptive MMSE Multiuser detection by Predrag. B. Rapajic in [20] was specifically used for co-operative systems by means of decision feedback equalization and relay nodes. The adaptive MMSE filter minimizes the error by an adaptive algorithm. A MMSE MUD techniques are effective to almost achieve the performance of a maximum likelihood estimator but on a linear complexity. A MMSE MUD provides robustness and mobility in a time variable frequency selective multi-path fading channel, improves the bit error rate performance and therefore enhances channel capacity of a multi-cellular environment. Adaptive MIMO OFDM was also presented by Wong [27] who assumes knowledge of the intravenous channel gain for bits and power allocation algorithm in all users to improve transmit power, bit error rate and coverage for a given outage probability. With no knowledge of the channel, the objective is to maximize the transmission rate, while guaranteeing a prescribed error performance, under the constraint of fixed transmit-power[28].

1.0.2 Wireless Local Area Networks

A wireless local area network (WLAN) links two or more devices using some wireless distribution methods (typically spread-spectrum or OFDM radio), and usually providing a connection through an access point to the wider internet. This gives users the mobility to move around within a local coverage area and still be connected to the network.

In the 1990's, wireless data systems such as wireless local area networks (WLANs) were on the increase demand for both voice and data communications. The growing demand for flexibility and availability of higher bandwidth wireless systems is expected. The coming of the 4G and 5G era will provide faster data transmission and higher bit rate and bandwidth. Taking advantages of both optical communication and wireless communication, OFDM Radio is characterized by its high speed, large capacity and high spectral efficiency. In principle, anything or everything that moves is a potential object for mobile/wireless communication.

WLANs for the 900MHz, 2.4GHz, and 5GHz license-free ISM (Industrial, Scientific and Medical) bands have been available, based on a range of proprietary techniques [9]. In June 1997 the Institute of Electrical and Electronics Engineers (IEEE) defined an international inter-operability standard, called IEEE 802.11. This standard specifies a number of Medium Access Control (MAC) protocols and three different physical layers (PHYs). Two of these physical layers are based on radio communication and use the 2.4GHZ band and the other PHY uses infrared light. All three PHY support a data rate of 1 Mbps and optionally 2 Mbps.

Users, demand for higher bit rates and the international availability of the 2.4 GHz band spurred the development of a higher speed extension to the 802.11 standard. In July 1998, a new standard was defined, named IEEE 802.11b, which describes a PHY providing a basic rate of 11 Mbps and a more robust rate ie., a fall-back rate, of 5.5 Mbps. Current widely-available products support both the 11 and 5.5 Mbps modes, as well as the 1 and 2 Mbps modes. Meanwhile, in Europe, the European Telecommunication standards Institute (ETSI) specified its own WLAN standard, called HIPERLAN/1 which defines data rates ranging from 1 Mbps to 20 Mpbs. In contrast to the IEEE 802.11b standard, no commercial products have been developed that support the HIPERLAN/1 standard.

The demand for higher data rates by the opening of the new unlicensed spectrum in the 5GHz for the use of a new category of equipment called unlicensed National Information Infrastructure (UNI) devices, a new IEEE 802.11 working group on 3G WLANs emerged. The group in 1998 selected OFDM as their chosen transmission technique for the new available spectrum in the 5GHz band. In the year 2000, the standard was ratified and called IEEE 802.11a. In 2003, IEEE standardization group finalized a similar standard for this band named IEEE 802.11g [29].

Following the selection of OFDM by IEEE 802.11a standardization group, the ETSI, Broadband Radio Acess Network (BRAN) and MMAC from Japan, working groups adopted OFDM for their PHY. The standardization groups worked in harmony to enable equipment compatibility worldwide. Based on the tremendous success of IEEE 802.11a and IEEE 802.11g products in terms of commercial availability of higher data rate and demand for higher data rates, IEEE802.11b was developed, and it is expected that the new product will surpass the former in terms of sold volumes per month.

1.0.3 Aims

The major aims of this research is "To show that the adaptive MMSE Multiuser Receivers in MIMO OFDM Wireless system provides higher data rate performance, higher mobility and higher carrier frequencies for easy and reliable multiuser transmission in wireless systems". Secondly this thesis mathematically analyzed "how to find the information capacity comparisons of mobile communication systems with MMSE DFE and OFDM receivers".

1.0.4 Objectives

The main objectives of this thesis include:

- Identification of the limitations associated with some existing channel estimation techniques for both single and multiple antenna Communication Systems.
- Deployment of OFDM transmission scheme to address the problem of ISI in both SISO and MIMO wireless Communication System.
- Designing effective channel estimation models for SISO-OFDM and MIMO-OFDM wireless Communication Systems.
- Deriving and proposing effective and less complex adaptive algorithms for implementation of the channel estimation AMUD MIMO OFDM receivers.
- Deriving an effective and less complex adaptive predictor for prediction of time varying channel for SISO-OFDM, MIMO-OFDM and AMUM MIMO OFDM wireless Communication Systems.
- Analyzing mathematically, supported with the simulation result, that the capacity of a stationary channel with intersymbol interference (ISI) is achievable by both the techniques:1) single carrier modulation with ideal MMSE-DFE receiver and 2) multicarrier modulation over narrow sub channels with OFDM receivers.

1.1 Research Motivation

The ever increasing growth of wireless communication systems has continued to drive the research efforts towards obtaining novel techniques by which system capacity can be increased, and at the same time maintaining high-quality of services. This, as earlier mentioned, has brought about the migration from single antenna, single input single output (SISO) systems to deployments of multiple antennas at both ends of the wireless communication Systems. Emerging from this migration is the multiple-input multiple-output (MIMO) systems. From the spectral efficiency angle of wireless communication is the emergence of orthogonal frequency multiplexing (OFDM) which finds deployment in both single antenna and multiple antenna wireless communication systems. The concepts of MIMO and OFDM were combined with the emerging intent of exploiting the advantages of both techniques. This combination has given the development to MIMO-OFDM wireless communication systems with the expectation of having spectrally efficient, high data rate system that is robust to frequency selective fading channels.

With the area of applications of the MIMO-OFDM system expanding very fast, the requirement for an improved functioning of the systems is becoming very high. As a result, more research efforts are being directed towards achieving better MIMO-OFDM Systems performance. However, one of the major challenges to either single antenna, SISO OFDM, or MIMO-OFDM communication systems is means of providing accurate channel state information (CSI) at the receiver end of the systems for coherent detection of the transmitted signal. If the CSI is not available at the receiver, the transmitted signal could only be demodulated and detected through a non-coherent method such as the differential demodulation technique. However, the employment of non-coherent detection method is at the expense of about 3-4 dB loss in signal-to-noise ratio (SNR) compared with using the coherent detection method [30]. In order to eliminate such a huge loss, it is imperative to develop an efficient and cost effective technique of providing channel state information at the receiver for coherent detection of the transmitted information in MIMO-OFDM wireless communication Systems.

There are different techniques by which channel state information can be obtained and these are classified as pilot-assisted (training-based), blind and decision-directed channel estimation methods. In the context of pilot-assisted channel estimation scheme, training-data that is known a priori at the receiver is transmitted along with the message data from the transmitter. These training data is then used to obtain the samples of CSI at the training data?s locations. The CSI at the message data locations are obtained from CSI at the training data locations by means of interpolation techniques. The insertion of the training data within the message signal will definitely induce additional overhead and thus reducing the data throughput. In blind channel estimation method, no training data sequence is needed; instead the statistical properties of the channel and certain information about the transmitted signal are employed to obtain the CSI. Consequently, there is saving in the bandwidth usage while employing blind channel estimation method in comparison with the training-based method. Though the blind channel estimation method has its advantage in that it has no overhead loss, unfortunately it can only be applied to slowly time-varying fading channels. This is because it will have to memorize the data record for a long time. Thus, it can not be applied in fast-varying channel scenarios that are peculiar to mobile wireless communication systems. Besides, blind channel estimation methods also tend to become heavier in terms of computational complexity [31].

In this thesis, the training-based channel estimation schemes for single and multi antenna system rather than the blind channel estimation method were developed. The investigations carried out, leads to developing a low complexity adaptive algorithm that is robust against both slow and fast fading channel scenarios.

1.2 Thesis Contribution

The capacity and mutual information of a broadband fading channel consisting of a finite number of time-varying paths was stated by Telatar in [32]. Full knowledge of the channel statistical parameters at the transmitter was assumed. This corresponds to an implicit assumption of use of an optimum MUD [4][20]. However, this assumption limits MIMO communication channels to a centralized operation, while the MIMO system is vulnerable to unknown channel interference. Also, the optimum MUD is of non linear computational complexity and thus the active number of nodes in the system should remain small. The MIMO OFDM system presented in this thesis involves the use of AMUD which enables mobility, while the system remains tolerant to both known and unknown channel interference. Computational complexity of MIMO OFDM is linear due to the concept of AMUD. In this work, Adaptive MUD in MIMO OFDM Wireless Communication were proposed as follows:

- Enhanced channel estimation and signal detection.
- Bit error rate achieved using AMUD at low SNR has a good performance compared to the existing MIMO OFDM.
- Technique with significant effect of AMUD as shown in Figure 4.1 and 4.2 shows the proposed scheme and the existing MIMO at low SNR less than 5dB intercept with each other depicting the graphical linear nature of AMUD to exponential of MIMO OFDM.
- The sum rate capacity result in the new technique is very close to MIMO theoretical upper bound (it offers significant insights into the factors determining capacity, in particular those of the antenna array geometry and number of antennas, which are becoming increasingly more important for realistic MIMO system designs) Figure 4.6
- With 8×8 antennas AMUD performs better as shown in Figure 4.3.
- As the number of antenna increases, better SNR performance is achieved as shown in Figure 4.4 and 4.5 respectively.

In the second research contribution, a mathematical analysis supported with the simulation results to estimate the quality of digital communication systems, the bit error rate (number of information bits received incorrectly normalized by the total number of information bits received) was analyzed. The information channel capacity as a fundamental measure of estimating the quality of digital communication channel which is possible with vanishingly small probability of bit error was investigated. Thus the capacity of a stationary channel with intersymbol interference (ISI) is achievable by both techniques:1) single carrier modulation with ideal MMSE-DFE receiver and 2) multicarrier modulation over narrow subchannels with OFDM receivers. The results imply that both techniques, single carrier or multicarrier, apart from different implementations, are essentially identical when it comes to criteria for achievable channel information capacity.

A novel adaptive iterative multiuser receivers scheme for MIMO OFDM, which we refer to as Iterative AMUD MIMO OFDM, the adaptive vector precoding schemes and adaptive multiuser receivers scheme for MIMO OFDM over Turbo-Equalization for Single Carrier Transmission were compared with the new technique. The result of the comparison shows a significant effect of the proposed and were all published. Thus it involves, the joint iteration of the adaptive minimum mean square error multiuser detection and decoding algorithm with prior information of the channel and interference cancelation in the spatial domain. For the iterative multiuser receivers, LMS algorithm and maximum a posteriori (MAP) algorithm are utilized in the receiver structures. A partially filtered gradient LMS (Adaptive) algorithm is also applied to improve the convergence speed and tracking ability of the adaptive detectors with a slight increase in computational complexity.

The new technique analysis, in a slow and fast Rayleigh fading channels MIMO OFDM systems, shows the suitability of turbo equalization as a means of achieving low bit error rate in the future high data communication systems. The Iterative equalization approach to coded data transmission over channels with Intersymbol interference (ISI) can yield additional improvement in bit error rate. The adaptive vector precoding schemes for the downlink multiuser requires pseudo inversion of the channel matrix, where this operation is only optimum when the transmitter power is unconstrained. This research work presents efficient methods to reduce the computational load of the algorithm by interpolating the precoding and decoding matrices corresponding to different OFDM subcarrier.

The thesis is organized as follows:

- Chapter 1 : Introduction and Thesis Contribution.
- Chapter 2 : Survey of MIMO OFDM Systems.
- Chapter 3 : Proposed Adaptive Multiuser Receivers for MIMO-OFDM Systems.
- Chapter 4 : Performance systems using the new proposed techniques by computer simulation.
- Chapter 5 : Information Capacity of the Communications Systems with Adaptive MMSE Receivers and MMSE DFE.
- Chapter 6 : Adaptive Information Capacity of Mobile Communication Systems with MMSE DFE and OFDM Receivers.
- Chapter 7 : Comparisons of Adaptive MMSE Multiuser Detection for MIMO OFDM Wireless Channel.
- Concluding remarks.
- Future recommendations.
- References.

Chapter 2

Survey of MIMO OFDM System

2.1 Overview of MIMO Systems

MIMO system is used in this research AMUD MIMO OFDM to enhance the channel model for effective transmission of the block of OFDM, it will provide good quality and large capacity to a wide range of wireless applications that will be requiring higher data rates, as it is required by this novel AMUD MIMO OFDM system.

Multiple transmit and multiple receive antennas have emerged as a promising technique for improving the performance of wireless digital transmission systems [15][1][33]. The limited resources of a wireless communication system, such as spectrum and power efficient broadband and mobile communications, can be efficiently used with multiple antennas to provide good quality and large capacity to a wide range of applications requiring higher data rates.

Multiple antenna systems at both transmitting and receiving can be described by a multiple-input multiple output (MIMO) system model, where the propagation environment is a quasi-static and frequency-flat rayleigh fading channel[15]. This assumption is necessary to establish simple code design criteria. Nevertheless, the codes designed under this simplifying assumption yield good performance in a wide variety of real world scenarios.

Multiple antenna technology today happens to be the so called multiple-input multiple-output (MIMO) system. The concept of MIMO dates back to the early 1970s [34][35]. In the following years, progress was not fast until the mid 1990s where the high demand for increased data rates over wireless channels made MIMO an important research topic. In the year 1999, the Shannon capacity of a fading Gaussian MIMO channel was demonstrated in a paper that became the landmark in MIMO communication systems [1]. The research of MIMO communication systems increased rapidly every year with an increased number of published papers.

Channel capacity of multiple antenna systems is directly dependent on spatial correlation between the antenna elements of a multi-antenna node. Spatial correlation is a consequence of a narrow spacing between the antenna elements of a single node resulting in electromagnetic antenna coupling as reported experimentally in [36] who stated that local scatterers at the base station tend to decrease the correlation between signals received at the two antennas. The spacing between antenna elements is defined in relation to the carrier wavelength of the wireless channel. It is noted that small spacing between the antenna elements of a MIMO system results in poor diversity. In order to achieve spatial diversity, the spacing between multi-antenna element in a device will have to be at least half wavelength apart [37].

Signal data transmission strategies in MIMO wireless communication systems are mainly defined by the transmit power control and transmit signal power allocation technique used. The most common transmit power allocation strategy is stated in [1], called the "Uniform power distribution" transmission technique, all the antenna elements of the transmitter are allocated the same portions of the total available SNR to transmit. The most effective transmission strategy in MIMO in terms of channel capacity and BER performance is "Waterfilling power distribution". By means of singular value decomposition at the communication channel modal analysis is performed as stated in [1][38][39].

The mode that offers the best wireless link (in the sense of highest singular value) is allocated with the majority of the available SNR as demonstrated in figure 2.1 of this chapter. The second best wireless link represented by the second highest singular value will be allocated with the second largest portion of SNR and so on. By this pattern, the transmit power allocation over the available channel is achieved and hence the highest possible channel capacity. The main disadvantage of Waterfilling transmission strategy is that the transmitter needs to have full statistical knowledge of the channel which makes this technique unsuitable for mobile applications, since the channel is unknown at every instance given the fact the node is moving. Other transmission strategies were proposed over the years, but not comparable with Waterfilling and Uniform power allocation strategies.

In wireless communication, the received signal exhibits amplitude fluctuations which are called channel fading, these amplitude fluctuations are composed of macroscopic channel fading which is originated by shadowing and microscopic channel fading is also caused by the random signal scattering between the transmitter and receiver of the communication system [39][7][40]. The envelope of the received

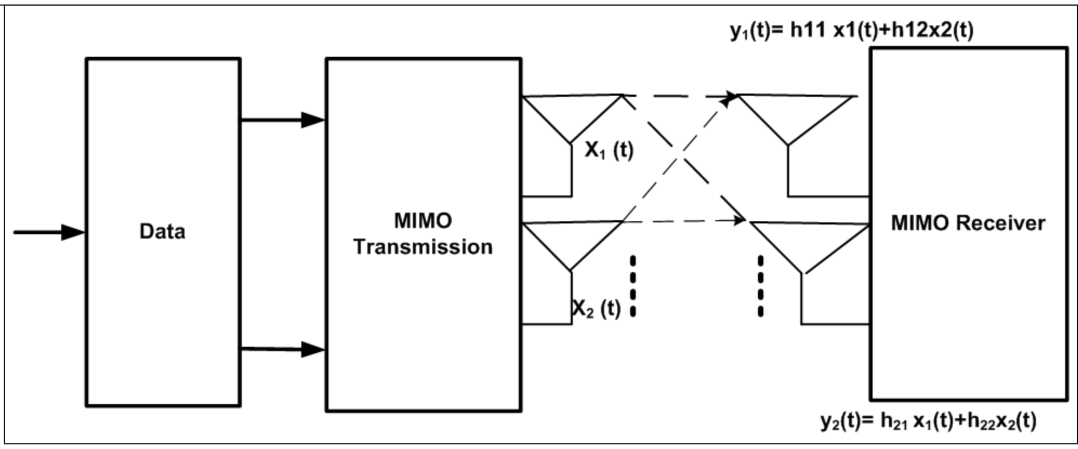

Figure 2.1: 2 x 2 MIMO System Model [1]

1. y = H x+n
2. y = Received signal
3. x = Transmit vectors
4. h=Channel matrix

signal normally follows a power density function such as rayleigh distribution for the indirect signal propagation or rican distribution which also contains a line of sight (LOS) signal component.

2.1.1 MIMO General System Model

MIMO systems employ multiple antennas at both the transmitter and receiver. They transmit data ,$(x1, x2, ..., xN)$ which are independently transmitted on different antennas simultaneously in the same frequency band. These independent signals $(x1, x2, ..., xN)$ are combined. Traditionally this "combination" has been treated as interference. However, by treating the channel as a matrix, the independent transmitted streams can be recovered. As multiple data streams are transmitted in parallel from different antennas, in this system there is a linear increase in throughput with every pair of antennas added to the system. An important fact to note is that unlike traditional means of increasing throughput, MIMO systems do not increase bandwidth in order to increase throughput, they simply exploit the spatial dimension by increasing the number of unique spatial paths between the transmitter and receiver. However, to ensure that the channel matrix is invertible, MIMO systems require an environment rich in multipath. A reasonable system can provide an increase in capacity for the same signal to noise ratio (SNR). Without increasing bandwidth or total transmit power, we can achieve substantial throughput improvement with MIMO.

The received signal model for a MIMO wireless communication channel is given as follows:

$$\mathbf{y} = \mathbf{H}\mathbf{x} + \mathbf{n} \tag{2.1}$$

where $\mathbf{y}$ is the $1 \times n_r$ received signal vector, $\mathbf{x}$ is the $n_t \times 1$ original transmit signal vector and $\mathbf{n}$ is the $n_t \times 1$ noise vector. The channel matrix $\mathbf{H}$ is composed of n_t transmitter and n_r receiver antenna elements and it is of an $n_r \times n_t$ size. The channel coefficients are Zero Mean Circular Symmetric Complex Gaussian (ZMCSCG) independent identically distributed (iid) random variables with unit variance. The total average transmit signal power is constrained to ρ

$$tr\left(\mathcal{E}\left|\mathbf{x}\mathbf{x}^H\right|\right) \leq \rho \tag{2.2}$$

where $tr(\cdot)$ denotes the trace of a matrix. The spatially uncorrelated channel matrix of which full statistical knowledge exists at both ends of the communication is called a "white channel matrix" [39]. A MIMO system model employing two antennas at both the transmitter and receiver is shown in Figure 2.1, while figure 2.2 is the capacity comparisons of single input single output (SISO) and multiple input multiple output (MIMO) of a 2×2, 3×2 and 4×4 antenna systems.

Figure 2.2 represents the information capacity performance improvement of a wireless communication system when multiple antenna elements are used. It is shown that spatial multiplexing achieves diversity which reflects, a significant improvement to the channel capacity when the number of spatially multiplexed antenna elements per node increases.

The effect of spatial correlation at the transmitter as shown in the figure 2.2 reflects how the antenna elements of a multi-antenna configuration can significantly degrade the information capacity performance of a system. It is also shown that partial or no knowledge of the channel statistics at the transmitter produces errors

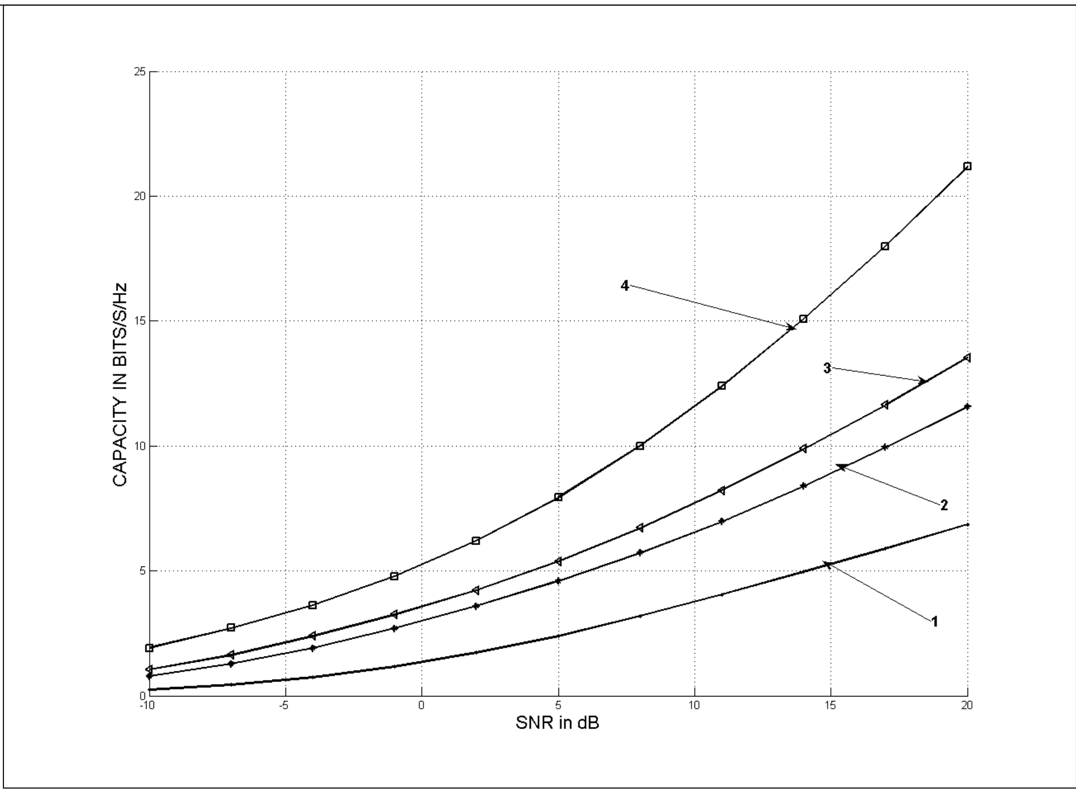

Figure 2.2: MIMO Channel Capacity Comparison

1. = SISO
2. = 2×2 MIMO
3. = 3×2 MIMO
4. = 4×4 MIMO

to the data sequences and hence the channel capacity performance saturates at high SNR range

2.1.2 Partial Channel State Information

Partial knowledge of the channel at the transmitter can lead to errors in the data transmission. Long distance communications or communications in an urban environment cause severe signal power attenuation and hence poor signal reception at the receiver side. Over a long period of time, errors seem to follow a pattern. By statistical estimation of the variance of error, it is possible to predict channel capacity.

The estimation of the channel at the receiver, normally denoted by $\hat{\mathbf{H}}$ is affected by the $\sqrt{1-\sigma_e^2}$ rule presented in [41].

Therefore estimation of the channel at the receiver is given by:

$$\hat{\mathbf{H}} = \left(\sqrt{1-\sigma_e^2}\right)\mathbf{H} \tag{2.3}$$

where σ_e^2 is the MSE of the signal at the receiver.

2.1.3 Uniform Power Distribution

Transmission strategies are normally regulated by the covariance matrix $\mathbf{S}$. The covariance matrix is the SNR regulator matrix, hence the transmit power allocation matrix. The total average SNR available is divided by the number of transmit antennas and equal portions of the total SNR is allocated to each of the antennas as shown in Figure 2.3. In other words, the covariance matrix becomes $\mathbf{S} = \frac{SNR}{n_t}$. For a system with spatially uncorrelated antenna elements where the transmitter has full knowledge of the statistics of the channel, hence the capacity formula for the particular MIMO channel is given by [1][42] as follows: Figure 2.3 expresses uniform power distribution model.

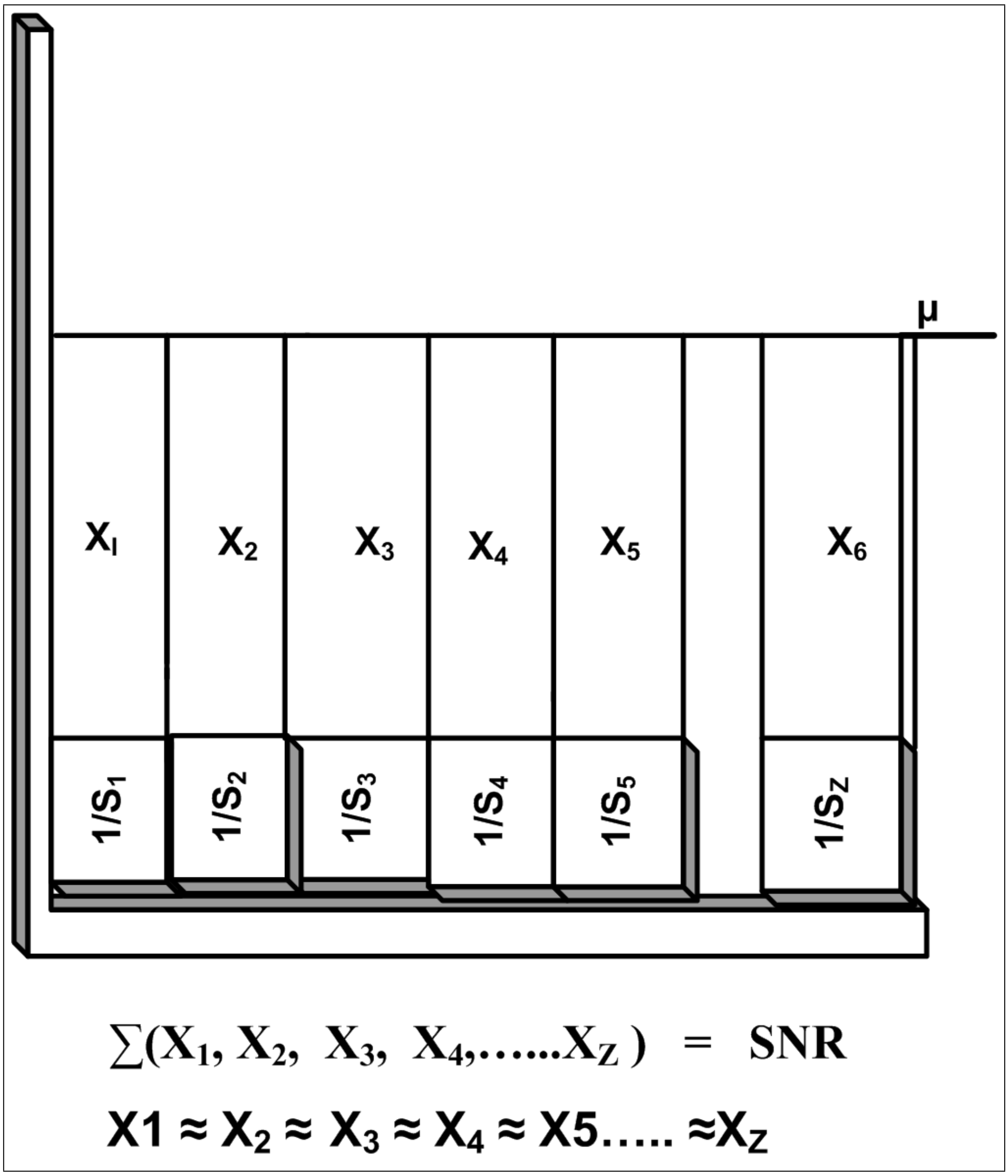

Figure 2.3: Uniform power Model
[43]

1. $\sum X_1, X_2, X_3, X_4, ..., X_Z$= SNR
2. S = Transmit power allocated
3. X = SNR
4. μ = Threshold level

$$C = \mathcal{E}\left[log_2\left|\mathbf{I}_r + S\mathbf{H}_\omega\mathbf{H}_\omega^H\right|\right] \tag{2.4}$$

similarly for a spatially correlated system with unit variance of noise ($\sigma_n^2 = 1$) with no errors at the signal detection at the receiver ($\sigma_e^2 = 0$), equation (2.5) becomes

$$C = \mathcal{E}\left[log_2\left|\mathbf{I}_r + S\mathbf{H}\mathbf{H}^H\right|\right] \tag{2.5}$$

Spatially uncorrelated system but with partial CSI equation (2.6) becomes

$$C = \mathcal{E}\left[log_2\left|\mathbf{I}_r + S\hat{\mathbf{H}}\hat{\mathbf{H}}^H\sigma_n^2 + \sigma_e^2 tr(\mathbf{I}_t S)\mathbf{I}_r\right|\right] \tag{2.6}$$

$$\Rightarrow C = \mathcal{E}\left[log_2\left|\mathbf{I}_r + \frac{S\hat{\mathbf{H}}\hat{\mathbf{H}}^H}{\mathbf{I}_r + \sigma_e^2 SNR\mathbf{I}_r}\right|\right] \tag{2.7}$$

Spatially correlated only at the transmitter with partial CSI equations (2.6 and 2.7) becomes

$$C = \mathcal{E}\left[log_2\left|\mathbf{I}_r + \frac{S\hat{\mathbf{H}}\hat{\mathbf{H}}^H}{\sigma_n^2 + \sigma_e^2 tr(S\mathbf{R}_t)}\right|\right] \tag{2.8}$$

System spatially correlated only at the receiver with partial CSI equation (2.9) becomes

$$C = \mathcal{E}\left[log_2\left|\mathbf{I}_r + \frac{S\hat{\mathbf{H}}\hat{\mathbf{H}}^H}{\sigma_n^2 + \sigma_e^2 SNR\mathbf{R}_r}\right|\right] \tag{2.9}$$

System spatially correlated on both the transmitter and the receiver with partial CSI equation (2.10) becomes

$$C = \mathcal{E}\left[log_2\left|\mathbf{I}_r + \frac{S\hat{\mathbf{H}}\hat{\mathbf{H}}^H}{\sigma_n^2 + \sigma_e^2 tr(S\mathbf{R}_t)\mathbf{R}_r}\right|\right] \tag{2.10}$$

2.1.4 Waterfilling Transmission Strategy

The modal weights are taken from eigen decomposition of the channel matrix. Singular valued decomposition is used to perform modal analysis in this proposed scheme as stated in [7][44][45]. The eigen values of the modes are put in a descending order and are inverted. The inverted weights are put in an increasing order so that the first weight will actually represent the strongest mode. A threshold level μ is selected and transmit power is "water-poured" up to μ. The total SNR is equal to the summation of all the SNR given to every mode as shown in Figure 2.4, only the modes below the threshold level are allocated with portions of the total SNR.

The threshold level μ is purely dependent on the available SNR and the singular values S_{ij} of the modes and is given by:

$$\mu = SNR + \sum_{i=1}^{n_t} \left(\frac{1}{S_{ij}} \right)^2 \tag{2.11}$$

the number of active antennas are decided by the number of non-negative elements are given by:

$$\mu - \left(\frac{1}{S_{i+1,j+1}} \right)^2 > 0 \tag{2.12}$$

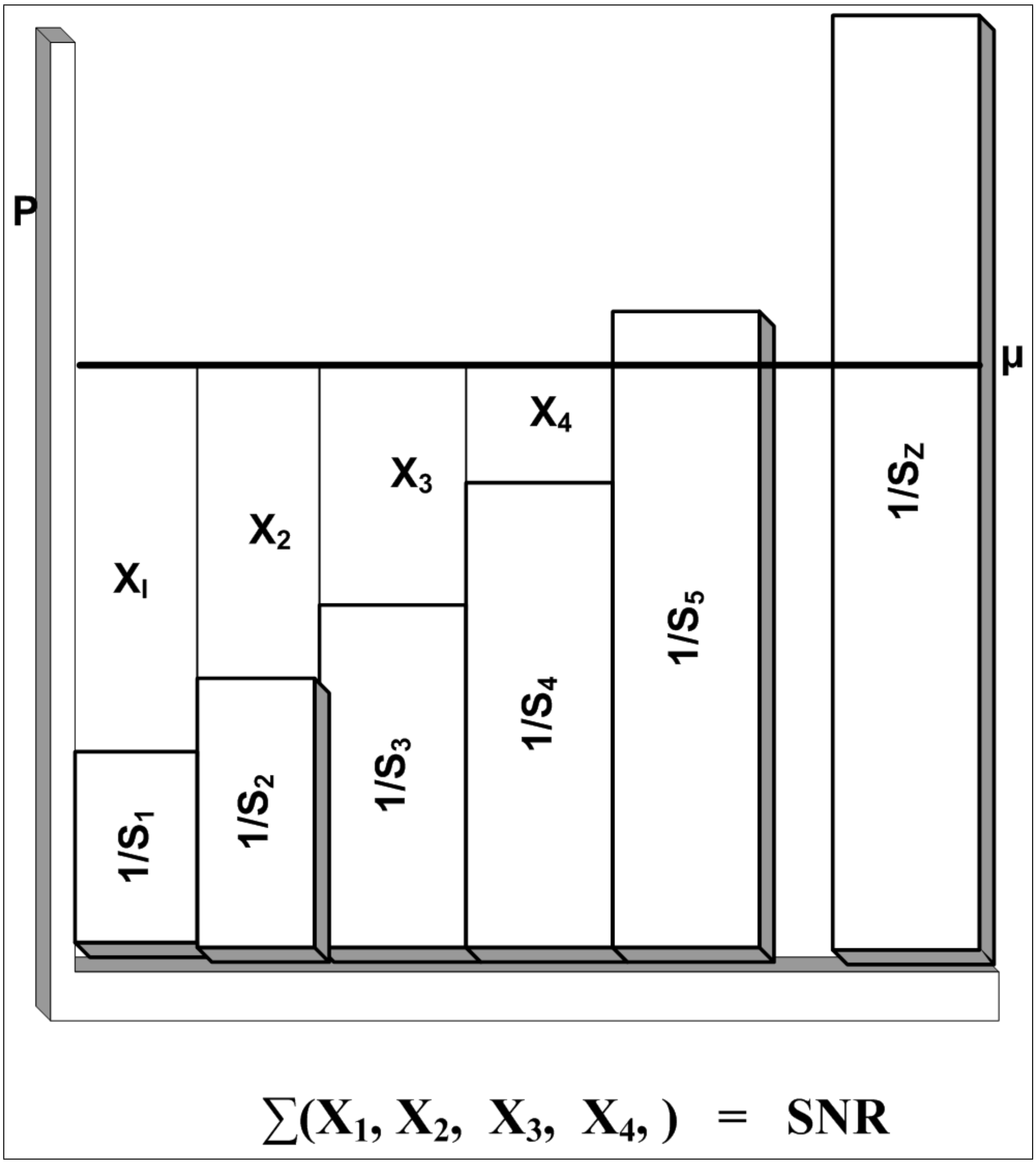

Figure 2.4: Waterfilling Model
[43]

1. $\sum X_1, X_2, X_3, X_4, ..., X_Z$= SNR
2. S = Allocated energy
3. X = SNR
4. μ = Threshold level

It is impossible to perform singular value decomposition(SVD) without full knowledge of the channel. Waterfilling becomes impossible and its power distribution strategy is used only when the transmission has full knowledge of the channel.

From the waterfilling strategy, systems with very high available SNR acts, as a system with uniform power distribution and those with very low available SNR act as a single beamformer as shown in Figures 2.3. When SNR is very high the threshold level μ is also extremely high. The available SNR is to be divided equally to each mode, hence it approaches uniform power distribution transmission strategy, were SNR and threshold levels are low, waterfilling strategy would only allow one mode to transmit and thus act as a beamformer as shown in figure (2.3)

2.1.5 Improved Water-Filling Power Allocation

Based on adaptive modulation MUD principals [46] applied in this research work, the adaptation techniques can be implemented from two aspects, i.e.,the adaptive power allocation under the transmit power constraint for the maximum transportation of adaptive bits, which allocates the transmit bits for minimum transmit power is stated in [25][27][46]. Under the constraints of total power given and the target bit error ratio (BER), the only consideration is how to conduct power allocation to orthogonal eigenmodes to maximize transmit bits.

In order to maximize the transported total bits, an improved water-filling power allocation scheme is given on the basis of classical water-filling schemes. According to this scheme, the adaptive power and bit allocation are conducted in two steps; firstly, an initial power allocation is given by classical water-filling scheme, i.e., the first step is executed to initially allocate the power for different orthogonal eigenmodes according to the classical water-filling scheme. Then, after determining the transported bits at channel eigenmodes, the residual power is reallocated among these eigenmodes to transport additional bits.

2.2 Overview of OFDM System

The first scheme for Orthogonal Frequency Division Multiplexing (OFDM) was proposed by Chang [47] for dispersive fading channels in 1966. Since Chang's proposal, other meaningful research contributions such as [10][11][12][48][49] and their wonderful contributions needs to be recognized. The OFDM scheme was standardized as European digital audio broadcasting (DAB) as well as digital video broadcast scheme (DVB). It is a credible scheme for the third generation mobile and recently selected scheme for High Performance Radio LAN (HIPERLAN) transmission technique as well as becoming part of the IEEE 802.11 wireless standard.

OFDM is a popular modulation scheme that is used in 802.11a, g, HIPERLAN/2 and in the Digital Video Broadcasting standard (DVBT). It is also used in the Asynchronous Digital Subscriber Line (ADSL) standard, where it is referred to as Discrete Multitone modulation. OFDM modulation divides a broadband channel into many parallel subchannels, which makes it a very efficient scheme for transmission in multipath wireless channels. The use of an FFT/IFFT pair for modulation and demodulation make it computationally efficient.

In OFDM, the transmitted signals arrive at the receiver after being reflected from many objects. Sometimes the reflected signals add up in phase leading to increased signal strength and sometimes they add up out of phase causing a fade. This causes the received signal strength to fluctuate constantly, also different subchannels are distorted differently. An OFDM receiver has to sense the channel and correct these distortions on each of the subchannels before the transmitted data can be extracted. OFDM is effective in correcting such frequency selective distortions.

OFDM has many advantages over other transmission techniques. One such advantage is high spectral efficiency (bits/sec/Hz). The Orthogonal part of the name refers to precise mathematical relationship between the frequencies of the subchannels that make up the OFDM system. Each of the frequencies is an integer multiple of a fundamental frequency. This ensures that, though the subchannels overlap they do not interfere with each other, this results in high spectral efficiency. The use of IFFT and FFT for modulation and demodulation results in computationally efficient

OFDM modems. The block diagram of an OFDM modulator and demodulator are as shown in Figure 2.5.

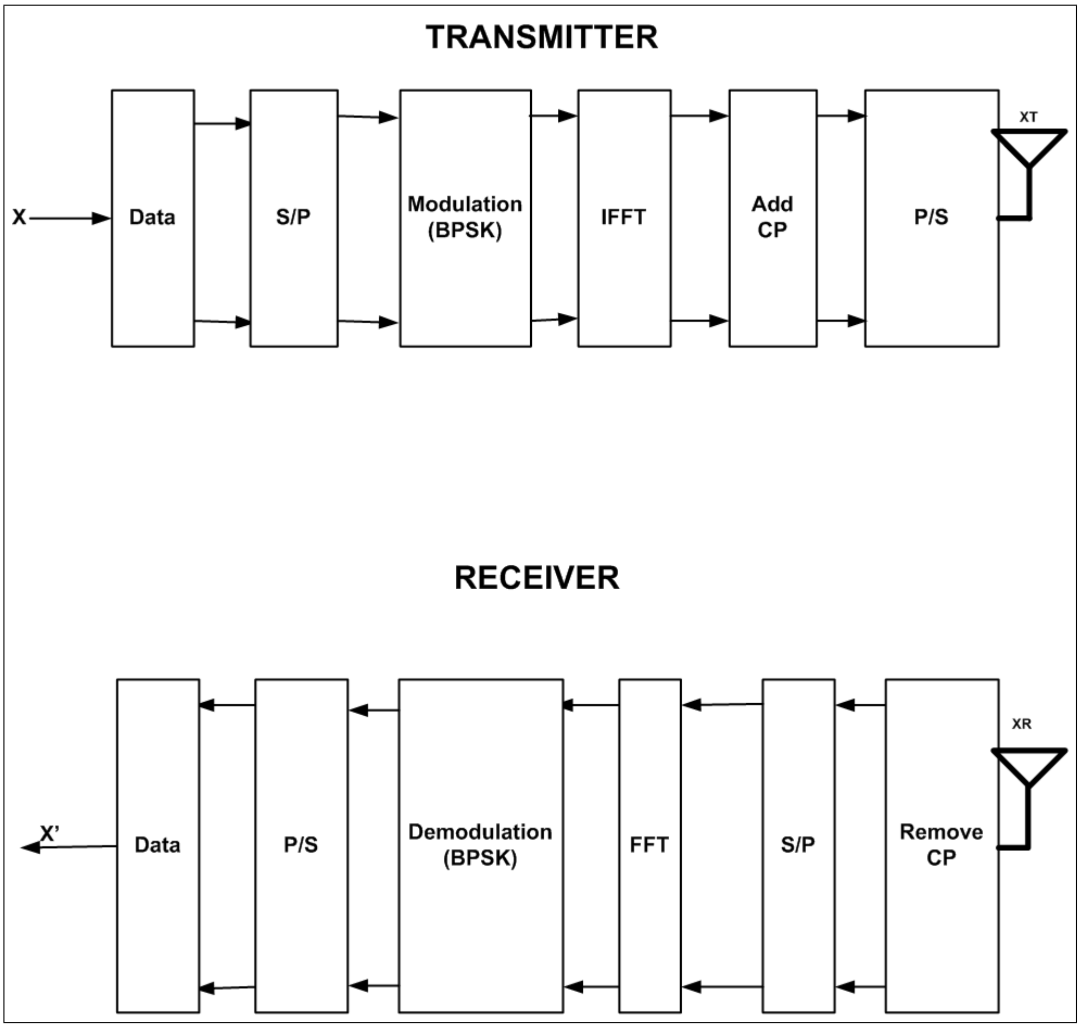

Figure 2.5: OFDM System Model[2]

X = block of OFDM symbol

XT = MIMO Transmit antenna

XR = MIMO Receive antenna

X' = Output OFDM symbol

In Figure 2.4, the signal data is converted from serial to parallel, BPSK is employed to modulate the signal and then IFFT converts the signal from frequency domain to time thereby orthogonalising the signal, cyclic prefix is added to remove all the ISI before transmitting via MIMO channel and on the receiver the opposite of all the procedures in the transmitter is applied to get the signal back.

2.2.1 OFDM Principles

Assuming a communication system with multi-carrier modulation transmits Nc complex-valued source symbols S_n, n = 0,..., $N_t - 1$, in parallel on to Nc sub-carriers. The source symbols may, for instance, be obtained after source and channel coding, interleaving, and symbol mapping. The source symbol duration T_d of the serial data symbols results after serial-to-parallel conversion in the OFDM symbol duration, below is the transmission of OFDM signals.

$$T_s = N_t T_d \tag{2.13}$$

The principle of OFDM is to modulate the Nc sub-streams on sub-carriers with a spacing of

$$F_s = \frac{1}{T_s} \tag{2.14}$$

in order to achieve orthogonality between the signals on the Nc sub-carriers, presuming a rectangular pulse shaping. The N_t parallel modulated source symbols S_n, n = 0, . . . , $N_t - 1$, are referred to as an OFDM symbol. The complex envelope of an OFDM symbol with rectangular pulse shaping has the form

$$x_t = \frac{1}{N_s} \sum_{n=0}^{N_t - 1} S_n e^{j2\pi f_n^t}, 0 \leq t < T_s \tag{2.15}$$

The N_t sub-carrier frequencies are as located in equation below

$$f_n = \frac{n}{T_s}, N = 0, ..., N_t - 1 \tag{2.16}$$

where T_s is the symbol duration, F_s is the frequency, x_t is the transmitted data symbol and f_n is the central frequency. The figure below shows the spectrum of OFDM with 8 subcarriers superimposed.

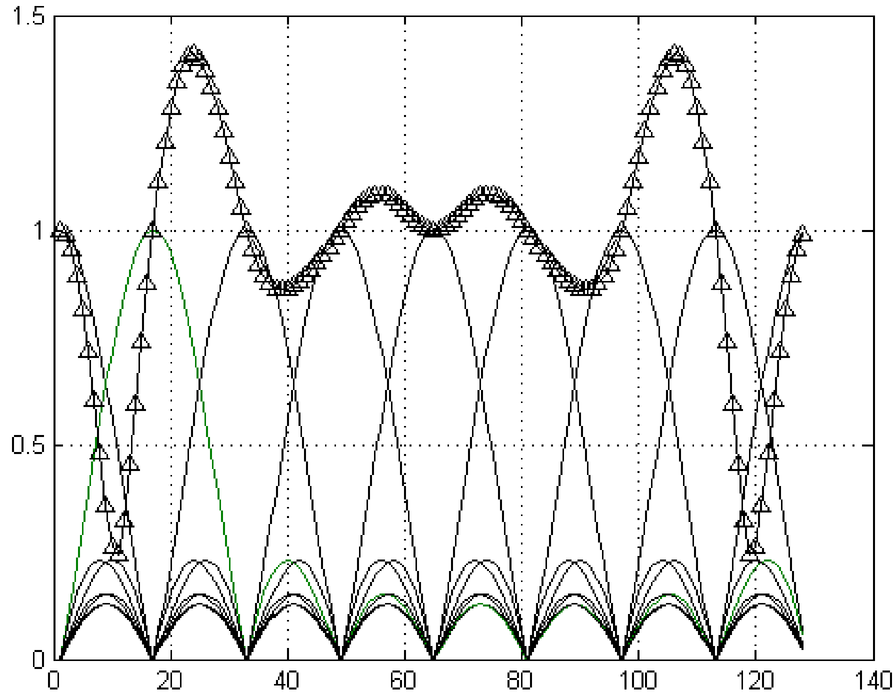

Figure 2.6: OFDM spectrum
OFDM Spectrum of 8 subcarrier superimposed

2.2.2 Table Describing brief overview of OFDM Technology

The rapid advances in multimedia applications involve increased demand for transmissions of graphical data, video and audio messages. The demand for high capacity broadband transmission links continues to increase rapidly. In recent years, wireless communications have drawn remarkable attractions for their flexibility. The market for wireless communications has enjoyed a tremendous growth. Wireless technology now reaches or is capable of reaching virtually every location on the surface of the Earth. Hundreds of millions of people exchange information every day in their personal or business activities using pagers, cellular telephones and other wireless communication products.

It seems that it is a feasible solution and market competitive for the broadband wireless communication systems to replace, or to complement the traditional fixed copper communication systems. Generally the wireless communication environment is more unfavorable than the fixed wired communication; it requires a reasonable system design or architecture to provide a reliable system performance. In the third generation (3G) wireless communication system, although the maximum data rate can be 2Mbps, the typical data rate is around 384kbps. To achieve the goals of broadband cellular service, it is very appealing to leap to the fourth generation (4G) networks. In the last few years, the orthogonal frequency division multiplexing (OFDM) broadband wireless communication system has attracted much interest for its advantages. It is also considered as one of the promising candidates for wireless communication standard. World recognised standards such as IEEE and ETSI are selected OFDM as the physical layer technique for the next generation of wireless systems.

OFDM is an old concept. It was first introduced in the late 60s, based on the multicarrier modulation technique used in the high frequency military radio. Many years after its introduction, however, the OFDM technique has not become popular. This is due to the requirements for large arrays of the sinusoidal generators and coherent demodulators in the transceiver. These are too expensive and too complex for practical deployment. Eventually the discrete Fourier transfer (DFT) and inverse DFT (IDFT) were introduced as an effective solution to the arrays of sinusoidal generators and demodulators, which lower the system complexity. With the constant advances in the technology of very large scale integration (VLSI), the implementation of fast Fourier transform (FFT) and inverse FFT (IFFT) become possible and economical.

In 1971 Weinstein and Ebert proposed the use of IFFT/FFT as an efficient way to realize the OFDM function and the concept of the guard interval to avoid the intersymbol interference (ISI) and inter-carrier interference (ICI). This proposal opened a new era for OFDM. The technique began to attract more and more attention and became very popular. OFDM has already been successfully adopted in many applications, such as digital audio broadcasting (DAB) and digital video terrestrial broadcasting (DVB-T). A brief history of OFDM technique and its applications are listed in Table 1.1. In the past few years, applying the OFDM technique in the wireless LAN (WLAN) has received considerable attention. OFDM technique has been adopted in the WLAN standards of IEEE 802.11a in North America and

Overview of OFDM System

OFDM Overview	
1957	Kineplex, multi-carrier high frequency (HF) modem
1966	R. W. Chang, Bell Labs, OFDM paper+patent
1971	Weinstein and Ebert proposed the use of FFT and guard interval
1985	Cimini described the use of OFDM for mobile communications
1987	Alard and Lasalle proposed the OFDM for digital broadcasting
1995	ETSI established the first OFDM based standard, DAB standard
1997	Digital video terrestrial broadcasting (DVB-T) standard was adopted
1997	Broadband internet with ADSL was employed
1998	Magic WAND project demonstrated OFDM modems for wireless LAN
1999	IEEE 802.11a and HIPERLAN/2 were established for LAN (WLAN)
2000	Vector OFDM (V-OFDM) for a fixed wireless access
2001	OFDM was considered for the IEEE 802.11g and the IEEE 802.16 standards

Table 2.1: Overview of OFDM Technology

HIPERLAN/2 in Europe. It was considered for the IEEE 802.11g and the IEEE 802.16 WLAN standards.

2.2.3 FFT/IFFT for OFDM Application

The IFFT/FFT is the most critical part of the OFDM system. FFT is an efficient way to calculate the discrete Fourier transform (DFT) to find the signal spectra. Since the DFT and inverse DFT (IDFT) basically involve the same type of computations, discussions of an efficient computational algorithm for the DFT also apply to the efficient computation of IDFT. The concept of the DFT is discussed first.

2.2.4 DFT/IDFT for OFDM Application

The DFT of an N- point sequence $x(n)$, is $\leq N-1$ is calculated as:

$$X(k) = \sum_{n=0}^{N-1} x(n) W_N^{kn}, K = 0, 1..., n-1 \tag{2.17}$$

where $K = 0, 1, ..., n-1$. Thus $X(k)$ denotes the K^{th} discrete spectral sample and W_N is defined as:

$$W_N = e^{-j^{2\pi}N} \tag{2.18}$$

The twiddle factor W_N^{kn} can be written as:

$$W_N^{kn} = e^{-j^{2\pi}N}kn \quad (2.19)$$

The IDFT of an N-point sequence $X(k)$, $0 \leq k \leq N-1$ is similarly defined as:

$$x(n) = \frac{1}{N}\sum_{n=0}^{N-1} x(n)W_N^{kn}, n = 0, 1..., \ N-1. \quad (2.20)$$

The sequence $x(n)$ contains N samples in the time domain and the sequence $X(k)$ contains N samples in the frequency domain. The sampling points in the frequency domain occur at the N equally spaced frequencies $\mathrm{w}_k = 2\pi k/N, \ k = 0, 1, ..., N-1$. With these sampling points, $X(k)$ uniquely represents the sequence of $x(n)$ in the frequency domain.

2.2.5 Cyclic Prefix

It is known that in a multipath fading channel environment, channel dispersion causes the consecutive blocks to overlap, creating ISI/ICI. This degrades the system performance. In order for the orthogonality of the OFDM sub-carriers to be preserved, typically in an OFDM system, a guard interval is inserted. Actually the guard interval can be realized by the insertion of zeros, but using the cyclic prefix as guard interval can transform the linear convolution with the channel into circular convolution. The insertion of a cyclic prefix is very simple. Assuming the length of the guard interval is l, it is just the last l samples to the original OFDM sample sequence at the transmitter. At the receiver the guard interval is removed. The process is shown in Figure 2.5. The length of the cyclic prefix is required to be equal to or longer than the maximum channel delay spread to be free from ISI/ICI. As already mentioned, this is simple, but it reduces the transmission efficiency of the information bits.

2.2.6 Synchronization

Time and frequency synchronization between the transmitter and receiver are very crucial with regards to OFDM performance. A wide variety of technique have been proposed for estimating and correcting both timing and carrier frequency offset at the OFDM receiver. Rough timing and frequency acquisition algorithm of the OFDM system rely on known pilot tones embedded into OFDM symbols. The starting time of the FFT window (timing synchronization), the frequency offset due to the inaccuracies of the transmitter and receiver oscillators [50], as well as the channel estimates if coherent reception is adopted, the synchronization can be generated by automatic gain control or using a training symbol as in AMUD (which can also be used for timing synchronization and possibly frequency synchronization). For the latter case, the same metric used for timing synchronization may be used together with the threshold decision. After detecting the presence of the signal, the signals are estimated. [50][2]

2.2.7 Sub-carrier Allocations

Considering the traditional OFDM system, e.g., IEEE 802.16, different users are assigned different frequencies, so that each users signals can be detected at different frequency bands without interfering with one another. As a result, OFDM enjoys the merit of easy decoding at the user side. Such simplicity is particularly appealing during downlink operations where the processing power at user terminals is often limited. For fixed or portable applications where the radio channels are slowly varying, an intrinsic advantage of OFDMA over other multiple access methods is its capability to exploit the so-called multiuser diversity embedded in diverse frequency-selective channels [51][52][53]. The promise of simpler receivers and high system performance has landed OFDMA as one of the prime multiple access schemes for future generation broadband wireless networks IEEE 802.16a-e.

In principle, Orthogonal Frequency Division Multiplexing Access (OFDMA) and MIMO can be synergistically integrated to offer the benefits of both system simplicity and high performance, which is indeed an active topic within the IEEE 802.16/20 standardization bodies. Despite these promises, a few fundamental questions remain to be answered, such as whether or not OFDM, MIMO, OFDMA and MIMO OFDM is the right choice for multiuser communications.

The optimality of MIMO OFDM in the multiuser multi-carrier system is yet to be established. To achieve the capacity bound, one must solve the multiuser sub-carrier allocation and the optimal power allocation jointly. The computational cost for finding the optimal solution is exponential with respect to the number of sub-carriers and polynomial with respect to the number of users. However for the suboptimal sub-carrier allocation criteria for MIMO OFDM systems namely; the Product-criterion and the Sum-criterion, the computation complexity of these suboptimal approaches still grow linearly with the number of users and the number of sub-carriers [54].

2.2.8 OFDM Applications

Due to its computational complexity, OFDM applications have been scarce until quite recently, however it has now been adopted as the new European standard for Digital Audio Broadcasting (DAB) as well as Terrestrial Digital Video Broadcasting (DVB) systems.

In fixed-wired applications, OFDM is employed in the asynchronous digital subscriber line (ADSL)and high-bit-rate digital subscriber line (HDSL) systems and it has also been suggested in power line communication systems due to its resilience to time dispersive channel and narrow band interferers.

Currently OFDM is being studied for European 4th generation framework for advanced Communication Technologies and Services (ACTS) Programme. OFDM combination with MIMO techniques as discussed in this thesis will thereby help to achieve high spectral efficiency and increased throughput.

2.2.9 Advantages of OFDM systems

- High spectral efficiency.
- Simple implementation by FFT (Fast Fourier transform).
- Low receiver computational, conceptual complexity.
- Robustability for high-data-rate transmission over multipath fading channels.

- High flexibility in terms of link adaptation.
- Makes efficient use of the frequency spectrum by allowing overlaping.
- By dividing the channel into narrowband flat fading subchannels, OFDM is more resistant to frequency selective fading than single carrier systems.
- Eliminates ISI and Inter symbol frequency interference(IFI) through the use of a cyclic prefix.
- Using adequate channel coding and interleaving one can recover symbols lost due to the frequency selectivity of the channel.
- Channel equalization becomes simpler, than using adaptive equalization techniques with single carrier systems.
- It is possible to use maximum likelihood decoding with reasonable complexity.
- OFDM is computationally efficient by using FFT techniques to implement the modulation and demodulation functions.
- OFDM is less sensitive to sample timing offsets than single carrier systems.
- Efficient in providing good protection against co-channel interference and impulsive parasitic noise.

2.2.10 Disadvantages of OFDM systems

- Sensitive to frequency offsets, timing errors and phase noise
- Relatively higher peak-to-average power ratio compared to single carrier system, which tends to reduce the power efficiency of the RF amplifier
- The OFDM signal has a noise like amplitude with a very large dynamic range, therefore it requires RF power amplifiers with a high peak to average power ratio.
- OFDM is more sensitive to carrier frequency offset and drift than single carrier systems are due to leakage of the DFT.

2.3 Overview of MIMO OFDM System

The quest and urge for higher data rates continues, as consumer demands for bandwidth hungry applications such gaming, audio and the video streaming leads to the invention of MIMO OFDM. Advancement in handset processors and further integration of technologies like higher mega-pixel cameras into handsets, create a never ending need for more bandwidth. 3G technology falls short in meeting this demand, as coverage is often worse than what customers were used to from 2.5G networks. On the other hand, wireless LAN, the technology initially expected to provide only limited range and bandwidth has come a long way.

Since the first IEEE 802.11 standard in 1997, the maximum data rate has increased from 2 to 54 Mbps [55]. Unfortunately, every increase in data rate comes at the expense of a loss in range. In the IEEE 802.11a/g standards, for instance, the highest data rate of 54 Mbps is achieved through the use of 64-QAM. The use of such highly spectral efficient higher order modulations requires a significantly larger SNR than the simple BPSK modulation used for the lowest 1 Mbps rate, resulting in a significant loss in range. In addition, the link becomes more vulnerable to co-channel interference, which reduces the total system capacity.

The solution to obtaining significantly higher data rates and increasing the range performance at the same time is by MIMO-OFDM (Multiple Input Multiple Output Orthogonal Frequency Division multiplexing) [3][56] applications. MIMO-OFDM increases the link capacity by simultaneously transmitting multiple data streams using multiple transmit and receive antennas. It makes it possible to reach data rates that are several times larger than the current highest 802.11a/g rate of 54 Mbps without having to employ a larger bandwidth or a less robust QAM constellation [57]. After almost a decade of research on MIMO-OFDM, this technique is now ready to succeed OFDM as the dominant transmission technique in wireless LAN. With the introduction of MIMO OFDM wireless LAN products in 2004 by Airgo Networks and the advent of the MIMO-OFDM based 802.11n standard, the performance of wireless LAN in terms of throughput and range has improved significantly, enabling new applications outside the traditional wireless LAN area. The

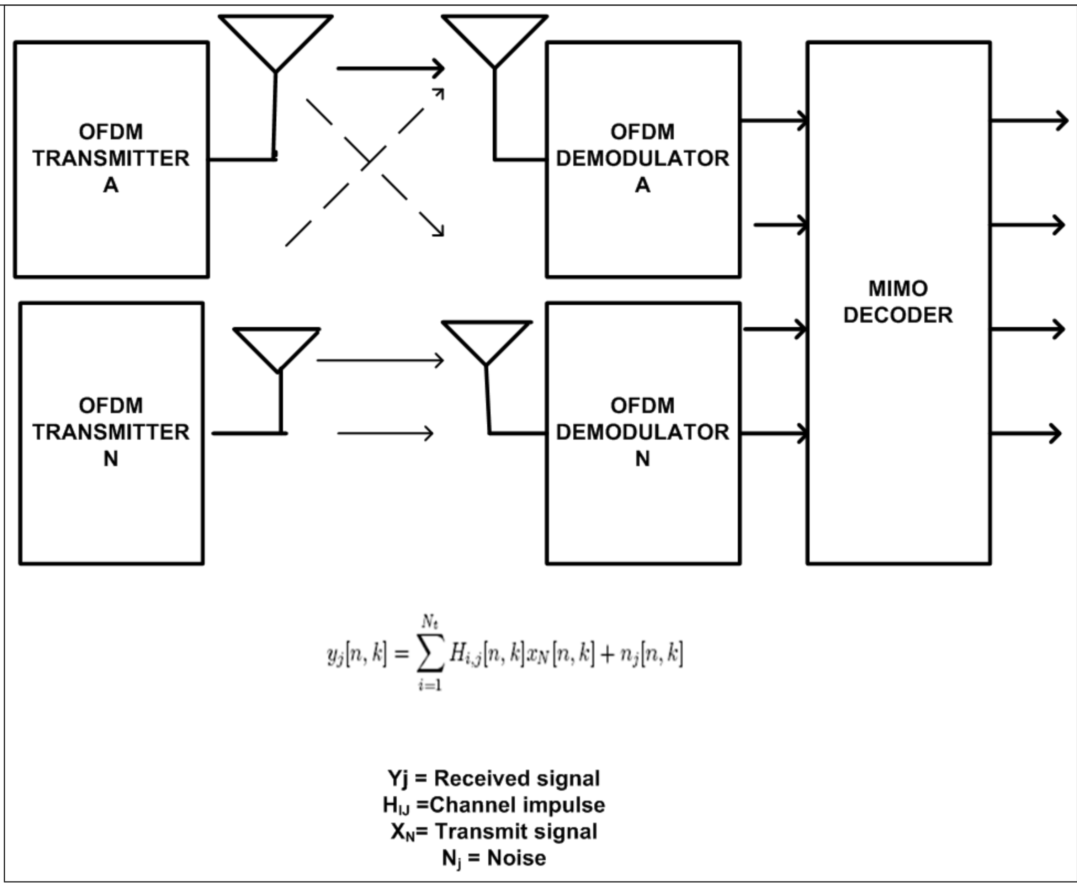

Figure 2.7: MIMO OFDM System Model [3]

one time vision to replace wires in home entertainment applications, such as TV cable replacement, has become a reality.

2.3.1 MIMO OFDM Performance Results

In 2004, Airgo Networks launched the first wireless LAN chipset based on MIMO-OFDM. This first generation MIMO-OFDM system uses a 20MHz channel to transmit at either standard 802.11a/g data rates with a large range increase compared to conventional wireless LAN, or at significantly higher data rates up to 108 Mbps. In 2005, a second generation MIMO-OFDM product was introduced which uses the Adaptive Channel Expansion to transmit either in a 20 or 40MHz channel, increasing the top data rate to 240 Mbps.

The BER simulation of the MIMO OFDM shows that MIMO OFDM below performs better to OFDM SISO, at BER of 10^4 MIMO OFDM has SNR of 7dB as

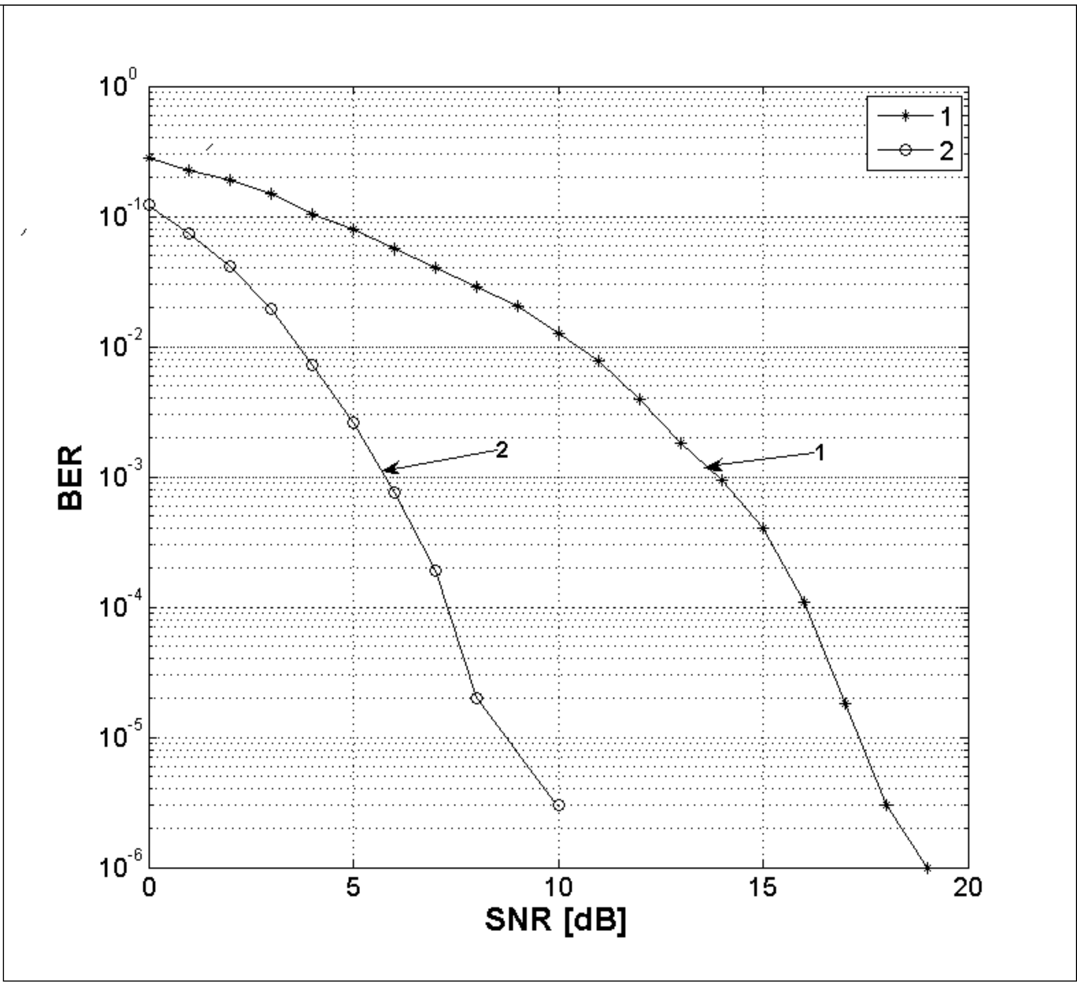

Figure 2.8: BER Comparison of MIMO OFDM and OFDM SISO

1. OFDM SISO
2. MIMO OFDM

compared with OFDM SISO with SNR of 17.5dB at BER of 10^4.

2.3.2 Link Adaptation Scheme

In this scheme, when channel parameters are known at the transmitter, the capacity of MIMO OFDM systems can be further increased by adaptively assigning transmitted power to orthogonal eigenmodes according to the water-filling rule [1]. At the transmitter, the transmitted signals of different carriers are usually eigen beamformed independently to orthogonal modes of the spatial channels at every sub-channel in MIMO OFDM systems [22][23][58], which can be formed via spatial filtering according to the singular value decomposition (SVD) of the channel matrix at transmitters. However, these eigenmodes can not be used to steer the data symbols encoded by spacetime codes, as one spacetime codeword is transferred simultaneously by multiple carriers, while the eigenmodes are obtained in every carrier. So, when coupled with adaptive power and bit allocation, these eigenmodes have many disadvantages relative to their counterparts of MIMO systems in single-carrier transmission.

- These eigenmodes ignore the effects of spacetime diversity gains on the equivalent signal to noise ratios of data symbols encoded by one spacetime coder.
- For MIMO OFDM system configured with low rate spacetime codes, it would be difficult to conduct adaptive power allocation as a large number of eigenmodes exist, compared with data symbols carried by one MIMO OFDM symbol.
- It is also difficult to determine the modulation order of data symbols encoded in one spacetime codeword, as one spacetime codeword is carried by many eigenmodes at multiple carriers.

Therefore, these eigenmodes can be viewed as the simple generalization of their counterparts of MIMO systems in single-carrier transmission for convenient analysis for system capacity, but not reflect the fact of one spacetime codeword being carried by multiple sub-channels.

2.4 sumary

In this section, a new approach to construct orthogonal eigenmodes in MIMO OFDM systems is presented. For the MIMO OFDM systems with least-squared decoders, orthogonal eigenmodes can be obtained by the SVD of equivalent channel matrix in system models, where one general spacetime code is considered in general way. The results of the eigenmodes corresponds to the data symbols encoded in spacetime code words carried by one MIMO OFDM symbol. Thus, the novel eigenmodes can be used directly to steer adaptive power allocation to data symbols and their bit allocations, as usually done in the MIMO systems with single-carrier transmission.

Major fundamentals that will be used in this thesis are discussed, their importance and contributions in communications are discussed in this chapter. Without the review of this fundamental, the AMUD MIMO OFDM would not have been possible. The major aim and objectives of this research dwell on how to improve on the quest and the urge for higher data rates transmission, as consumer demands for higher bandwidth applications such as the gaming, audio and the video streaming which leads to the invention of MIMO OFDM and now AMUD MIMO OFDM.

Chapter 3

Proposed Adaptive Multiuser Receivers for MIMO-OFDM Systems

3.1 Introduction

The adaptive Multiuser detection is the preferred detection technique in this thesis because it sends in training signals to monitor the parameters of the channel and adjusts the parameters of its filter to suit the desired signals. The effect, importance and advantages of the fundamentals discussed in chapter 2 will facilitate and make it possible for the aims of this research work to be achieved thus it is the foundation in which we explore our research.

Multiuser Detection provides the first comprehensive treatment of the subject of multiuser digital communications. Multiuser detection deals with demodulation of the mutually interfering digital streams of information that occur in areas such as wireless communications, high-speed data transmission, satellite communication, digital television, and magnetic recording. The development of multiuser detection techniques is one of the most important recent advances in communications technology. There are various detection technique to be discussed in this chapter.

Adaptive MMSE Multiuser detection (A MMSE MUD) is for demodulation of digitally modulated signals with multiple access interferences (MAI). This scheme was designed for total elimination of MAI in the system. In a single user environment, every match filter maximum likelihood receiver plays the role of Adaptive MMSE maximum likelihood receiver [4][20].

In the implementation of Adaptive Minimum Mean Square Error Multiuser Detection (A MMSE MUD), it provides robustness and mobility in a time variable frequency selective multipath fading channel; it improves the bit error rate performance and therefore enhances channel capacity of a multi-cellular environment. MIMO OFDM mitigates multiple access interference and increases capacity [59][22]. In [20] A MMSE MUD techniques was used effectively to achieve the performance of a maximum likelihood estimator but on a linear complexity.

3.2 Multiuser Detection

Considering various multi-user detectors (MUDs), the classic linear least squares (LS) and MMSE MUDs exhibit low computational complexity at the cost of a limited performance. In contrast, the high-complexity optimum maximum-likelihood (ML) MUD is capable of achieving the best performance due to invoking an exhaustive search, which imposes a computational complexity typically increasing exponentially with the number of simultaneous users supported by the MIMO OFDM system and thus rendering its implementation prohibitive in high-user-load scenarios [26][2][5].

In most research papers, a range of suboptimal nonlinear MUDs have been proposed, such as the MUDs based on successive interference cancelation (SIC) and picture interference cancelation (PIC) techniques [2][5]. Explicitly, instead of detecting and demodulating user's signals in a sequential manner, as the LS and MMSE MUDs do, the PIC and SIC MUDs invoke an iterative processing technique that combines detection and demodulation. More specifically, the output signal generated during the previous detection iteration is demodulated and fed back to the input of the MUD for the next iterative detection step. Similar techniques invoking decision-feedback have also been applied in the context of classic channel equalization.

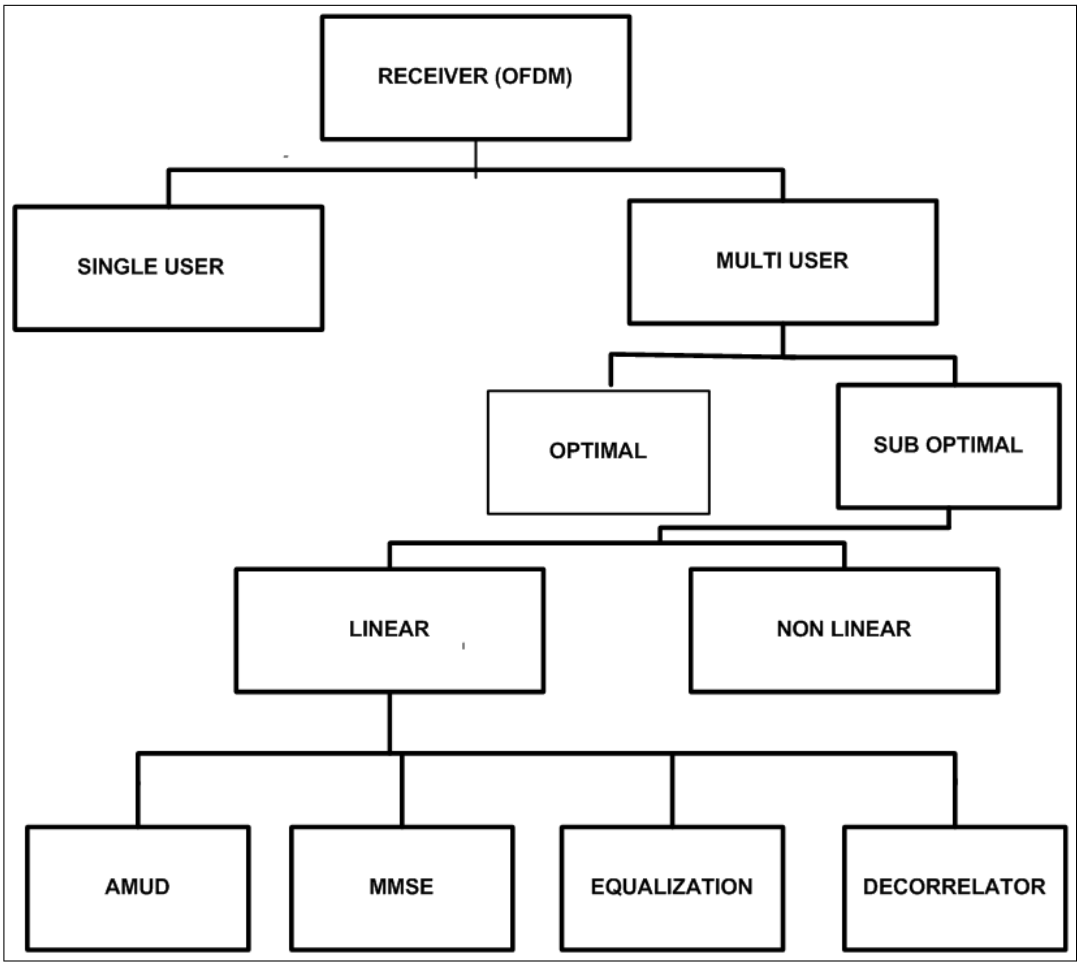

Figure 3.1: Proposed OFDM Receiver Hierarchy [4][5][6]

1. Matchfilter [5]
2. Decorelator [5]
3. Equalizer [60]
4. MMSE = [6]
5. AMUD = [20][4]

Nevertheless, since the philosophy of both the PIC and SIC MUDs is based on the principle of removing the effects of the interfering users during each detection stage, they are prone to error propagation occurring during the consecutive detection stages due to the erroneously detected signals of the previous stages. A typical OFDM receiver block diagram below depicts the hierarchy on which the proposed technique functions as shown in Figure 3.1. OFDM receivers are either single-user or multiuser detectors. A conventional matched filter is the most typical single-user detector, as shown in Figure 3.2.

3.2.1 Matched filter

The distinguishing characteristic of a Matched Filter is the step response which approximates a ramp, and the impulse response approximating a pulse. The purpose of the Matched Filter in this thesis is to maximize the signal to noise ratio and to minimize the probability of undetected errors received from a signal.[5]

Matched Filter is used to optimize the signal to noise ratio at the sampling point of a bit stream. This happens if the filter is applied to the bit stream. It has an impulse response that is the time inverse of the pulse shape that is being sampled. If the pulse is rectangular, the filter impulse response must therefore also be a rectangle, and the step response is a ramp.

Filter Solutions and Filter Light allow you to define your Matched Filter by setting the rise time of the ramp. The proper use of the Matched Filter is to set the rise time to be equal to the pulse width of the pulses in a bit stream. The integration of the square of the error between the filter impulse response and the ideal impulse response (a square pulse) is minimized under the mentioned restraint conditions. The function of a Matched Filter is to optimize the signal to noise ratio at the sampling point of a bit stream.

The ideal continuous and infinite impulse response (IIR) Matched Filter solutions are not realizable, they must be approximated. Filter Solutions use an approximate solution that optimizes the time response of the filter with the constraint that the transfer function zeros remain on the axis. Specifically, the integration of the square of the error between the filter impulse response and the ideal impulse response (a square pulse) is minimized under the mentioned restraint conditions. The purpose of the zero constraint is to allow the filter to be realized with passive elements.

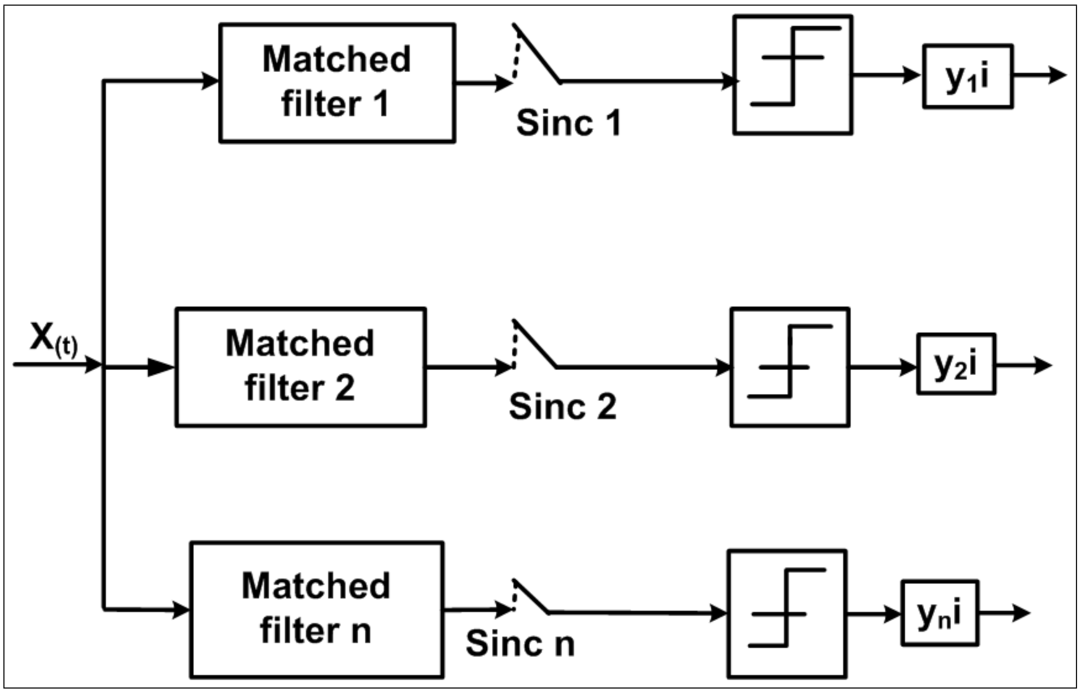

Figure 3.2: Bank of Single user Matched filter [5][7]

1. x_t = Matched filter receiver
2. y_n^i = Bank of Single user Matched filter output

Multiuser detectors are either optimal or sub-optimal as shown in Matched Filter diagram in Figure 3.2. The optimal detection refereed to MLSE eliminates MAI, however its complexity grows exponentially with the numbers of active users [5][61]. The increased complexity issue makes the optimal detection inapplicable, hence a number of sub-optimal multiuser detectors have been invented that are either linear systems which can only provide a marginal channel capacity and BER reliability improvement, or non linear systems where their complexity can be very high [62].

3.2.2 Multiuser Detection Technique

The MLSE detector proposed by Verdu in [61] is known as the optimal MUD, which is fully capable of suppressing MAI. The digital signal detection on an MLSE estimator is made by joint sequence decision at the Matched Filter outputs from all users. MLSE estimators demonstrate a significant information capacity enhancement over the conventional single user detector. The optimal MUD achieves a BER performance that approaches the single user bound, which means that it performs like no other users operate within the channel. However, due to its high complexity, the MLSE MUD technique is inappropriate for contemporary wireless communication systems.

In statistics, maximum-likelihood estimation (MLE) is a method of estimating the parameters of a statistical model. When applied to a data set and given a statistical model as shown in Figure 3.3, maximum-likelihood estimation provides estimates for the model's parameters.

Maximum likelihood corresponds to many well-known estimation methods in statistics. For example, one may be interested in the heights of adult female giraffes, but be unable due to cost or time constraints, to measure the height of every single giraffe in a population. Assuming that the heights are normally (Gaussian) distributed with some unknown mean and variance, the mean and variance can be estimated with MLE while only knowing the heights of some sample of the overall population. MLE would accomplish this by taking the mean and variance as parameters and finding particular parametric values that make the observed results the most probable (given the model).

In general, for a fixed set of data and underlying statistical model, the method of maximum likelihood selects values of the model parameters that produce a distribution that gives the observed data the greatest probability (i.e., parameters that maximize the likelihood function). Maximum-likelihood estimation gives a unified approach to estimation, which is well-defined in the case of the normal distribution and many other problems. However, in some complicated problems, difficulties do occur: in such problems, maximum-likelihood estimators are unsuitable or do not exist.

The major reason in literature for MLSE is increasing information : For the asymptotes to hold in cases where the assumption of independent identically distributed observations does not hold, a basic requirement is that the amount of information in the data increases indefinitely as the sample size increases. Such a requirement may not be met if either there is too much dependence in the data (for example, if new observations are essentially identical to existing observations), or if new independent observations are subject to an increasing observation error.

Some regularity conditions which ensure this behavior are:

- The first and second derivatives of the log-likelihood function must be defined.
- The Fisher information matrix must not be zero, and must be continuous as a function of the parameter.
- The maximum likelihood estimator is consistent

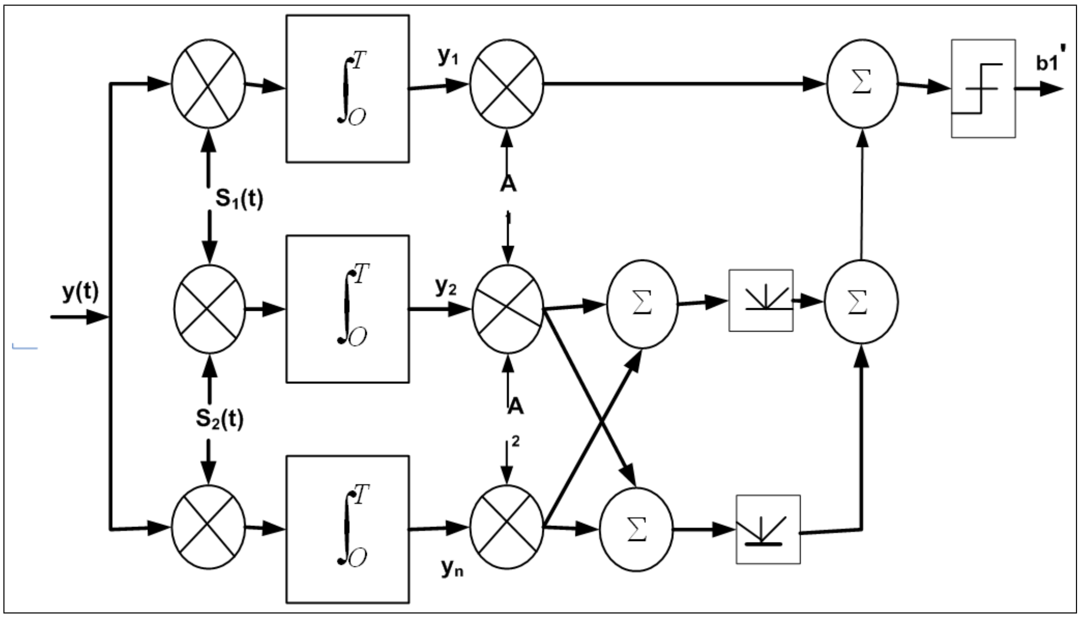

Figure 3.3: MLSE detection with one synchronous interferer [5]

1. $A|y_1|, A_2|y_2| \geq A_1A_2|P|$= Optimium Decision
2. y_1, y_n = Received waveform
3. S_1, S_2 = Signature waveform
4. b_1 = Joint Optimum decision

Therefore, only the linear complexity MUD systems can be considered suitable for the demands of mobile communication networks.

3.2.3 Decorrelator

The decorrelator algorithms are linear, although non-linear algorithms also exist. Decorrelation is used to reduce autocorrelation within a signal, or cross-correlation within a set of signals, while preserving other aspects of the signal. A frequently used method of decorrelation in this thesis is matched linear filter, to reduce the autocorrelation of a signal as far as possible. Since the minimum possible autocorrelation for a given signal energy is achieved by equalizing the power spectrum of the signal to be similar to that of a white noise signal, this is often referred to as signal whitening.

Lupas [63] introduced a decorrelator that is used to eliminate the cross-correlation that occurs within the transmitted signals of a multiple-access channel. A very common technique for decorrelation of a data signal is the use of linear complexity matched filters at the receiver to reduce the cross-correlation within the incoming data signals, assuming negligible noise, and those sets of data signals within the channel are linearly independent. In a multiple-access channel where a set of independent users operate, the decorrelating detector is independent of the energy of other users. In [63], it was stated that in the synchronous case the performance achieved by linear multiuser detectors is similar to that of optimum multiuser detection. Thus the decorrelating detector is of linear complexity. The ideal decorrelating detector would pre-multiply the inverse cross-correlation matrix of the received signal vector. In practice this scenario is totally hypothetical since noise is inevitable and its components are always correlated to the received signal and channel coefficients [5].

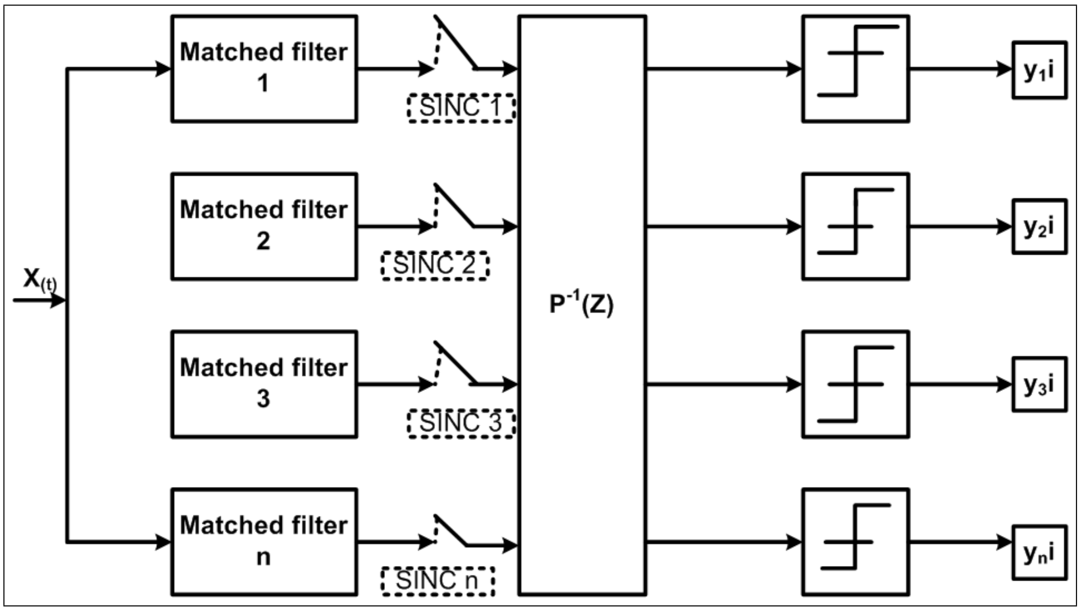

Figure 3.4: Decorrelator Model [5]

1. $P^{-1}(z)$ = Bank of matched filter output
2. X_t = received input
3. y_1, y_n^i = Output

3.2.4 Minimum Mean Square Error

In model-based estimation of unobserved components, the minimum mean squared error estimator of the noise component is different from white noise. The variance of the component is always underestimated, and the smaller the noise variance, the larger the underestimation. Estimators of small-variance noise components will also have large autocorrelations. In the context of an application, the sample autocorrelation function of the estimated noise will perform well even when the variance is small and the series is of relatively short length.

The equalization techniques are used to mitigate MAI in multiple access channels and it is linearly complex in sub-optimal multiuser detection systems. The MMSE detectors do not require any statistical or explicit knowledge of the MAI parameters; it is composed of a bank of n Matched Filters shown in Figure 3.2 that adapt to the incoming digital signal to achieve MMSE solution. An MMSE equalization scheme was proposed by Madhow in [6].

The first MMSE equalization scheme assumes a chip-rate sampling of the channel and, by the use of N-tap adaptive FIR filter at the receiver, the MSE between the original digital data sequence and the received data sequence is minimized. The second scheme assumes a single match filter detector samples X times per symbol interval on the same configuration with the first technique. The advantage of the sub-optimal MMSE equalization technique is that of linear complexity, but on the other hand the system is totally centralized, making it inapplicable to mobile communication systems.

For the channel capacity estimation, a set of definitions are used to determine the performance of MMSE. Calculations Definitions are as follows:

1. Auto covariance matrix $\mathbf{R} = \mathcal{E}\left\{\mathbf{y}\mathbf{y}^H\right\}$
2. Cross correlation vector $\mathbf{p} = \mathcal{E}\left\{x_k^*\mathbf{y}\right\}$
3. Filter output statistic $\hat{x}_k = \mathbf{w}^H\mathbf{y}$

where x_k is the training signal of the k^{th} user and k is constrained to the total number of users, $\mathbf{y}$ is the received signal and $\mathbf{w}$ represents the matched filter coefficients.

The error function is defined as:

$$J(\mathbf{w}) = \mathcal{E}\left\{|x_k - \hat{x}_k|^2\right\} \tag{3.1}$$

expanding equation (3.1) yields:

$$J(\mathbf{w}) = \mathcal{E}\left\{x_k^*(x_k - \hat{x}_k)\right\} - \mathcal{E}\left\{\hat{x}_k^*(x_k - \hat{x}_k)\right\}$$

Lemma 1 : For MMSE $\mathcal{E}\left\{\hat{x}_k^*(x_k - \hat{x}_k)\right\} = 0$, where on average, the estimate $\hat{x}_k$ is orthogonal to the error.

Proof :

$$\mathcal{E}\left\{\left(\mathbf{w}^H\mathbf{y}\right)^*\left(x_k - \mathbf{y}^H\mathbf{w}\right)\right\} = \mathcal{E}\left\{\mathbf{w}^H\mathbf{y}x_k^*\right\} - \mathcal{E}\left\{\mathbf{w}^H\mathbf{y}\mathbf{y}^H\mathbf{w}\right\}$$

Since $\mathbf{w}$ is constant, then

$$\mathcal{E}\left\{\left(\mathbf{w}^H\mathbf{y}\right)^*\left(x_k - \mathbf{y}^H\mathbf{w}\right)\right\} = \mathbf{w}^H\mathcal{E}\left\{\mathbf{y}x_k^*\right\} - \mathbf{w}^H\mathcal{E}\left\{\mathbf{y}\mathbf{y}^H\right\}\mathbf{w}$$

$$\mathcal{E}\left\{\left(\mathbf{w}^H\mathbf{y}\right)^*\left(x_k - \mathbf{y}^H\mathbf{w}\right)\right\} = \mathbf{w}^H\mathbf{p} - \mathbf{w}^H\mathbf{R}\mathbf{w} \tag{3.2}$$

Corollary 1 : The MMSE solution is $\mathbf{w} = \mathbf{R}^{-1}\mathbf{p}$.

Hence, by substitution

$$\mathbf{w}^H\mathbf{p} - \mathbf{w}^H\mathbf{R}\mathbf{w} = 0$$

Therefore for MMSE $\mathcal{E}\left\{\hat{x}_k^*(x_k - \hat{x}_k)\right\} = 0$.

For the MMSE, when $\mathbf{w} = \mathbf{R}^{-1}\mathbf{p}$, it is obvious that

$$J(\mathbf{w}) = \mathcal{E}\left\{x_k^*\left(x_k - \hat{x}_k\right)\right\} \tag{3.3}$$

Given Lemma 1,

$$J(\mathbf{w}) = \sigma_x^2 - \mathbf{w}^H\mathbf{p}$$

therefore,

$$J(\mathbf{w}) = \sigma_e^2 = \sigma_x^2 - \mathbf{p}^H\mathbf{R}^{-1}\mathbf{p} \tag{3.4}$$

where σ_e^2 is the variance of error. Note that $J(\mathbf{w})$ is the error function, where for $\mathbf{w} = \mathbf{R}^{-1}\mathbf{p}$, it is the minimum mean square error.

By approximation of the optimum filter weights in a practical manner utilizing the Least Mean Square (LMS) adaptive algorithm [4]. The LMS is given as:

$$\mathbf{w}_{k+1} = \mathbf{w}_k + \alpha e_k^* \mathbf{y} \tag{3.5}$$

where e_k^* is the conjugate of the instantaneous error and α is the step size parameter which is shown in [4] to be bounded by:

$$0 < \alpha < \frac{2}{\lambda_{max}}$$

$$\sum_{i=1}^{2M+1} \frac{\alpha\lambda_i}{2 - \alpha\lambda_i} < 1$$

where λ_i is the i^{th} eigenvalue of the autocorrelation matrix $\mathbf{R}$, λ_{max} is the maximum eigenvalue and $2M + 1$ is the number of filter coefficients.

It can be shown that the steady state MSE for the LMS algorithm is given by:

$$e(\infty) = \frac{J(\mathbf{w})}{1 - \sum_{i=1}^{2M+1} \frac{\alpha\lambda_i}{2-\alpha\lambda_i}} \tag{3.6}$$

Furthermore, provided that α is small enough, the steady state error is approximately $J(\mathbf{w})$.

Lemma 2 : The channel capacity of an adaptive system with a bank of MMSE filters was stated by Rapajic in [20] as:

$$C = I_{max}(x_k; \hat{x}_k) = log\left(\frac{\mathcal{E}\left\{x_k^2\right\}}{\mathcal{E}\left\{e^2\right\}}\right) = log\left(\frac{1}{\sigma_e^2}\right) \tag{3.7}$$

where x_k is $N(0, \sigma^2)$.

Proof : From Lemma 1, if a vector of coefficients $\mathbf{w}_{opt}$ is chosen to minimize mean error, then the error signal is orthogonal to the symbol estimate ($\mathcal{E}\left\{\hat{x}_k^*(x_k - \hat{x}_k)\right\} = 0$). Now if $x_1, x_2, ..., x_k$ are Gaussian distributed random variables with zero mean, then:

1. $\hat{x}_k$ is also Gaussian

2. $(\hat{x}_k - x_k)$ is also zero mean Gaussian

Lemma 3 : [33] Given that $p(x)$ is a one dimensional distribution and subject to the condition that the standard deviation of x is fixed at σ_x, the maximum entropy $H(x) = \sigma_x log\left(\sqrt{2\pi e}\right)$.

Lemma 4 : [64] Given two independent variables α and β. The entropy of α given β is given by:

$$H(\alpha|\beta) = H(\alpha) \tag{3.8}$$

Lemma 5 : [64] For any two random variables α and β

$$H(\alpha, \beta|\beta) = H(\alpha|\beta) \tag{3.9}$$

By taking into account Lemmas 1-5, the mutual information is given by:

$$I(x_k; \hat{x}_k) = H(x_k) - H(x_k|\hat{x}_k)$$

From Lemma 5

$$I(x_k; \hat{x}_k) = H(x_k) - H(x_k - \hat{x}_k|\hat{x}_k)$$

$$I_{max}(x_k; \hat{x}_k) = log(\sigma_x^2) - log(\mathcal{E}(n_e^2))$$

Lemma 2, assumes transmit signal power normalized to unit energy, $\sigma_x^2 = 1$

$$C = I_{max}(x_k; \hat{x}_k) log\left(\frac{1}{\sigma_e^2}\right) \tag{3.10}$$

By substitution of (3.4) to (3.10) we get:

$$C = log\left(\frac{1}{1 - \mathbf{p}^H\mathbf{R}^{-1}\mathbf{p}}\right) \tag{3.11}$$

$$0 \leq \mathbf{p}^H\mathbf{R}^{-1}\mathbf{p} < 1$$

for standard MMSE approach [5]

$$\mathbf{R} = \mathbf{H}^H\mathbf{Q}\mathbf{H} + \sigma_{\mathbf{v}}^2$$

where $\mathrm{Q} = \mathcal{E}\left|\mathrm{xx}^{\mathcal{H}}\right|$ and $tr(\mathrm{Q}) \leq P$. where from definitions 1, 2 & 3

1. $\mathbf{R}_{LCO} = \mathcal{E}\left\{\mathbf{y}_{LCO}\mathbf{y}_{LCO}^H\right\}$
2. $\mathbf{p}_{LCO} = \mathcal{E}\left\{x_k^*\mathbf{y}_{LCO}\right\}$
3. $\mathbf{R}_{LCO} = \mathbf{H}_{LCO}^H\mathbf{Q}\mathbf{H}_{LCO} + \sigma_{\mathbf{v}}^2$

Hence, the information capacity c, at the output of the system is given from equation (3.11)

$$C = log\left(\frac{1}{1 - \mathbf{p}_{LCO}^H\mathbf{R}_{LCO}^{-1}\mathbf{p}_{LCO}}\right) \tag{3.12}$$

3.2.5 Spatial Multiplexing

The V-BLAST architecture has been proposed for achieving high spectral efficiency over wireless channels characterized by rich scattering multi path channel [14]. In this V-Blast approach, one way of detection is to use the proposed AMUD, i.e., linear combining elimination. Conceptually, each stream (i.e., layer) in turn is considered to be the desired signal, while regarding the remaining signals as interference. Nulling is performed by linearly weighting the received signals to satisfy some performance related gain in Zero-Forcing or MMSE. This linear elimination approach is viable, but superior performance is obtained if nonlinear techniques are used.

One particularly attractive nonlinear alternative is to exploit symbol cancelation as well as linear elimination to perform detection. Using symbol cancelation, interference from already-detected components is subtracted from the received signal vector; it would reduce the interference. In this work ordered successive interference cancelation with AMUD employing MMSE was also applied as reference, a maximum likelihood (ML) decoding receiver was considered. It was assumed that the $H_{ij}(k)$ is the channel coefficient from j_{th} transmit antenna to i_{th} receive antenna and n is white noise as seen in this model.

3.2.6 Diversity

Space-time block codes (STBC) efficiently exploit transmit diversity to combat multipath fading while keeping decoding complexity to a minimum. It was shown in previous work by Tarokh that there is no STBC with full-rate and full-diversity for more than two transmit antennas, and it was proposed that the 3/4 rate, full-diversity code for four transmit antennas [17], the number of sub-carrier that transmits the same information, determines the order of diversity. It is easier to achieve a higher diversity in this proposed technique, than in direct sequence CDMA (DS CDMA) [9][7] and conventional MIMO OFDM. However, the reciprocal of the multipath spread is a measure of the coherence bandwidth of the channel, the maximum achievable order of frequency diversity, L, in a specific channel is approximately given by [7] as:

$$L \approx \frac{1}{(\Delta f)c} \tag{3.13}$$

where $(\Delta f)c$ is its coherence bandwidth. Hence, spreading a symbol over more than the number of sub-carriers is expected to have no more benefit in terms of diversity gain. Instead, as the number of users increases, the MUI will increase significantly, thus reducing the overall performance of MC-OFDM system, but will not affect AMUD technique based on the principle of its operation.

3.2.7 Interference Cancelation

Interference occurs when electromagnetic waves correlate with each other. It is one of the major problems of wireless communication networks. The correlations between electromagnetic waves are due to carrier frequencies of radio signals generated from the same source. Interference disturbs the radio signals and limits or obstructs the BER reliability and channel capacity performance of a wireless communication system. The problem of channel interference becomes more severe when multiple users access the same communication channel which is known as MAI. It is known that channel capacity performance of a MIMO OFDM wireless communication system is degraded by MAI caused by the cross-correlation between the unique spreading codes assigned to each active user within the system.

Many research works have been carried out in the past to find solutions to the problem of MAI. This research leads to the invention of techniques that are capable of significantly suppressing interference. It has been proven that by MAI cancelation, the BER reliability of wireless systems and wireless channel capacity has been considerably improved. The techniques developed towards the MAI cancelation over multiple access channels cannot fully eliminate MAI but can keep it low.

3.3 Adaptive Filters

A Wiener filter requires prior information about the statistics of the data to be processed. It is optimum only when the statistical characteristics of the input data match the prior information upon which the design of the filter is based. However, if the Wiener is not possible, the design is no longer optimum. This has generated a lot of concern and thus in real time operation, this procedure has the disadvantage of excess cost of hardware, which could be addressed with an adaptive filter.

This recursive algorithm makes it possible for the filter to perform satisfactorily in an environment where complete knowledge of the relevant signal characteristics is not available. The algorithm will eventually converge to the Wiener solution in some statistical sense, no matter the nature of the environment.

The applications of a recursive algorithm to the parameters of the adaptive filters are updated in the iterations and thus it is data dependent. It is classed nonlinear because it does not obey superposition. It could be classed linear or nonlinear depending on what its input-output map obeys. It is said to be linear if superimposed, otherwise it is nonlinear.

3.3.1 Factors affecting adaptive filters

Adaptive filters could be affected by the following:

- Misadjusting: The parameter provides a quantitative measure of the amount by which the final value of the square error, averaged over an ensemble of adaptive filters deviates from MSE produced by Wiener.

- Rate of convergence: This has to do with the number of iterations required for the algorithm, in response to stationary inputs, to converge to the optimium Wiener solution in the MSE sense.

- Tracking: In a non-stationary environment, it tracks the statistical variations by rate of convergence or steady state fluctuation due to noise.

- Robustness: Small estimation error is caused by small disturbances. It could be internal or external to the filter.

- Computational Requirement: This is a result of size of the memory, the number of operations and the programming.

- Structure: Information structure determines the manner of implementation.

- Numerical properties: In implementing the algorithm numerically, inaccuracies are produced due to quantization errors, which poses a serious design error. The numerical stability and accuracy are thus very essential, such that numerical stability is an inherent characteristic of an adaptive filter while the numerical accuracy is determined by the number of bits of data and filter coefficient. Thus it is said to be robust in word-length used in its digital implementation.

3.3.2 Linear Adaptive filters

This involves a filtering process designed to produce an output in response to a sequence of input data. An adaptive process provides a set of parameters used in the filtering. The impulse response of the linear filter determines the filter's memory. The FIR and IIR are characterized by finite and infinite long but fading memory.

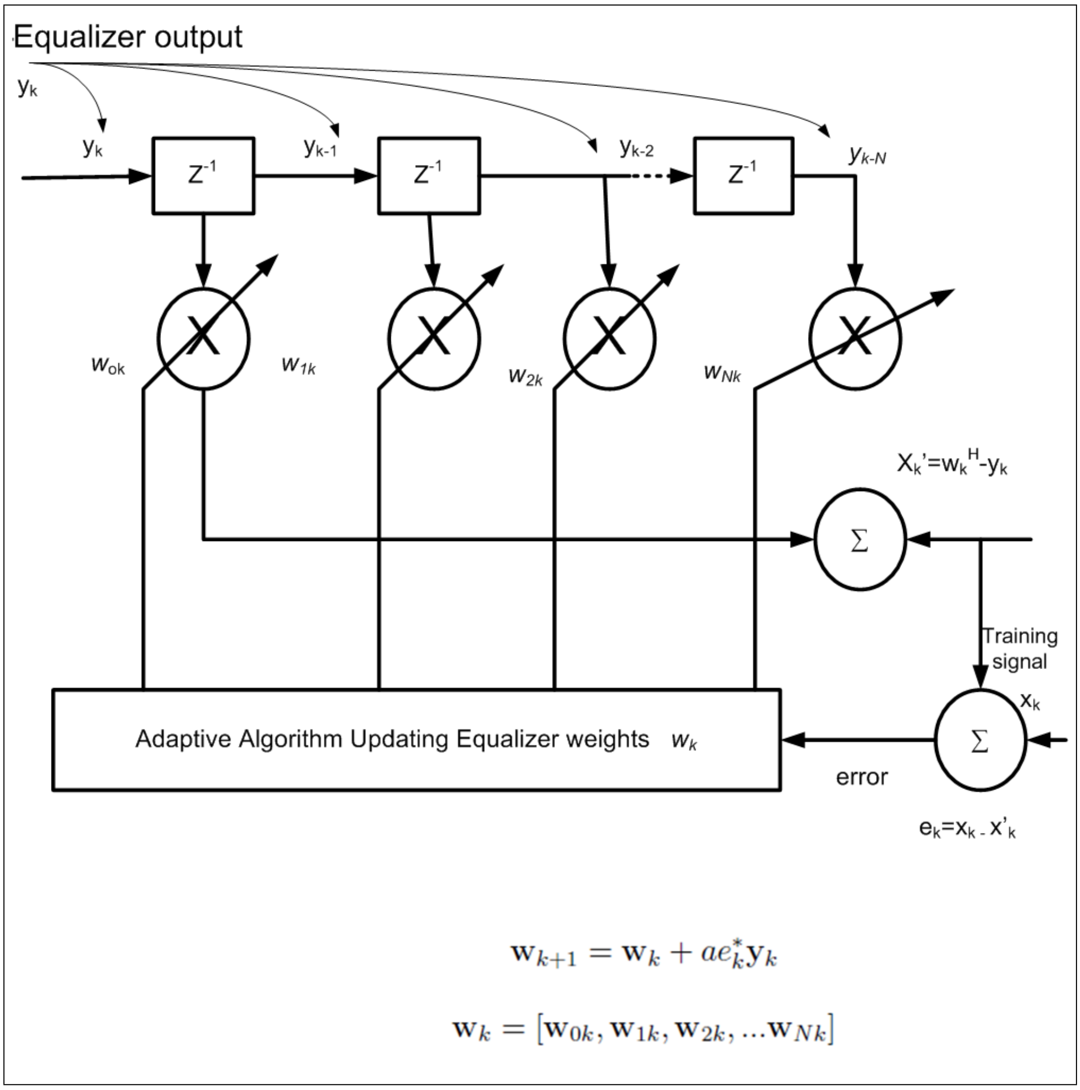

Figure 3.5: Adaptive Linear Equalize Model [8]

1. y_k = Equalizer input
2. w_k = Vector coefficient
3. X_k' = Equalizer output
4. e_k = Untrained error signal

3.3.3 Adaptive algorithm

Taking into consideration the equalization survey below: The adaptive algorithms, the LMS; RLS; RLS fast; etc. The approaches to developing linear adaptive filters can be deduced from the above block diagram. The challenges facing users of adaptive filtering is to understand the capabilities and limitations of various adaptive filtering algorithms and secondly the understanding in selecting the appropriate algorithm for a specific task. The stochastic gradient approach uses taped delay or transversal filters. The stationary input (MMSE) or the cost function is called the performance index to the achieved LMS.

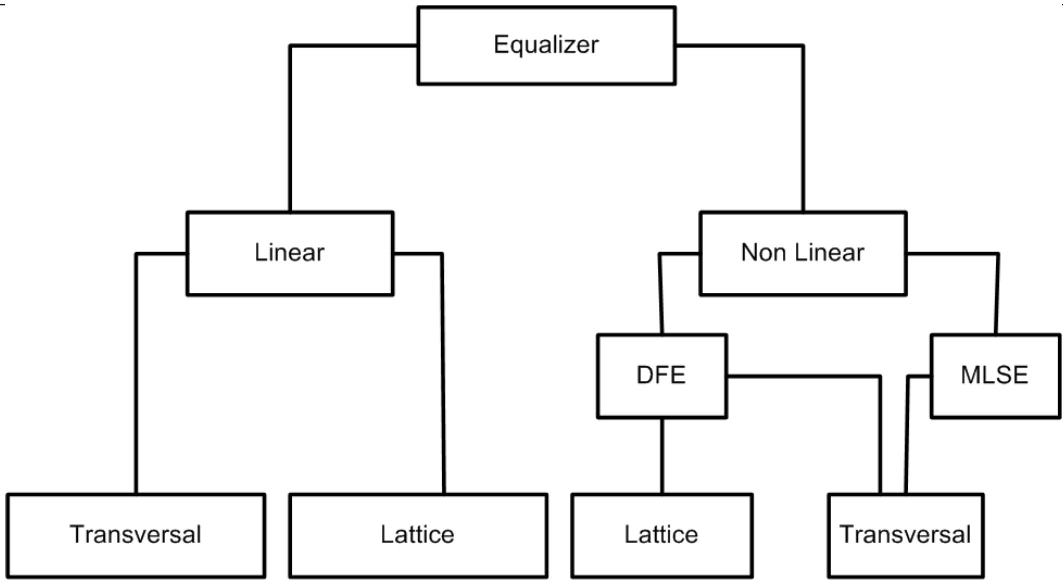

Figure 3.6: Equalizer Survey

3.3.4 Least square estimation (LMS)

This tends to the development of a linear adaptive filtering algorithm based on the method of least square to minimize the cost function or the error squares or the difference between some of the desired responses and that of the actual filter output. It could be explained as block estimation, whereby the update is arranged on a block by block basis.

In the recursive estimation (taped weight of transversal filter) they are updated on a sample by sample basis. Recursive estimate requires less storage than block by block and thus it is used more in comparison to the block by block type. The recursive least square estimation may be reviewed as a special case of Kalman filtering.

3.3.5 Adaptive Multiuser system

Multiuser system is defined as various ways in which multiple users' access common channel to transmit and receive information. The diagram below shows that each user has its unique set of coefficient signature, denoted as δ.

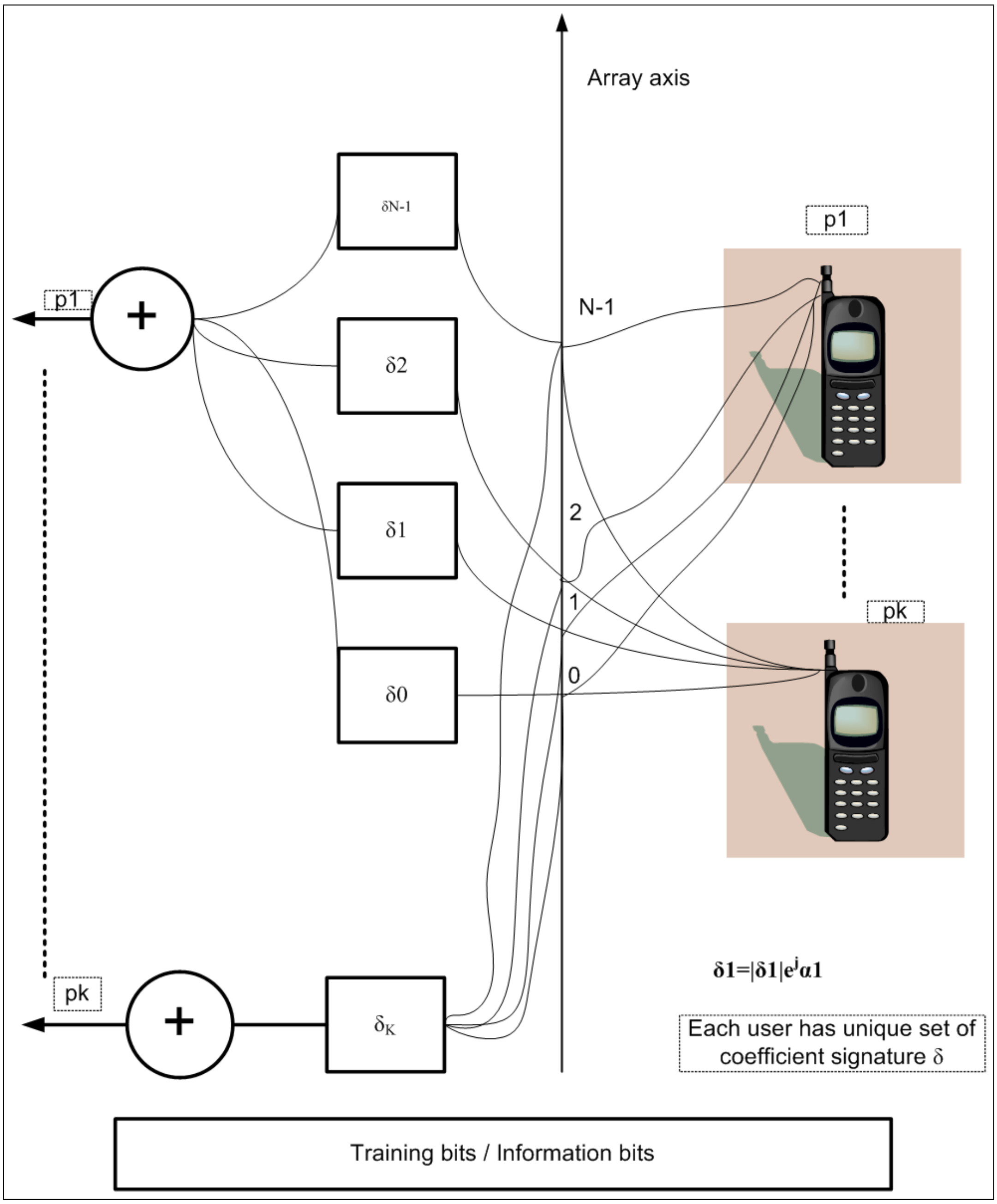

Figure 3.7: Adaptive Multiuser System [8]

1. δ = Users
2. $p1$ and pk = Transmission and Reception

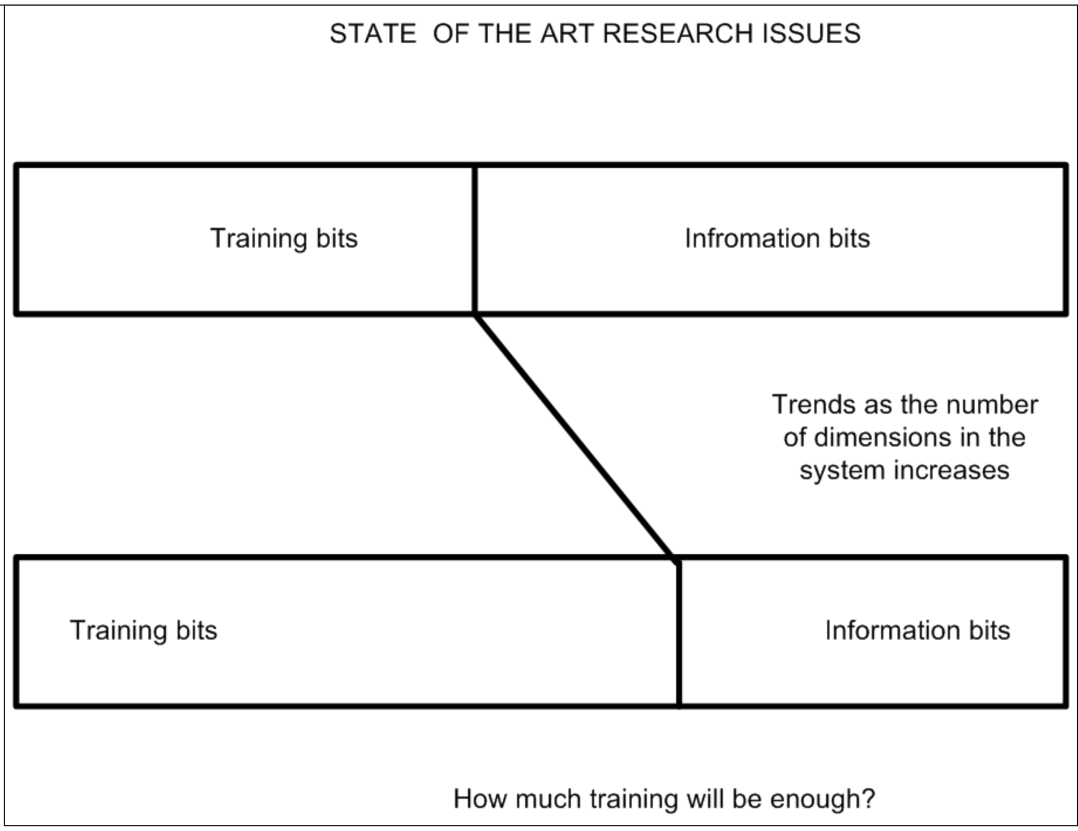

Figure 3.8: Current Issue

The current research issues are based on the Adaptive multiuser detection which is the basis of this research. It has to do with the training bits, information bits and how much training will be enough for a specific task? See figure 3.8.

3.3.6 Overview of the proposed Adaptive Multiuser Detection for MIMO OFDM Systems

MIMO-OFDM combines OFDM and MIMO techniques thereby achieving spectral efficiency and increased throughput. A MIMO-OFDM system transmits independent OFDM modulated data from multiple antennas simultaneously. At the receiver, after OFDM demodulation, MIMO decoding on each of the subchannels extracts the data from all the transmit antennas on all the subchannels. The block diagram of AMUD MIMO-OFDM system is shown in Figure 3.9.

Orthogonal Frequency Division Multiplexing (OFDM) is a wireless technology patented in 1970 which functions on the principle of transmitting data by dividing the data stream into smaller multiple parallel bit streams that have a much lower bit rate. These sub-streams are used to modulate several carriers. Although OFDM has been around since the 1960s, only recently has it been recognized as an outstanding method for high speed, bi-directional wireless network.

OFDM is a special form of multi-carrier modulation, which was originally used in high frequency military radio. An efficient way to implement OFDM is by means of a Discrete-time Fourier Transform (DFT) which was proposed by Weinstein in 1971 [48]. The computational complexity can be further reduced by a Fast Fourier Transform (FFT). However, OFDM was not popular at that time because the implementation of large-size FFTs was still too expensive, and thus not economically viable for communication systems. Recent advances in Very large scale integration (VLSI) technologies have enabled cheap and fast implementation of IFFTs and FFTs. In the 1980s, Cimini first investigated the use of OFDM for mobile communications [10]. Since then, OFDM has gained in popularity. In the 1990s, OFDM was adopted in the standards of Digital Audio broadcasting (DAB), Digital Video Broadcasting (DVB), Asymmetric Digital Subscriber Line (ADSL), and IEEE 802.11a. OFDM is also being considered in the new fixed broadband wireless access system specifications.

The concept of MIMO dates back to the early 1970s [34] [35]. Progress was not fast until the mid 1990s where the high demand for increased data rates over wireless channels made MIMO an important research topic. In 1999, the Shannon capacity of a fading Gaussian MIMO channel was demonstrated in a paper that became a trade mark in MIMO communication systems [32]. From this point on, the research of MIMO communication systems increased rapidly and every year an increased number of published papers in this area are noticed.

The channel capacity of multiple antenna systems is directly dependent on spatial correlation between the antenna elements of a multi-antenna node. Spatial correlation is a consequence of the narrow spacing between the antenna elements of a single node resulting in electromagnetic antenna coupling as experimentally reported in [36]. The spacing between antenna elements is defined in relation to the carrier wavelength of the wireless channel. It is noted that small spacing between the antenna elements of a system results in a poor channel capacity. According to the practical rule the spacing between the multi-antenna elements in a device has to be at least half a wavelength [37] in order to achieve spatial diversity.

The MIMO data signal transmission strategies in MIMO wireless communication systems are mainly defined by the transmit power control and transmit signal power allocation technique used on a MIMO system. The most common transmit power allocation strategy is the one stated in [32], called the "Uniform power distribution" transmission technique. All the antenna elements of the transmitter are allocated the same portions of the total available SNR to transmit. Waterfilling power distribution is the most effective transmission strategy for AMUD MIMO OFDM in terms of channel capacity and BER performance. Singular value decomposition [32][38] at the communication channel modal analysis is performed as stated in [39][38] and the modes are formed. The mode that offers the best wireless link (in the sense of highest singular value) is allocated with the majority of the available SNR.

There has recently been considerable interest in applying Orthogonal Frequency Division Multiplexing (OFDM) with Multiple-Input Multiple-Output (MIMO) technology to further enhance systems performance in BER and increased capacity. Under the assumption of instantaneous channel state information (CSI) at the transmitter, it is demonstrated that the adaptive transmitters were designed for the fading channels that are capable of achieving significant performance in BER and capacity improvement [25][27][28][68]. There are multi-dimensional parameters which can be adapted for radio resource allocation, such as power level, bit, subcarrier, space and user. Due to the fading independence of different users, an adaptive multiuser detection for MIMO OFDM is proposed to eliminate MAI.

Since MIMO OFDM depends crucially on AMUD for its application in this research, this section briefly examines the fundamental aspects and how they relate to the research. The main concept of MUD is to simultaneously detect digitally modulated data streams transmitted over a common channel from a number of different users, each of which is using a unique signature signal sequence. Signature signal sequences should be decorrelated in order to eliminate the inevitable interference between the transmitted signals of different users.

The optimal approach to MUD is via maximum likelihood sequence estimation (MLSE) [61]. However the complexity is non polynomial and subsequently unsuitable if the local cloud contains several users. A suboptimum approach is the MMSE based multiuser receiver having polynomial complexity, which is completely centralized [6].

AMUD enables decentralized detection with the advantage of linear complexity with BER and channel capacity performance equivalent to the one shot MMSE [4][6] approach. This is a situation corresponding in some respect to the single user detection problem and methods mentioned in [4][69] are necessary to mitigating MAI.

3.4 Proposed Adaptive Multiuser Receivers for AMUD MIMO OFDM

Adaptive Minimum Mean Square Error multiuser detection replaces the bank of match filters with MMSE filters for Maximum Likelihood computation to generate sufficient statistics at the receiver. This adopts an alternative approach to the conventional MMSE for detecting the signal that will use matched filter per signal by ignoring the cross-correlation between signals of different users. In the Adaptive filtering, the parameters of the filter continuously change due to the received training sequence from the transmitter, which will inform the receiver to adjust the parameters of its filters to match the desired signal. In the single user environment, every Match Filter maximum likelihood receiver plays the role of Adaptive MMSE maximum likelihood receiver [4][20].

An adaptive MMSE filter minimizes the error by an adaptive algorithm. A steepest decent algorithm was employed in the AMUD MIMO OFDM system to minimize the mean square error (MSE). In adaptive MMSE decode forward scheme bank of match filters were assigned to each receiver at relay or destination, which will eliminate the interference from other users, while in the amplify and forward, Adaptive MMSE is used only at the destination. For the simplicity of description we use fractionally spaced adaptive linear transversal filter for Adaptive MMSE detection, which is insensitive to the time differences in the signal arrival times of different users. Thus the receiver timing recovery is extremely simplified [4][65].

The Adaptive filter is in contrast to the multiuser receiver where the observation vector is not the output from the bank of matched filters, but the sampled signal itself. Consider the received signals symbols $y_1[n,k]$, $y_2[n,k]$ and $y_3[n,k]$ and let their general form for any node and any path in the network be $y_N[n,k] = r_n[m]$. where n is the specific number assigned to the signals at nodes. $\mathbf{y_1}[n,k]$, $\mathbf{y_2}[n,k]$ and $\mathbf{y_3}[n,k]$ received digital outputs symbol block from adaptive filters is $b'[n,k]$.

In a multi-cellular environment, the transmitter transmits information independently. Therefore, a non orthogonally transmitted signal from independent users arrives asynchronously at the receiver and the delay cannot be neglected [66][67]. Due to the non orthogonal nature of the spreading code, correlation will exist between the spreading codes at the receiver. The co-efficient of correlation is given by

$\mathcal{E}[\mathrm{r}_M[m]\mathrm{r}_N^*[m]]=\varrho(M,N) = R_{(M,N)} = \int s_M s_N dt$

and R correlation matrix is given by equation (3.19)

The digital output of the n^{th} filter for the m^{th} symbol period on relay or destination is given by

$$\mathrm{r}_n[m] = \mathrm{RH}\mathrm{x}_n[m] + \mathrm{v}_n[m] \tag{3.14}$$

Where H is matrix of respective channels.

The error between the reference signal and the output of the adaptive filter is

$$\epsilon = (\mathrm{x}_n[m] - \hat{\mathrm{x}}_n[m])$$

$$\epsilon = ([\mathrm{x}_n[m] - \mathrm{a}_n^H[m]\mathrm{r}_n[m]) \tag{3.15}$$

$\mathrm{a}_n^H[m]$ is M dimensional complex valued weight vector at m^{th} symbol time when the variable filter estimates the desired signal by convolving the input signal with impulse response.

$a_n[m] = [a_1, a_2......., a_M]$ M are tap of filter

and $r_n[m] = [r_1, r_2........., r_M]$. During the adaptation mode the weight parameters are adjusted such that mean square error J_{a_n} is minimized in m^{th} symbol time. m is associated with every term of the following equation but for simplicity of description it has been neglected

$$J_{a_n} = \mathcal{E}[\epsilon_n \epsilon_n^*] \tag{3.16}$$

from equation (3.15)

$$J_{c_n} = \mathcal{E}[(\mathrm{x}_n - \mathrm{a}_n^H \mathrm{r}_n)][(\mathrm{x}_n - \mathrm{a}_n^H \mathrm{r}_n)^*] \tag{3.17}$$

$$J_{c_n} = \mathcal{E}[\mathrm{x}_n \mathrm{x}_n^*] + \mathrm{c}_n^H \mathcal{E}[\mathrm{r}_n \mathrm{r}_n^H]\mathrm{c}_n - \mathrm{c}_n^H \mathcal{E}[\mathrm{r}_n \mathrm{x}_n^*] - \mathcal{E}[\mathrm{x}_n \mathrm{r}_n^H]\mathrm{c}_n \tag{3.18}$$

The first term in equation (3.15), represents the variance of the desired signal. The expectation $\mathcal{E}[\mathrm{r}_n \mathrm{r}_n^H]$ denotes M by N correlation matrix of the received signal given by

$$R = \begin{pmatrix} \varrho(1,1) & \varrho(1,2) & ... & \varrho(1,N) \\ \varrho(2,1) & \varrho(2,2) & ... & \varrho(2,N) \\ ... & ... & ... & ... \\ \varrho(M,1) & \varrho(M,2) & ... & \varrho(M,N) \end{pmatrix} \tag{3.19}$$

The matrix R is Hermitian and can be uniquely defined by specifying the values of the correlation coefficients $\varrho(M, N)$, where $\varrho(M, N) = \varrho^*(N, M)$

$$Z = \mathcal{E}[\mathrm{r}_n \mathrm{x}_n^*] \tag{3.20}$$

The expectation is M by N cross-correlation matrix vector between the received components and the reference sequence, and the expectation $\mathcal{E}[\mathrm{x}_{(n)}\mathrm{r}_{(n)}^H] = Z^H$.

where $Z^H = [z_1^*, z_2^*, ...z_M^*]$. The co-efficient z_i is given by $z_i = \mathcal{E}[\mathrm{r}_{(n)}\mathrm{x}_{(n)}^*]$ For stationary input and reference signals at the surface are obtained by plotting the mean square error $J_{(a_n)}$ versus the weight co-efficient has a fixed shape and the curvature i_{th} has a unique minimum point; the adaptive process seeks that minimum point at which the weight vector is optimal. Differentiating the mean squared error function $J_{(a_n)}$ with respect to each coefficient of the weight vector a_n yields the gradient ∇_n.

$$\nabla_n = \partial J(a_n)/\partial a_n = \begin{pmatrix} \partial J(a_n)/\partial a_1 \\ \partial J(a_n)/\partial a_2 \\ ..... \\ \partial J(a_n)/\partial a_M \end{pmatrix} \tag{3.21}$$

The optimal weight vector a_{opt} can be determined by setting the gradient ∇_n equal to zero,

$$\nabla_n = -2Z + 2Ra_n = 0 \tag{3.22}$$

where 0 is an M by 1 null vector at the minimum point of the error surface, the adaptive MUD is optimum in the mean squared error sense, and the equation can be simplified in the form $Ra_{opt} = Z$ which is the Wiener-Hopf equation or the normal equation, where the vector representing the estimation error is normal to the vector representing the output of the combiner. One possible solution of this equation is matrix inversion,

$$Z = R^{-1}a_{opt} \tag{3.23}$$

Another simple solution that does not require matrix inversion or explicit calculations of the correlation coefficients is the Steepest Descent Method. The Steepest

Descent Method is a recursive procedure that can be used to calculate the optimal weight vector a_{opt}. Let a_n and ∇_n denote the values of the weight vector and the gradient vector at time m, respectively. Then succeeding values of the weight vector are obtained by the recursive relation. After each symbol period m the weight of the filter is updated until the optimum coefficient gets its best cross correlation value. The filter can then go to decision directed mode where the coefficient will continuously change with the variation of the channel.

$$a_n = a_n - \mu \nabla_n \tag{3.24}$$

Where μ is a step size constant that controls stability and the rate of adaptation. If we express ∇_n in terms of instantaneous estimates $\hat{Z} = r_n x_n^*$ and $\hat{P} = r_n r_n^H$, then the equation can be simplified as

$$a_n[m+1] = a_n[m] + 2\mu r_n[m][x_n^*[m] - r_n^H[m]a_n[m] \tag{3.25}$$

which can be expressed in terms of $\epsilon_n^*[m]$ as,

$$a_n[m+1] = a_n[m] + 2\mu r_n[m]\epsilon_n^*[m] \tag{3.26}$$

where $m = 0, 1, 3........$ till a_{opt} is achieved.

$2\mu r_n[m]\epsilon_n^*[m]$ is the correction factor. The equation states that the updated weight vector is computed from the current weight vector by adding the input vector scaled by the complex conjugate value of the error and by μ which control the size of correction. Thus one can get an approximation by the optimum weight of the filter. All this computation done is during m^{th} symbol time of duration T_r such that $T_r > T$.

3.4.1 General System Model for AMUD MIMO-OFDM

The system has N_t transmit and N_r receive antennas and k sub-carrier in one OFDM block as shown in Figure 3.9. The channel between each pair of the N_t and N_r antennas are uncorrelated to each other. At time n, during transmission interval, a stream of binary bits b is coded into the N_t antenna symbol blocks. The signal on the k_{th} sub-carrier at the i_{th} antenna is denoted by $x_i[n,k]$, where $i = 1,...N_t$, $k = 0, ..., ..., K-1$, $n = 0, ..., N-1$. Though the figure shows MIMO OFDM with four transmit antennas, the scheme developed in this thesis can be directly applied to OFDM systems with any number of transmit antennas. The received signal N_r antenna j is:

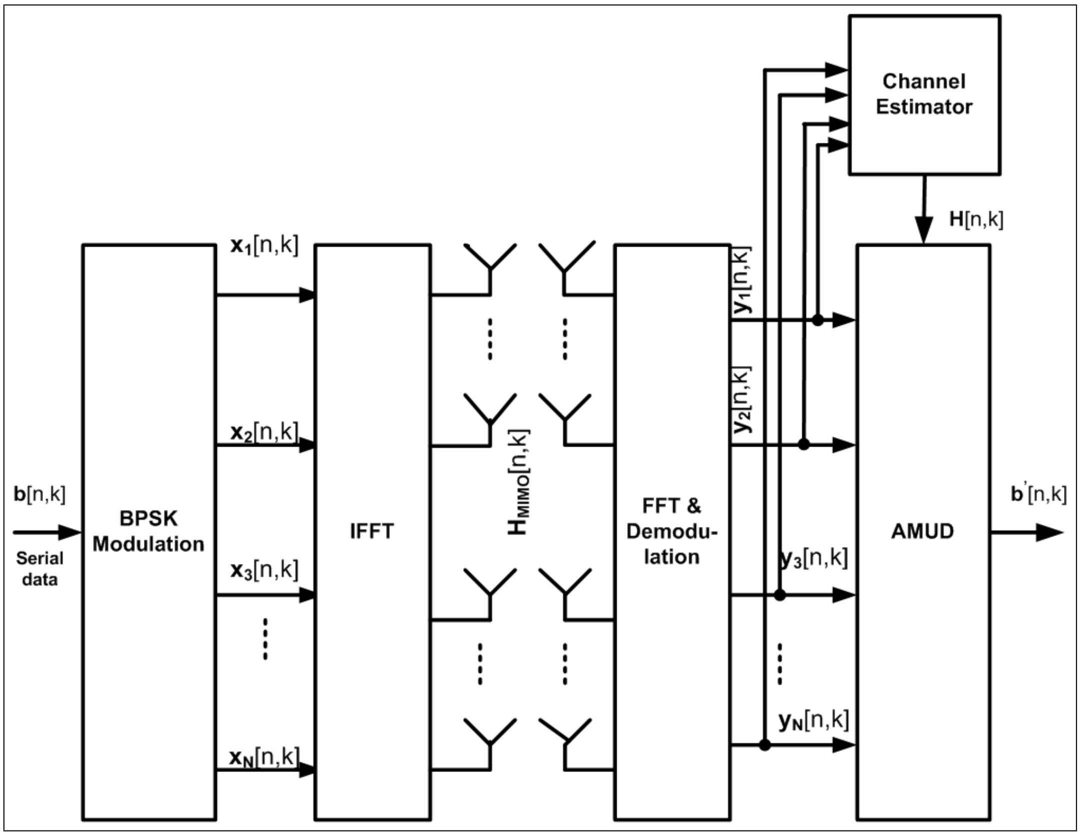

Figure 3.9: General System Model for AMUD MIMO OFDM

1. $b[n,k]$=block of OFDM symbols
2. $x[n,k]$=Transmit vectors
3. H_{MIMO}= MIMO channel
4. $y[n,k]$ = Received symbols
5. $b'[n,k]$ = Output symbols

$$y_j[n,k] = \sum_{i=1}^{N_t} H_{i,j}[n,k]x_N[n,k] + n_j[n,k] \tag{3.27}$$

where $H_{i,j}[n,k]$ is the channel frequency response between antennas i and j, $n_j[n,k]$ is the additive gaussian noise with zero mean and variance σ_n^2. The above equation can be written as:

$$\mathbf{y}_j[n,k] = \mathbf{H}_{i,j}[n,k]\mathbf{x}_N[n,k] + \mathbf{n}_j[n,k] \tag{3.28}$$

The equations above (3.27 and 3.28) were further developed as:

$$y_j[n,k] = \sum_{i=1}^{4} H_{ij}[n,k]x_i[n,k] + n_j[n,k] \tag{3.29}$$

Where $H_{i,j}[n,k]$ indicates the channel frequency response from transmitter i to receiver j at the k$_{th}$ tone of the OFDM block at time n and noise $n_j[n,k]$ is assumed to be zero-mean with variance σ_n^2 and uncorrelated for different $n's$, $k's$ or $j's$, $H_{ij}[n,k]$ denotes the channel frequency response for the k_{th} tone at time n, corresponding to ith transmit and jth receive antenna. The statistical characteristics of wireless channels are briefly described in this thesis. The vector form of OFDM input and output relationship are as follows:

$$\mathbf{y}[n,k] = \mathbf{H}_{i,j}[n,k]\mathbf{x}[n,k] + \mathbf{n}[n,k] \tag{3.30}$$

where

$$\mathbf{y}[n,k] \triangleq \begin{pmatrix} x_1[n,k] \\ ... \\ x_p[n,k] \end{pmatrix} \tag{3.31}$$

$$\mathbf{x}_1[n,k] \triangleq \begin{pmatrix} x_{2i-1}[n,k] \\ ... \\ x_{2i}[n,k] \end{pmatrix} \tag{3.32}$$

$$\mathbf{n}[n,k] \triangleq \begin{pmatrix} n_1[n,k] \\ ... \\ n_p[n,k] \end{pmatrix} \tag{3.33}$$

$$\mathbf{H}_{i,j}[n,k] \triangleq \begin{pmatrix} H_{2i}-1[n,k] & H_{2i}1[n,k] \\ \\ ... & ... \\ \\ H_{2i}-1p[n,k] & H_{2i}p[n,k] \\ \end{pmatrix} \tag{3.34}$$

The receiver first must estimate and correct for frequency offset and the symbol timing, e.g., by using the training symbols in the preamble. Subsequently, fast Fourier transformation (FFT) is performed per receiver branch. Spreading is done to increase resistance to natural interference and jamming that may prevent detection. AMUD detection was employed per OFDM subcarrier to recover the data signals transmitted on that subcarrier [21][3]. The symbols per transmit stream are combined, and finally detection is performed for the parallel streams and the resulting data are combined to obtain the signal.

3.4.2 Training for AMUD MIMO OFDM

Adaptive MIMO OFDM receivers require a training sequence, at the initial period, so that the receiver converges to its steady state, and thereafter it can be made to run in a directed mode. Adaptive MMSE is attractive as its computational complexity is similar to the MF receiver. The Adaptive MMSE ML receiver structure, where the bank of MF filters is replaced by bank of MMSE filter bank and thus does not require separate estimation of system parameters such as signal phase, signal amplitude and signal delay/timing. In training adaptive AMUD MIMO OFDM by employing MMSE, the fractionally spaced discrete time received sample vector $\mathbf{y}_j[n,k]$ of equation (3.27), chanel impulse responds $\mathbf{H}_{i,j}[n,k]\mathbf{x}_N[n,k]$ is represented by $\mathbf{Xb}$(n) and noise $\mathbf{n}$(n) at time n, over a running window of length (2p + 1), can be expressed in a matrix form as follows:

$$\mathbf{y}_j[n,k] = \mathbf{Xb}(\mathrm{n}) + \mathbf{n}(\mathrm{n}) \tag{3.35}$$

where $\mathbf{X}$ is the matrix of fractionally spaced sample signatures, vector $\mathbf{b}$(n) contains the transmitted symbols during that window period, and $\mathbf{n}$(n) is AWGN with covariance $\mathrm{E}\left[\mathbf{n}(\mathrm{n})\mathbf{b}^H(\mathrm{n})\right] = \sigma^2\mathbf{1}$. In order to simplify derivations, the symbol powers are normalized to one, $\mathrm{E}\left[\mathbf{b}(\mathrm{n})\mathbf{b}^H(\mathrm{n})\right] = \mathbf{1}$. This normalization does not mean equal signal power for all users, as the power of signatures might be different. The vector $\mathbf{b}(\mathrm{n})$ is expressed as

$$\mathbf{b}(\mathrm{n}) = \mathbf{b}_D\mathrm{n} + \mathbf{b}_U(\mathrm{n}) \tag{3.36}$$

where $\mathbf{b}_D\mathrm{n}$ contains known MIMO OFDM symbols with unknown symbols set to zero and $\mathbf{b}_U(\mathrm{n})$ contains unknown symbols with known MIMO OFDM symbols set to zero. Accordingly, the signature matrix $\mathbf{X}$ is split into two parts $\mathbf{X} = \mathbf{X}_D + \mathbf{X}_U$, where $\mathbf{X}_D$ consists of signatures corresponding to symbols in $\mathbf{b}_D(\mathrm{n})$ with signatures corresponding to unknown symbols being set to zero. Similarly, $\mathbf{X}_U$ corresponds to symbols in $\mathbf{b}_U(\mathrm{n})$. The filter coefficients are obtained by minimizing the mean square error (MSE), $\mathrm{E}\left[|e_k(\mathrm{n})|^2\right]$, where $e_k(\mathrm{n}) = b_k(\mathrm{n}) - \hat{b}_k(\mathrm{n}) = \mathbf{c}_{\mathrm{k}}^H(\mathrm{n})\mathbf{y}(\mathrm{n}) - \mathbf{d}_{\mathrm{k}}^H(\mathrm{n})\mathbf{b}_D$, and $\mathbf{c}_{\mathrm{k}}(n)$ is the MMSE FIR filter coefficient vector whose elements are defined in equation (3.27). There are other ways to obtain optimal coefficients $\mathbf{d}_{\mathrm{k}}$ and $\mathbf{c}_{\mathrm{k}}$ [20][8].

3.4.3 Proposed AMUD MIMO OFDM Channel Estimation

In AMUD MIMO-OFDM, the channel gain of the pilot-added subcarrier is first estimated by simply coherently multiplying the pilot symbol by its received signal. Since pilot symbols for each signal stream are added to every subcarrier at each time domain pilot slot, channel gains of other non-pilot-added subcarriers are estimated by using linear interpolation. Finally, the channel gain at each subcarrier is estimated by averaging over the OFDM pilot slots. AWGN power is estimated by averaging the residual power of the signal obtained by subtracting the received pilot signal replica formed by using the estimated channel from the received signal [66][2].

In AMUD MIMO OFDM, channel estimation error is caused by AWGN added at the receiver and multipath interference from the channel. Multipath interference causes channel estimation error by destroying the orthogonality among spreading codes in the coherent accumulation process in the linear interpolation process in

OFDM. In high SNR region, the channel estimation error due to multipath interference becomes more significant than AWGN, while in low SNR region, the channel estimation error due to AWGN is more significant.

The baseband representation of a mobile wireless channel impulse response as reported in [66] can be described by the partial knowledge of the channel at the transmitter leading to errors in the data transmission. Long distance communications or communications in an urban environment cause severe signal power attenuation and hence poor signal reception at the receiver side. Over a long period of time errors seem to follow a pattern. By statistical estimation of the variance of error it is possible to predict channel capacity [66].

$$\mathrm{h}(x,\tau) = \sum_{k} \mathrm{yk(x)c}(\tau - \tau_k) \tag{3.37}$$

where τ_k is the the delay of k_{th} path, $\mathrm{yk}(t)$ is the corresponding complex amplitude. Due to motion of vehicle, $\mathrm{yk}(t)'s$ are wide-sense stationary (WSS), narrow band complex Gaussian processes, which are independent for each path. The average powers of $\mathrm{yk}(x)'s$ depends on channel delay profiles, which is determined by the environment. The channel corresponding to different transmit and receive antennas in MIMO systems usually have the same delay profile. From the equation above, the frequency response at time x is

$$\mathrm{H}(x,f) = \int_{-\infty}^{+\infty} \mathrm{h(x},\tau)\mathrm{e}^{-j2\pi f\tau} d_{\tau} \tag{3.38}$$

then

$$\mathrm{C}(f) = \sum_{k} \mathrm{yk}(x)\mathrm{e}^{-j2\pi f\tau k} \tag{3.39}$$

where

$$\mathrm{C}(f) = \int_{-\infty}^{+\infty} \mathrm{c}(\tau)\mathrm{e}^{-j2\pi f\tau} d\tau \tag{3.40}$$

For OFDM systems, it can be seen from discussion in [66] that with tolerable leakage, the channel frequency response can be expressed as:

$$\mathrm{H}[n,k] = \mathrm{H}(n\Phi f, k\Delta f) = \sum_{l=0}^{k_o-1} \mathrm{h}[n,l] N_K^{kl} \tag{3.41}$$

In equation above $\mathrm{h}[n,l] = \mathrm{h}(n\Phi f, k\phi s/K)$, $N_K = exp(-j2\pi/K$, and K is the number of tones in an OFDM block. Φf and Δf are the block length and tone spacing respectively. While Φs is the OFDM symbol duration which is related to Δf by $\Phi s = 1/\Delta f$. In consideration of $\mathrm{h}[n,l]'s$ for l = 0, 1, ..., $K_o - 1$, are WSS, narrow-band complex Gaussian processes. The average power of $\mathrm{h}[n,l]$ and index $K_o(< K)$ depends on the delay profiles of the wireless channels.

3.4.4 MIMO OFDM Channel Capacity

As we have stated earlier, MIMO systems consist of transmit and receive antennas. It is considered a network with transmission paths connecting each input to output. From [1] the MIMO OFDM system capacity is:

$$C = log_2 \left[I_m + (\frac{p}{n})\mathbf{H}\mathbf{H}^H \right] b/s/Hz \tag{3.42}$$

Where C is the system capacity, H is complex transpose channel correlation matrix whose components are given by equation (3.27), transmitter i to receiver j at the k_{th} tone of the OFDM. The capacity formula for the MIMO OFDM is further developed as:

$$C = \mathcal{E} \left[\sum_{i=1}^{m} log(1 + \frac{p}{n})\lambda_{est} \right] b/s/Hz \tag{3.43}$$

Where λ_{est} is the complex transpose and $\mathcal{E}$ is an estimation of the capacity. p/n is SNR. Thus the capacity formula for MIMO OFDM is as shown below and the simulation result of channel capacity in Figure 4.4 based on the assumption that the channel matrix which consists of independent and identically distributed iid Rayleigh fading coefficients shows that the developed technology sum rate capacity in Figure 4.4.

$$C = log_2 \left[(1 + \frac{p}{n})\lambda_{est} \right] b/s/Hz \tag{3.44}$$

Thus the MIMO OFDM capacity formula is as shown below and the simulation of channel capacity in Figure.4.4 based on the assumption that the channel matrix which consists of independent and identically distributed iid, Rayleigh fading coefficients predicts that the developed technology system capacity is very close to the MIMO theoretical upper bound.

$$C = log_2 \left[(1 + \frac{p}{n}) \lambda_{est} \right] b/s/Hz \tag{3.45}$$

3.5 Summary

This chapter explains the different multiuser detection/receivers techniques stated in the literature survey as a benchmark to the proposed technique. This leads to the basic preliminaries of the thesis first contribution. It shows how the proposed technique was derived and the performance result will be explained in the next chapter. The basic system model for AMUD MIMO OFDM and its principle of operation was well explained in the chapter.

Chapter 4

Proposed AMUD MIMO-OFDM Performance and Simulations

4.1 Performance Comparison and Simulations

The linear relationship between the input and output of AMUD MIMO OFDM system (on a per subcarrier basis) is given, where the channel can be written as a random matrix with complex entries. The transmitter and receiver adapt dynamically to different channel conditions and interference environments leading to a higher reliability and spectral efficiency.

Simulation results shows that AMUD MIMO OFDM is spectrally efficient and outperforms conventional MIMO OFDM. Therefore, the new technique is a promising candidate for future wireless communications. The state of the art research was ensured such that its performance is discussed as a benchmark for thesis contribution. The performance evaluation criteria was well justified both mathematically and otherwise.

Typical urban and hilly terrain delay profiles with varied doppler frequencies were considered in these simulation results. The additive white Gaussian noise wireless channel is spatially uncorrelated with zero means and unit variance. The channel corresponds to different transmit and receive antennas, which have the same channel statistics. System parameters for the simulation are as shown in table below:

System Parameters	
Modulation	BPSK
Carrier Frequency	2.4GHz
Subcarriers	64
Partial channel state interference	Assumed
Channel Model	Rayleigh
Antenna numbers (Tx and Rx)	$(2\times2, 4 \times 4, 8 \times 8, 12 \times 12, 16 \times 16)$
Training/Payload	300/1000 bits
Data formation	1000/1300 bits
Spreading factor (Gain)	32
Cell Size (Length/width)	50/50m
Data Transmission period	16ms
symbol period for antenna	4ms
Target BER	10^{-5}

Table 4.1: Simulation Parameters

In the OFDM signal, entire bandwidth of 2.5MHz divided into 64 subchannels was assumed. To make orthogonal to each other, the symbol duration is $204.8\mu/s$, from the ISI due to multipath delay spread. BPSK modulation is used in the simulation, each data block contains 1000 bits of information, for example, OFDM with four transmit antennas can transmit four data blocks (4000 bits in total) in parallel, each time slot consists OFDM blocks, with the first block used as training and the following blocks used for data transmission. The described system can transmit 8Mb/s over the 2.50 MHz channel.

4.1.1 Results

A fair comparison is provided, were several system parameters were held at a constraint during the simulations. The achievable bit error rate of the following three cases:

- OFDM SISO systems.
- MIMO-OFDM systems.

- AMUD MIMO-OFDM systems

were compared using Monte Carlo simulation. Perfect channel state information is assumed. BPSK Modulation and flat fading models were used in the simulation. The configurations parameters that were considered for the OFDM simulation are; 64 subcarrier, 16 symbol time periods and 4 symbol period for antenna configurations $N_t = N_r$ = 2,4,8,12 and 16.

Figure 4.1 and Figure 4.2 shows the BER versus the SNR in dB of the SISO OFDM, MIMO OFDM and AMUD MIMO OFDM for antenna configurations $N_t = N_r$ =2,4,8, 12 and $N_t = N_r = 16$. The simulation results presented show that at an average BER of 10^{-4} with the antenna configuration of $N_t = N_r = 2$, AMUD MIMO OFDM performs better than other configurations, although their was a crossing in the initial stage which might be due to environmental issues, when the $N_t = N_r = 4$, MIMO OFDM perform better to others, however at low SNR less than (5dB), the AMUD MIMO OFDM performance is better than others. As the SNR increases, MIMO OFDM performance appreciates justifying the theory, taking into consideration the principles of the Maximum Ratio Combiner(MRC) on which MIMO operates. With antenna configuration 8×8, the AMUD MIMO OFDM provides a 2dB SNR gain to the conventional MIMO OFDM as shown in Figure 4.3. At reduced SNR and an increased number of antennas, AMUD MIMO OFDM has slightly better bit error rate to MIMO. This indicates the applicability of the AMUD to the uplink channel where power transmission at the mobile station is a constraint.

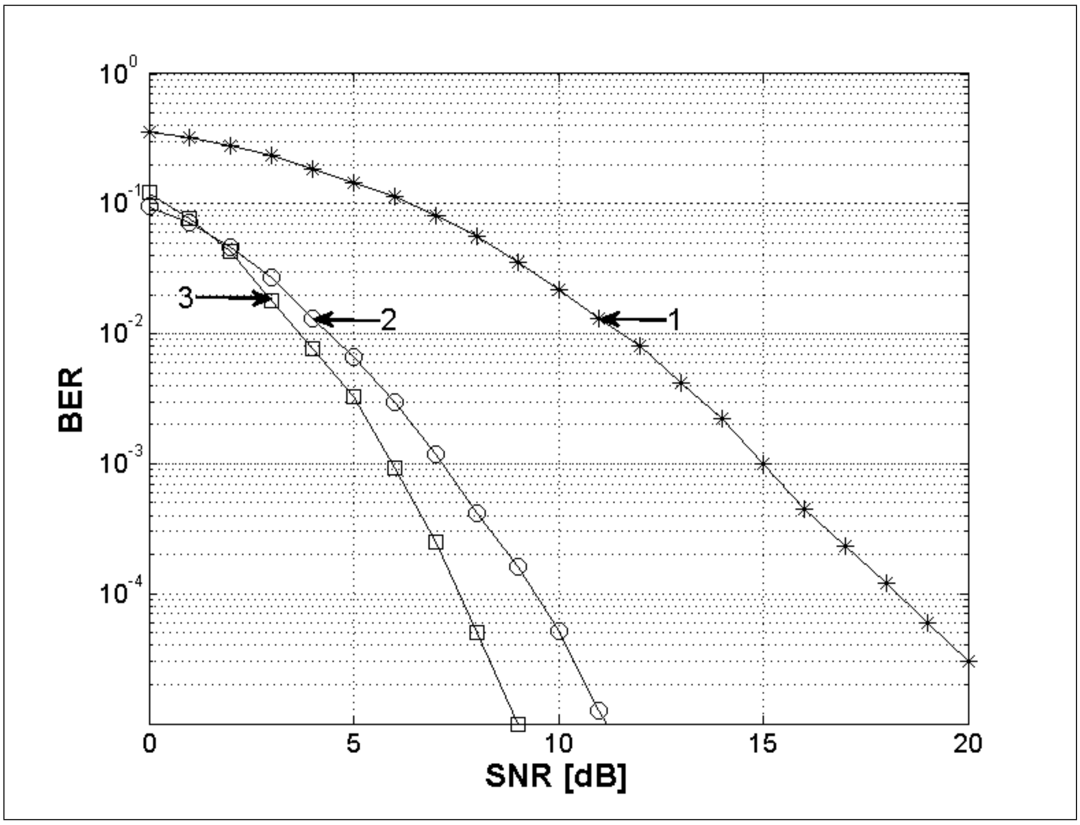

Figure 4.1: BER comparison of 2×2 OFDM MIMO and AMUD OFDM MIMO

1. OFDM SISO
2. OFDM MIMO
3. AMUD OFDM MIMO

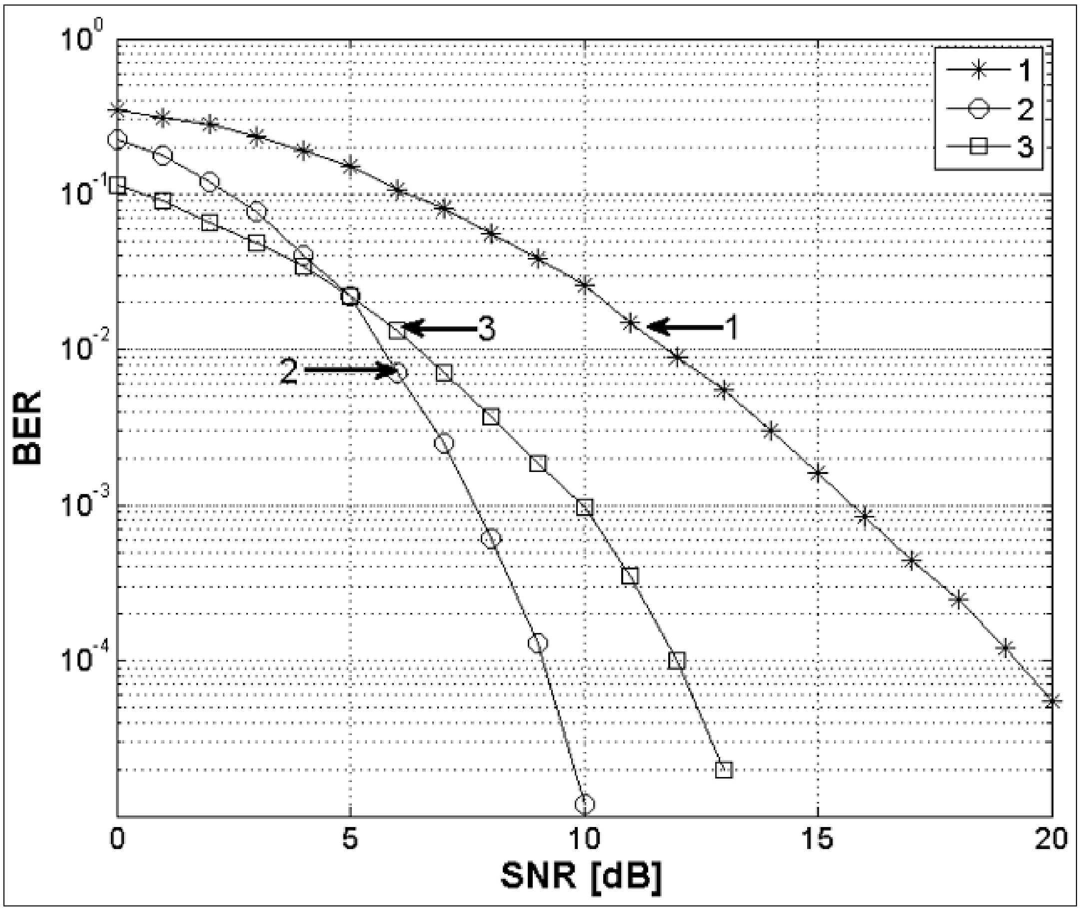

Figure 4.2: BER comparison of 4×4 OFDM MIMO and AMUD OFDM MIMO

1. OFDM SISO
2. OFDM MIMO
3. AMUD OFDM MIMO

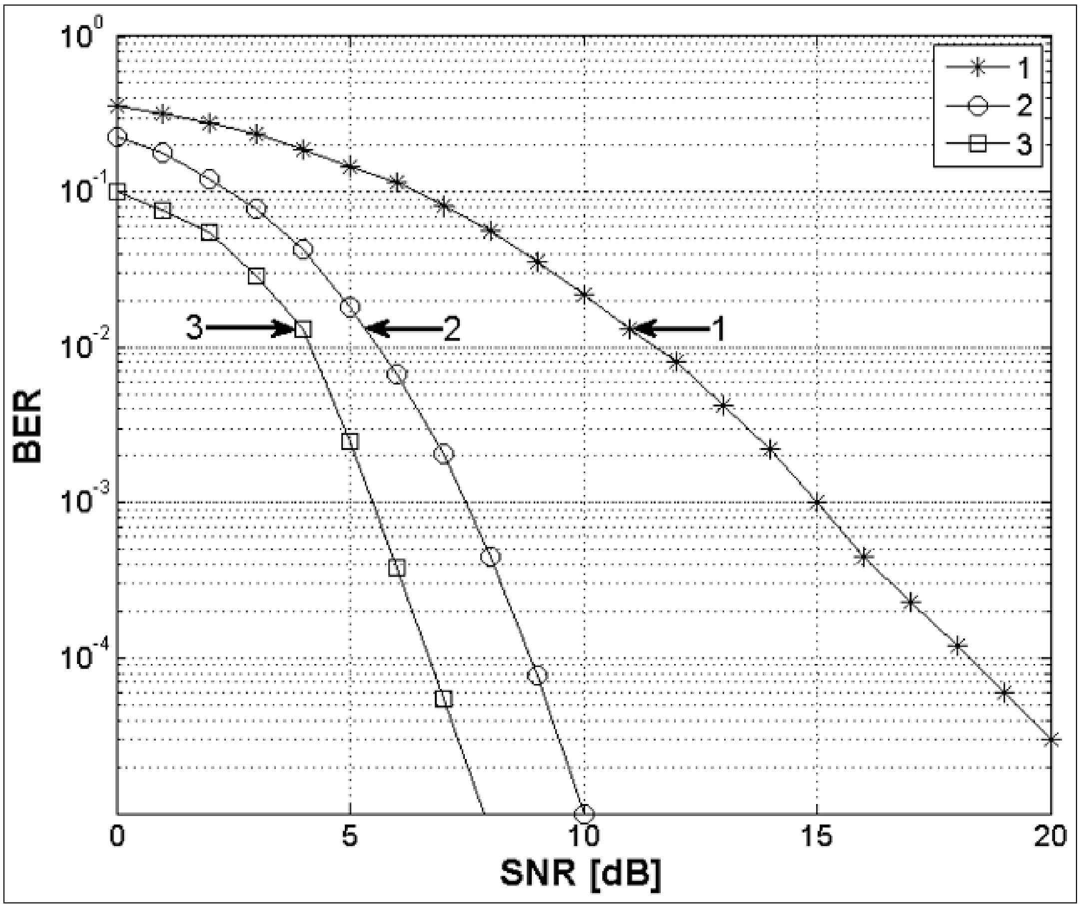

Figure 4.3: BER comparison of 8 × 8 OFDM MIMO and AMUD OFDM MIMO

1. OFDM SISO
2. OFDM MIMO
3. AMUD OFDM MIMO

With the higher MIMO 12×12 antenna configuration, the platform is intended for cooperative joint transmission and detection demonstrations for 3GPP LTE+, but it can also be used for other systems like future evolution of WIMAX and WLAN. The implementation results regarding signal processing performance and bandwidths are promising, it includes channel interpolation by Wiener filtering for each of the 144 transmit-receive antenna pairs, simulation parameters of the 12×12 configuration is the same with others and estimation of common phase error and SINR per resource block of 12 subcarrier. For parallelization, the computational load is divided into work units of 48 subcarrier covering 1 ms.

Figure 4.4 is the BER comparison of 12×12 OFDM SISO, OFDM MIMO and AMUD OFDM MIMO has a dB SNR gain, when compared to the conventional MIMO OFDM.

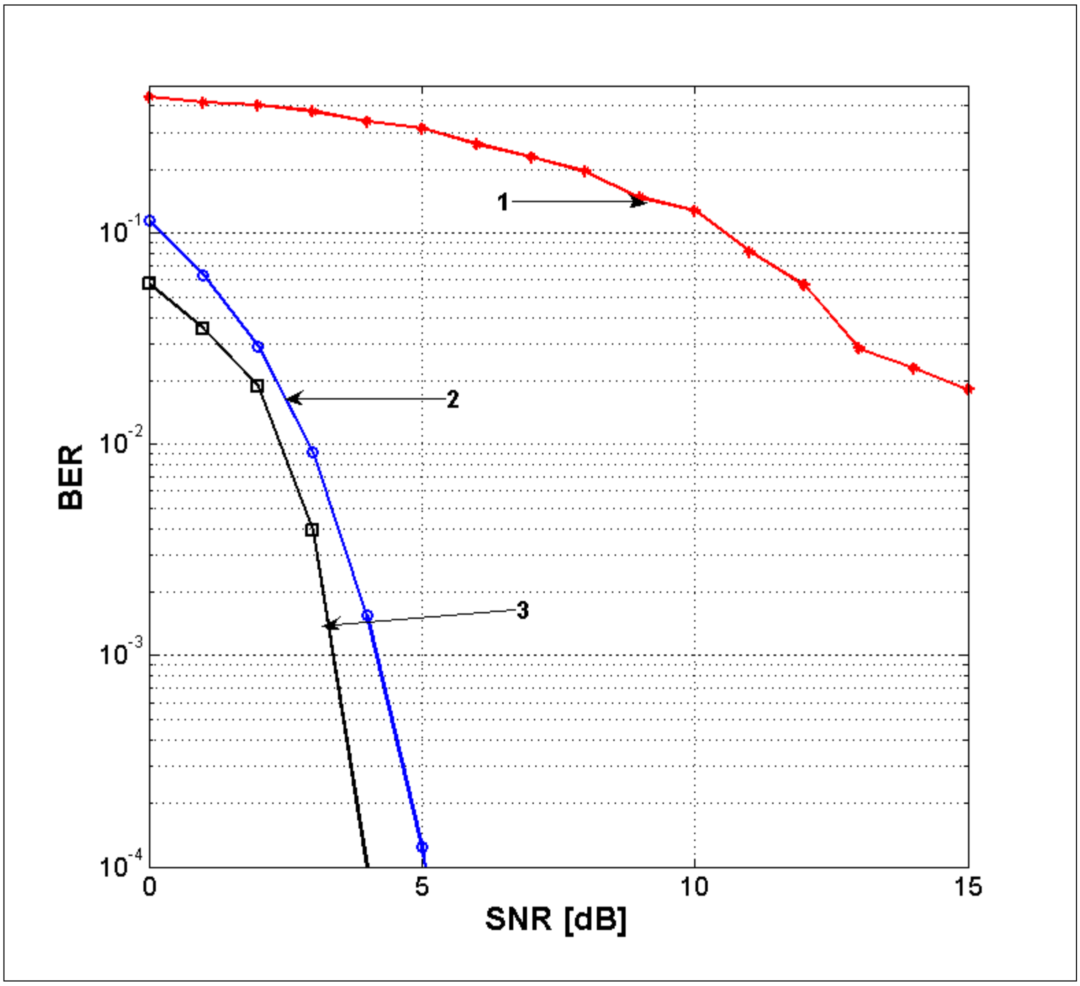

Figure 4.4: BER comparison of 12×12 OFDM MIMO and AMUD OFDM MIMO

1. OFDM SISO
2. OFDM MIMO
3. AMUD OFDM MIMO

In the higher MIMO 16×16 antenna configuration, just like in the 12×12, the platform is intended for cooperative joint transmission and detection demonstrations for 3GPP LTE+, but it can also be used for other systems like future evolution of WIMAX and WLAN. Following the same simulation parameters in the other antenna configurations a similar result to the 12×12 was achieved with lower SNR. Implementing the algorithm that provides best theoretical channel capacity might not always be feasible due to the computational complexity under real-time operation constraints. The simulation result of 16×16 provides a 3dB SNR gain by the new technique when compared to the conventional MIMO MOFDM, thus the higher the number of antenna configuration the better the performance.

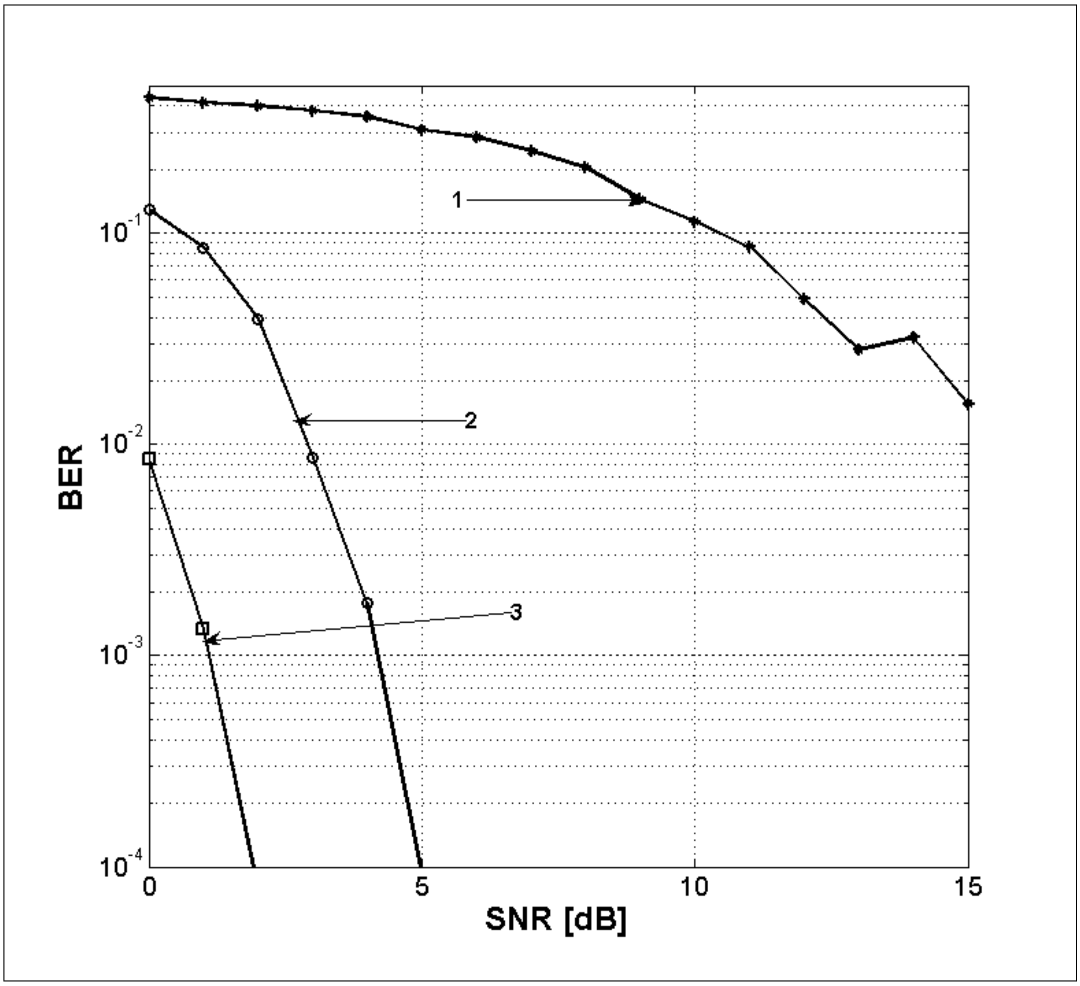

Figure 4.5: BER comparison of 16×16 OFDM MIMO and AMUD OFDM MIMO

1. OFDM SISO
2. OFDM MIMO
3. AMUD OFDM MIMO

The sample rate for a system that uses 20 MHz bandwidth has to be at least 40 MHz with I and Q channel having a resolution of 16 bit each. A 4x4-antenna system requires 256 I/O signals and a total bandwidth of 640 MB/s for either transmit or receive direction. 16×16-antenna system requires 1024 I/O signals and 2560 MB/s in either transmit or receive direction.

4.1.2 AMUD Capacity equation

The fundamental issues concerning the performance of adaptive MIMO OFDM systems and the behavior of the channel across frequency was considered. Focusing on wideband channel variations in the frequency domain, we have considered both outage and data rate metrics and derived exact results for their means and variances.

As i have stated earlier, MIMO systems consist of transmit and receive antennas, it is considered a network with transmission paths connecting each input to output.

Thus the capacity formula for this proposed scheme is as stated below [20] and the simulation of channel capacity is as shown in Figure 4.6 based on the assumption that the channel matrix which consists of independent and identically distributed (iid) Rayleigh fading coefficients shows that the proposed technology sum rate capacity in Figure 4.6 is very close to MIMO capacity upper bound. The capacity formula for adaptive multiuser detection by [20] is as follows :

$$C = log\left(\frac{1}{\sigma_e^2}\right) \tag{4.1}$$

The simulation result in Figure 4.6, is the sum rate capacity comparative results of the AMUD MIMO OFDM, MIMO OFDM and SISO OFDM schemes in bits/second/Hz, with the AMUD MIMO OFDM very close to MIMO capacity upper bound. The theoretical upper bound of MIMO system by Emre Telatar shows that the channel capacity (a theoretical upper bound on system throughput) for a MIMO system is increased as the number of antennas is increased, which is proportional to the minimum number of transmit and receive antennas. The case where the numbers of antennas at all the transmitters and receivers are equal. The SNR parameters play a key role in the upper bound and the lower bound.

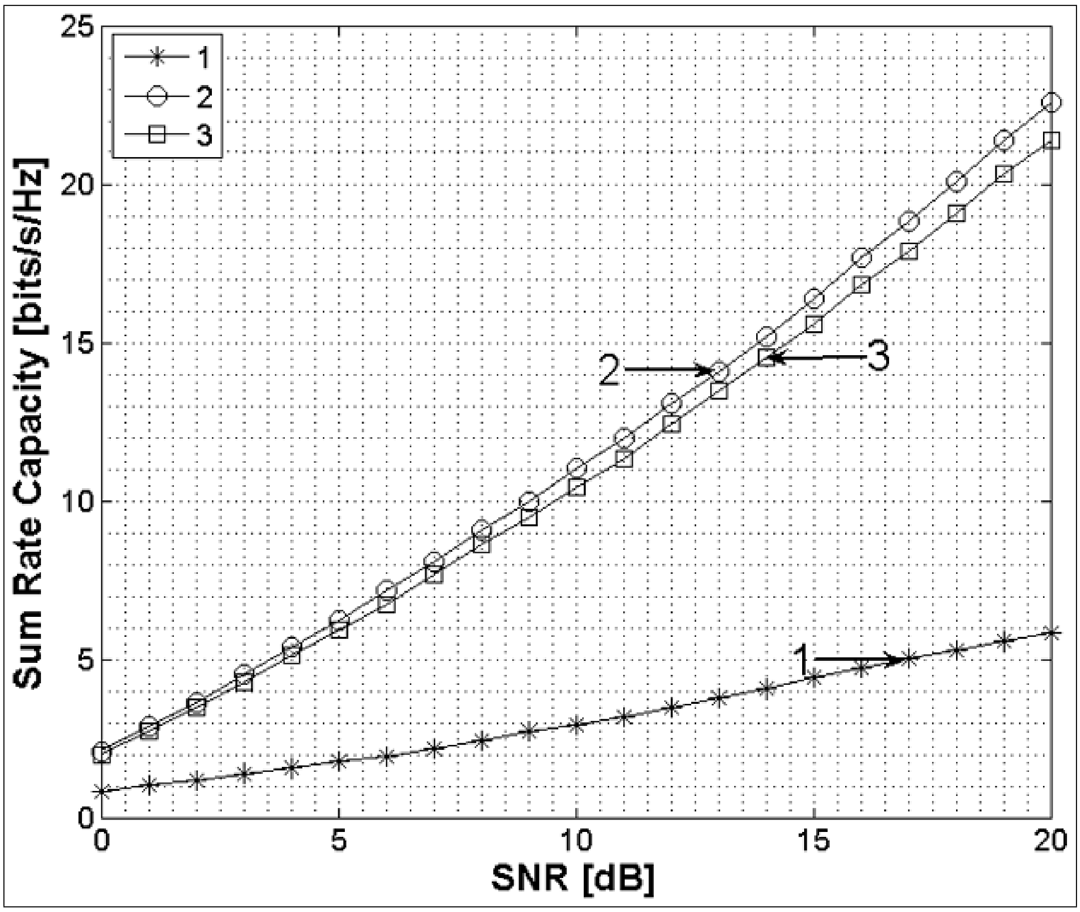

Figure 4.6: Information Capacity Comparison

1. OFDM SISO - Sum rate capacity
2. OFDM MIMO - Sum rate capacity
3. AMUD OFDM MIMO - Sum rate capacity

4.2 sumary

The achievable bit error rate of the following three cases (OFDM MIMO, OFDM SISO and AMUD OFDM MIMO) were compared using different antenna configurations, BPSK Modulation and flat fading channel models were used in the simulation. The results achieved shows that, as the SNR increases, MIMO OFDM performance appreciates justifying the theory, taking into consideration the principles of the Maximum Ratio Combiner(MRC) on which MIMO operates.

At reduced SNR and an increased number of antennas, AMUD MIMO OFDM has a better bit error rate to MIMO OFDM. This indicates the applicability of the AMUD OFDM MIMO to the uplink channel where power transmission at the mobile station is a constraint. The sum rate capacity comparative results of the AMUD MIMO OFDM, MIMO OFDM and SISO OFDM schemes in bits/second/Hz, shows that the AMUD MIMO OFDM sum rate capacity is very close to MIMO theoretical capacity upper bound. The results achieved shows that as the number of antenna increases, the new technique achieves a better performance result in BER and capacity.

Chapter 5

Information Capacity of the Communications Systems with Adaptive MMSE Receivers and MMSE DFE

5.1 Introduction

The introduction of mobile internet multimedia services (video and audio), compounded by increased demand for the existing mobile phone services, will require significantly increased information capacity from the mobile networks of the future. The information capacity of fixed (as opposed to mobile) communications has been increased rapidly by technological advances in the area of optical fiber communications and wireless. In mobile communications, the dominant physical carrier of information are still radio-waves, and there is a limited frequency spectrum available for mobile communications. There is a clear need to use available frequency spectra as efficiently as possible.

Implementation of adaptive antenna arrays (multisensor receivers) in cellular mobile communications has been considered by many authors as a promising way of increasing the information capacity of cellular mobile communication systems [70][71][72][73].

In [74] a zero forcing equalization approach is used to separate users of interest from Multiple Access Interference (MAI) based on different multipath-multiangle signal propagation for different users caused by different mobile terminal spatial positions. The presence of the thermal Gaussian noise is neglected for the sake of the analysis clarity. If the N-element antenna array is used, it is shown [74] that it is possible to accommodate N - 1 (times) more users in the cellular uplink system in comparison to the omnidirectional base-station antenna system. The exact quantitative analysis of the system information theoretic capacity was not considered.

The performance of adaptive equalizers suppressing ISI is given by the output minimum mean square error (MMSE). In section 5.1.3 the output MMSE is given for the optimum (Wiener solution) linear and decision feedback equalizer, ε_{opt} (5.17)

$$\varepsilon_{opt} = 1 - \mathbf{h}^H \mathbf{F}_u^{-1} \mathbf{h}. \tag{5.1}$$

Where h is the channel impulse response, and F_U is the channel correlation matrix which depends on the input signal to noise ratio and the channel impulse response.

Explanations and derivations are found in the section 5.3. The loss due to the adaptive nature of the receiver implementing the Least Mean Square (LMS) algorithm, provided that the algorithm had enough time to converge to its steady state, is given in section 5.3 by equation (5.47) [5].

$$\varepsilon_{(\infty)} = \frac{\varepsilon_{opt}}{1 - \sum_{i=1}^{2M+1} \alpha\lambda_i/(2-\alpha\lambda_i)} \tag{5.2}$$

Where α is the LMS algorithm step size and λ_i are the eigenvalues of the channel autocorrelation matrix. It should be noted that occasions may arise where the LMS algorithm has not converged to its steady state. Cases like this will be subject of future study[60]. The next analytical step is linking information capacity C of a system with MMSE receivers with the output MMSE in general and with reference to the result of equation (5.47). The capacity in terms of the output MMSE is given by equation (5.23) [4]

$$\mathrm{C} = \frac{1}{2} log \frac{1}{\varepsilon} \tag{5.3}$$

where ε is the output MMSE and the capacity C is the maximum data rate achievable with vanishingly small probability of error. The result on information capacity requires specific optimum modulation format. The symbol probability distribution should be Gaussian with infinite alphabet providing maximum input signal entropy for a given average power limitation, and then the optimum channel coding scheme (turbo coding) is being used. None of these are satisfied in the system of interest. The modulation scheme is 8 PAM [7][75] where three bits of information are mapped into the output symbol alphabets consisting of 8 equidistant amplitude levels. Since the modulation format is defined then a tighter upper limit for the capacity in terms of the output of MMSE is found, which is called the cutoff rate R_0.

5.1.1 System Model

The signal in additive white Gaussian noise may be expressed as

$$y_t = \sum_{i=M}^{M} a(i)h(t-iT) + n(t) \tag{5.4}$$

Where a(i) is the ith symbol, ht is the channel response, T is the inverse symbol rate and n(t) = $\sigma\omega(t)$ where $\omega(t)$ is normalized white Gaussian noise. The discrete time received sample vector **y** of equation (5.4) at time n, over a running window of length $(2p+1)$, can be expressed in a matrix form:

$$\mathbf{y}(n) = \mathbf{H}\mathbf{a}(n) + \mathbf{n}(n) \tag{5.5}$$

where **H** is the Toeplitz matrix obtained from the channel impulse response in order to present convolution as matrix multiplication. Symbols during that window period, $\mathbf{n}(n)$ is AWGN with covariance E$\mathbf{n}$(n)$\mathbf{n}^H$(n) $= \sigma^2\mathbf{I}$. The receiver structure consists of an adaptive symbol spaced finite impulse response (FIR) filter.

5.1.2 Information Capacity of a System With ISI

As a benchmark it is illustrative to find the capacity of channel with ISI [32][76]. The T- spaced received sample vector $\mathbf{y}(n)$ of length N at time n, is y(n) = Hb(n)+n(n), where the matrix H contains the symbol spaced channel response. Then the capacity formula of the channel is given by

$$\mathrm{C} = \frac{1}{2}log\left|\mathbf{I} + \frac{\mathbf{H}\mathbf{H}^H}{\sigma^2}\right| = \sum_{n=1}^{N} log\left(1 + \frac{\lambda_n}{\sigma^2}\right) \tag{5.6}$$

where $\lambda_n, n, ...N$, are the eignevalue of the matrix H$\mathbf{H}^H$. The non zero eigenvalues H$\mathbf{H}^H$ are also to the non zero eigenvalues $\mathbf{H}^H$H.

5.1.3 MMSE Optimum (Wiener Solution)

The mean square error for the symbol b(n) at time instant n is

$$\varepsilon = \mathrm{E}\{|e(n)|^2\} = \mathrm{E}\{|a(n) - \hat{a}(n)|^2\} \tag{5.7}$$

Although the transient behavior of $e(n)$ is important from the application point of view, we do not discuss the transient behavior for a while, and the variable n will be omitted. The symbol estimate $\hat{a}$ is obtained as $\hat{a} = \mathrm{f}^H\mathrm{y} - \mathrm{d}^H\mathrm{a}_D$. Then the MSE from equation (5.7) can be represented in the following form:

$$\varepsilon = \mathrm{E}(|\mathbf{f}^H(\mathbf{H}\mathbf{a} + \mathbf{n}) - \mathbf{d}^H\mathbf{a}_D - a|^2) \tag{5.8}$$

By substituting equation (5.41) into equation (5.8), we get:

$$\varepsilon = \mathrm{E}(|\mathbf{f}^H(\mathbf{H}\mathbf{a}_U + \mathbf{n}) - (\mathbf{d}^H - \mathbf{f}^H\mathbf{H})\mathbf{a}_D - a|^2) \tag{5.9}$$

After performing the indicated expectation the MSE becomes:

$$\varepsilon = \mathbf{f}^H\mathbf{F}_U\mathbf{f} - (\mathbf{f}^H\mathbf{h} + \mathbf{h}^H\mathbf{f}) + 1 + \mathbf{Q}_D \tag{5.10}$$

Where h = E$\{a$y$\}$ is the physical representation associated with a, equal in shape to the channel response. Without loss of generality we assume $\mathrm{h}^H\mathrm{h} = 1$. The channel gain is normalized to 1. Channel Correlation matrix F_U is given by:

$$\mathbf{F}_U = \mathbf{H}E\{\mathbf{a}_U.\mathbf{a}_U^H\}\mathbf{H}^H + \sigma^2\mathbf{I} = \mathbf{H}_U\mathbf{H}_U^H + \sigma^2\mathbf{I} \tag{5.11}$$

Q_D in Eq. (5.10) is a quadratic form defined by:

$$\begin{aligned}\mathbf{Q}_D = (\mathbf{d}^H - \mathbf{f}^H\mathbf{H})\mathrm{E}\{\mathbf{a}_D.\mathbf{a}_D^H\}(\mathbf{d}^H - \mathbf{f}^H\mathbf{H})^H \\ = (\mathbf{d}^H - \mathbf{f}^H\mathbf{H}_D)(\mathbf{d}^H - \mathbf{f}^H\mathbf{H}_D)\end{aligned} \tag{5.12}$$

Note that $\mathrm{E}(\mathbf{a}_D.\mathbf{a}_D^H)$ is an identity matrix. The equation defining the optimum receiver coefficient can be obtained from (5.10) by minimizing the MSE. Since $\mathbf{Q}_D$ is in a quadratic form, its minimum value will be 0. Setting

$$\mathbf{Q}_D = 0 \tag{5.13}$$

and taking derivatives of

$$\varepsilon = \mathbf{f}^H\mathbf{F}_U\mathbf{f} - (\mathbf{f}^H\mathbf{h} + h^H\mathbf{f}) + 1 \tag{5.14}$$

we get the equation for the optimum linear FIR filter coefficient in the form:

$$\mathbf{F}_U\mathbf{f}_{opt} = \mathbf{h} \tag{5.15}$$

By solving $\mathbf{f}_{opt}$ from equation (5.15) and substituting it into equation (5.13) we get the tentative decision aided coefficient sequence in the form:

$$\mathbf{d}_{opt} = \mathbf{H}_D^H\mathbf{f}_{opt} \tag{5.16}$$

The MMSE is then

$$\varepsilon_{opt} = 1 - \mathbf{h}^H \mathbf{f}_{opt} = 1 - \mathbf{h}^H \mathbf{F}_U^{-1} \mathbf{h}. \tag{5.17}$$

Equations (5.15), (5.16) and (5.17) define the optimum coefficient sequences $\mathbf{f}_{opt}$, $\mathbf{d}_{opt}$ and the MMSE ε_{opt}, for a general adaptive receiver structure under the condition that the matrix $\mathbf{F}_u$ is the time invariant [69][6][35].

For illustration purposes an equalizer with no ISI will be analyzed. It looks at first glance that there is little sense in analyzing an adaptive equalizer for the channel with ISI because the presence of ISI was the reason to introduce an equalizer in the first place. It should be mentioned here that an adaptive receiver (in this case called equalizer) plays a much wider role than the ISI elimination. Such roles are:

- Fine (AGC) Automatic Gain Control (besides a separate coarse system)
- Fine timing control (especially fractionally spaced equalizers)
- Carrier phase compensation.

5.1.4 Matched Filter Example

It is shown that in the absence of ISI the MMSE filter becomes the matched filter (MF). We start from equation (5.15),

$$\mathbf{f}_{opt} = \mathbf{F}_U^{-1} \mathbf{h} \tag{5.18}$$

But since there is no ISI matrix, $\mathbf{F}_U$ becomes:

$$\mathbf{F}_U = \mathbf{h}\mathbf{h}^H + \sigma^2 \mathbf{I} \tag{5.19}$$

With the matrix inversion lemma applied we have :

$$\mathbf{F}_U^{-1} = \frac{\mathbf{I}}{\sigma^2} - \frac{\mathbf{h}\mathbf{h}^H}{\sigma^2(\sigma^2 + 1)} \tag{5.20}$$

Then

$$\mathbf{f}_{opt} = \frac{\mathbf{h}}{\sigma^2 + 1} = \eta.\mathbf{h} \tag{5.21}$$

Where $\eta = \frac{1}{\sigma^2+1}$ is the gain factor of the matched filter. Thus, in the absence of ISI the MMSE filter becomes the matched filter (MF). The output MMSE becomes

$$\varepsilon_{MF} = 1 - \mathbf{h}^H \mathbf{f}_{opt} = \frac{\sigma^2}{1 + \sigma^2} \tag{5.22}$$

5.2 Information Capacity of a System With MMSE Receiver

The key part of this section is the following proposition. Proposition: The maximum mutual information over probability distribution of a, called information capacity, [32] [77][33] of the channel with the optimum MMSE filter is given by:

$$\mathrm{C} = \mathrm{I}_{max}(a;\hat{a}) = log\frac{E(a^2)}{E(e^2)} = \frac{1}{2}log\frac{1}{\varepsilon} \tag{5.23}$$

where ε is the average minimum mean square error. The received signal $\mathbf{y}$ contains information about a which is fed into linear digital adaptive FIR filter with coefficients $\mathbf{f}_{opt}$. The output of the filter is the sequence of symbols $\hat{a}$. Symbols $\hat{a}$ are optimum MMSE estimates of the transmitted symbols a. That is the coefficients $\mathbf{c}_{opt}$ are chosen such that $\varepsilon^2 = \mathrm{E}\{|\hat{a}_1 - a|^2\}$ is minimum. Eq. (5.7).

In [64] Lemma: The mean square estimation orthogonality principle with adjusted notation for the purpose of this research work, states: If the vector of coefficients $\mathbf{c}_{opt}$ is chosen to maximize the mean squared error $\mathrm{E}\{|\hat{a} - a|^2\}$, then the error signal $(\hat{a} - a)$ is orthogonal to the symbol estimate $\hat{a}$, in the following sense.

$$\mathrm{E}\{(\hat{a} - a)\hat{a}^2\} = 0 \tag{5.24}$$

Comment; If a, including other symbols from a are zero mean Gaussian, then:
a) â which is zero mean Gaussian, since it is a linear combination of zero mean Gaussian variables, which are the components of the vector a and the AWGN of n.
b) $(\hat{a} - a)$ is also a zero mean Gaussian.
Because $\hat{a}$ and $(\hat{a} - a)$ are zero mean Gaussian and orthogonal, they are mutually independent.

In [33] Lemma 2; Let p(a) be one dimensional distribution. The form of p(a) giving by the maximum entropy subject to the condition that the standard deviation of a can be fixed at σa which is Gaussian with the entropy $\mathrm{H}(a) = log\sqrt{2\pi e \sigma a}$
In [64] Lemma 3; for two independent $r.v$ α and β the following is true:

$$\mathrm{H}(\alpha/\beta) = \mathrm{H}(\alpha) \tag{5.25}$$

Knowing β does not change average uncertainty (information) about α, where the uncertainty is measured by the entropy (H(.)).

Lemma 4. For any two r.v α and β,

$$\mathrm{H}(\alpha, \beta/\beta) = \mathrm{H}(\alpha/\beta) \tag{5.26}$$

The entropy $\mathrm{H}(\alpha/\beta)$, of α when β is known, it will not change if β is added to the list of "unknown" variables. In other words adding known to the list of uncertain facts does not increase uncertainty.

The proof of proposition 1 consists of several steps invoking Lemma 1 to 4. The information about a when $\hat{a}$ is known, is given by:

$$\mathrm{I}(a;\hat{a}) = \mathrm{H}(a) - \mathrm{H}(a/\hat{a}) \tag{5.27}$$

Since $\mathrm{H}(a/\hat{a}) = \mathrm{H}(a - \hat{a}/\hat{a})$ from Lemma 4, then,

$$\mathrm{I}(a;\hat{a}) = \mathrm{H}(a) - \mathrm{H}(a - \hat{a}/\hat{a}) \tag{5.28}$$

Since $\hat{a}$ and $(\hat{a} - a)$ are mutually independent and Gaussian (Lemma 3.) then,

$$\mathrm{I}_{max}(a;\hat{a}) = \mathrm{H}(a) - \mathrm{H}(a - \hat{a}) = \frac{1}{2} log \sigma^2 a - \frac{1}{2} log \mathrm{E}(n_e^2) \tag{5.29}$$

$$\mathrm{C} = \mathrm{I}_{max}(a;\hat{a}) = \frac{1}{2} log \frac{1}{\varepsilon} \tag{5.30}$$

where signal power is normalized, $\sigma_a^2 = 1$ and $\mathrm{E}(n_e^2) = \varepsilon$. Observe that (5.30) has been derived under the general set of assumptions. It is noted that the assumption of stationarity is not an explicit or implicit condition to arrive at equation (5.30) .

Since the capacity could be formerly expressed in terms of the output signal to noise ratio (SNR),

$$\mathrm{C} = \frac{1}{2} log(1 + SNR) \tag{5.31}$$

Then

$$SNR = \frac{1}{\varepsilon} - 1 \tag{5.32}$$

Compare Eq. in [78]

5.2.1 Matched Filter Example Revisited

Equation (5.22) shows that in the absence of ISI the MMSE filter becomes MF and the quantitative measure for the output MMSE of the matched filter was given as:

$$\varepsilon_{MF} = \frac{\alpha^2}{1 + \sigma^2} \tag{5.33}$$

Then by using equation (5.30), the capacity of a power limited channel with the average signal power 1, and average noise power σ^2 where the information detection takes place after the matched filter becomes:

$$\mathrm{C}_{MF} = \frac{1}{2} log \left(1 + \frac{1}{\sigma^2}\right) \tag{5.34}$$

5.2.2 Adaptive MMSE Receivers

The linear MMSE equalizer is considered as a special case of the Decision Feedback Equalization (DFE) when all decision feedback coefficients are equal to zero. The output of MMSE filter at the nth symbol interval is

$$\mathrm{b}(n) = \sum_{m=-P}^{P} f(m) y_k(nT - mT) \tag{5.35}$$

where f(m) are the adaptive filters coefficients, T is the symbol interval. The total number of adaptive equalizer coefficients is $(2p + 1)$. The symbol estimate $\hat{a}(n)$ is obtained as:

$$\hat{a}(n) = b(n) - \mathbf{d^H}(n)\mathbf{a}_D(n) \tag{5.36}$$

where $\mathbf{d}(n)$ is a vector of decision aided coefficient sequences, defined as,

$$\mathbf{d}(n) = [d_1, d_2, ..., d_k]^T. \tag{5.37}$$

The elements of $\mathbf{d}(n)$ represent the weighting coefficients which multiply the respective known symbols. The vector $\mathbf{a}_D(n)$ contains symbols known to the receiver with unknown symbols set to zero. It is defined as:

$$\mathbf{a}_D(n) = [a(n+1), a(n+2), ..., a(n+K)]^T \tag{5.38}$$

The coefficients of $\mathbf{d}(n)$ and $\mathbf{f}(n)$ are obtained adaptively during a training period. After the training period, the coefficients $\mathbf{d}(n)$ and $\mathbf{f}(n)$ can be kept during data detection. Alternatively, in a decision directed mode, these coefficients can be updated by tentative decisions [4][8].

5.2.3 LMS Adaptive Algorithm

The following steps correspond to the LMS algorithm as stated in [4]:

$$\mathbf{f}(n+1) = \mathbf{f}(n) + \alpha_1 e^*(n)\mathbf{y}(n) \tag{5.39}$$

$$\mathbf{d}(n+1) = \mathbf{d}(n) - \alpha_2 e^*(n)\mathbf{a}_D(n) \tag{5.40}$$

for n $= 0, 1, 2, ...,$ where f(n) is the linear filter coefficient sequence and d(n) is the decision aided coefficient sequence, both at the n^{th} symbol iteration, and $(e)^*$ denotes conjugation, α_1 and α_2 being step sizes. Similarly, the Recursive Least Square (RLS) algorithm can also be used to provide faster convergence. The coefficients are updated once every symbol interval [60][4].

5.2.4 Training of the Adaptive MMSE Receiver

In order to simplify derivations, the symbol powers are normalized to 1, $\mathrm{E}\mathbf{a}(n)\mathbf{a}^H(n) = I$. The vector is expressed as:

$$\mathbf{a}(n) = \mathbf{a}_D(n) + \mathbf{a}_U(n) \tag{5.41}$$

where $\mathrm{a}_D(n)$ contains known symbols and $\mathrm{a}_U(n)$ contains unknown symbols. Accordingly, the channel matrix H is split into two parts $\mathrm{H} = \mathrm{H}_D + \mathrm{H}_U$, where H_D consists of channel responses corresponding to symbols in $\mathrm{a}_D(n)$ and the H_U correspond to the symbol in $\mathrm{a}_U(n)$. The filter coefficients are obtained by minimizing the MSE, $\mathrm{E}[|e^n|^2]$, where $e(n) = a(n) - \hat{a}(n)$, $\hat{a}(n) = \mathrm{f}^H(n)\mathrm{y}(n) - \mathrm{d}^H(n)\mathrm{a}_D$. There is a range of adaptive algorithms offering simple adaptive solutions [8] to obtain the optimal coefficients d and f.

5.3 Channel Capacity Loss due to Imperfect Estimation

The analytic and experimental results on the convergence rate for the LMS and other types of adaptive algorithms are given in [8] and references therein, in consideration of the channel capacity loss due to imperfect channel estimations by the LMS Adaptive Algorithm and the Excess MMSE. We present only a brief discussion on the convergence conditions and rate for the adaptive algorithm of the adaptive linear equalizer and concentrate on the properties relevant to the increase in the MMSE in comparison to the Wiener solution given by equation (5.17) .

The mean squared error $\varepsilon(n)$ converges to a steady-state value denoted by $\varepsilon(\infty)$, if and only if, the step size parameter α satisfies the following two conditions [8]. Condition 1:

$$0 < \alpha < \frac{2}{\lambda_{max}} \tag{5.42}$$

Condition 2:

$$\sum_{i=1}^{2M+1} \frac{\alpha\lambda_i}{2-\alpha\lambda_i} < 1 \tag{5.43}$$

Where λ_1 are the eigenvalues of the channel correlation matrix F_U, and $2M+1$ is the number of filter coefficients; λ_{max} is the largest eigenvalue of F_U. When these two conditions are satisfied, the LMS algorithm is convergent in the means square. When the two conditions above are satisfied, the LMS algorithm becomes convergent in the means square. If condition 1 is satisfied, then condition 2 can be replaced by a weaker form:

$$\sum_{i=1}^{2M+1} \frac{\alpha\lambda_i}{2} < \sum_{i=1}^{2M+1} \frac{\alpha\lambda_i}{2-\alpha\lambda_i} < 1 \tag{5.44}$$

Eq.(5.44) can be written as

$$\alpha < \frac{2}{\sum\limits_{i=1}^{2M+1} \lambda_i} = \frac{2}{P_t} \tag{5.45}$$

since from [8],

$$\sum_{i=1}^{2M+1} \lambda_i = \mathbf{tr}(\mathbf{F}_U) = P_t \tag{5.46}$$

Where P_t is the total input power. Eq.(5.45) shows that the convergence speed of the adaptive algorithm is limited by the total received signal power contained in the receiver observation vector. If the time span of the received signal is larger, the convergence rate of the LMS algorithm decreases, under the condition that other parameters are equal. An additional convergence speed reduction occurs when there is a significant ISI caused by uneven amplitude transfer characteristics of the channel, with possible deep attenuation in certain ranges of the channel frequency band. Better results, in some cases of interest, could be achieved by faster adaptive algorithms [8].

$$\varepsilon(\infty) = \frac{\varepsilon_{opt}}{1 - \sum\limits_{i=1}^{2M+1} \alpha\lambda_i/(2 - \alpha\lambda_1)} \tag{5.47}$$

Eq. (5.47) shows that the steady state error is proportional to the number of eignevalues. The convergence speed is an important parameter since it determines the multipath fading rate (channel time variations) that can be handled successfully. What MMSE can be achieved by given adaptive convergence speed is determined by the existing training sequence length as well. By knowing the MMSE, then the ultimate system information capacity can be obtained based on the results in the next section.

5.3.1 Adaptive modulation with constant power and MMSE-DFE equalizer

In this section, we propose and investigate a modulation switching protocol based on the SNR at the equalizer output with an unbiased decision rule. In fact, it was shown in [79] that the channel capacity, for any ISI channel, depends on the optimized SNR at the unbiased MMSE-DFE equalizer output. Cioffi et al in [79] affirm that the best limit on the achievable data rate is determined by the SNR-DFE, U and is independent of any other parameter. The relationship between channel capacity and the SNR-DFE, U is given by

$$log\frac{1}{\varepsilon_{MMSE-DFE}} = \int_0^W log\left[\frac{S_a(f)}{N_0}|S_{hh}(f)|^2 + 1\right] df \tag{5.48}$$

5.4 MMSE-DFE Capacity Comparison

The equation (5.17) is the result for the DFE MMSE in time discrete domain. The equation could be used to calculate the information capacity achievable by DFE receiver and it could be shown that the ideal MSE-DFE is the information capacity achievable (canonical) device [80]. For the sake of comparison with multicarier modulation, where the frequency representation is used, it is more appropriate to use the expression for DFE MMSE in [80][81][79].

$$log\frac{1}{\varepsilon_{MMSE-DFE}} = \int_0^W log\left[\frac{S_a(f)}{N_0}|S_{hh}(f)|^2 + 1\right] df \tag{5.49}$$

where $S_a(f)$ is the average symbol power spectral density, $(S_a(f) = 1)$ in our case. In general, $S_a(f) = 1$ does not have to be a constant. However, if the symbol sequence is uncorrelated then $(S_a(f) = 1)$ is constant and without loss of generality it can be assumed to be 1. AWGN spectral density is denoted by N_0 and $S_h(f)$ is the fourier transform of the channel response h autocorrelation function.

$$C_{MMSE-DFE} = \int_0^W log\left(1 + \frac{S_h(f)^2}{N_0}\right) df \tag{5.50}$$

5.4.1 Simulation results

The computer simulation presented in [7] for classical adaptive combining, the step size is usually very small or according to the power of received signal and Wiener solution, however the inverse variance factor in step size tends to produce accurate weight estimate. Adaptive filter convergence involves signal to noise ratio which was analyzed mathematical by Wiener's filter solution. The average mean square error performance of classical LMS, were presented by the LMS and RLS algorithms in Gaussian channel and the convergence of LMS and RLS algorithm are very fast. In the simulation, 50 to 60 bits iterations are enough for steady state of adaptive combining. However the equations stated in the graph legend is used to demonstrate to generate it in mat-lab and the convergence of RLS algorithm is faster than proposed LMS algorithms. The noise variance are unity, therefore, the performance is equal and the convergence of proposed LMS algorithm is close to that of the RLS.

The classical scheme converge into steady state by requiring very long training for a more accurate and better convergence. Equation (5.49) is the Shannon capacity formula with average power constraint [7]. The developed tool analyzes the capacity performance of MMSE estimation and the adaptive filter in a two channel environment.

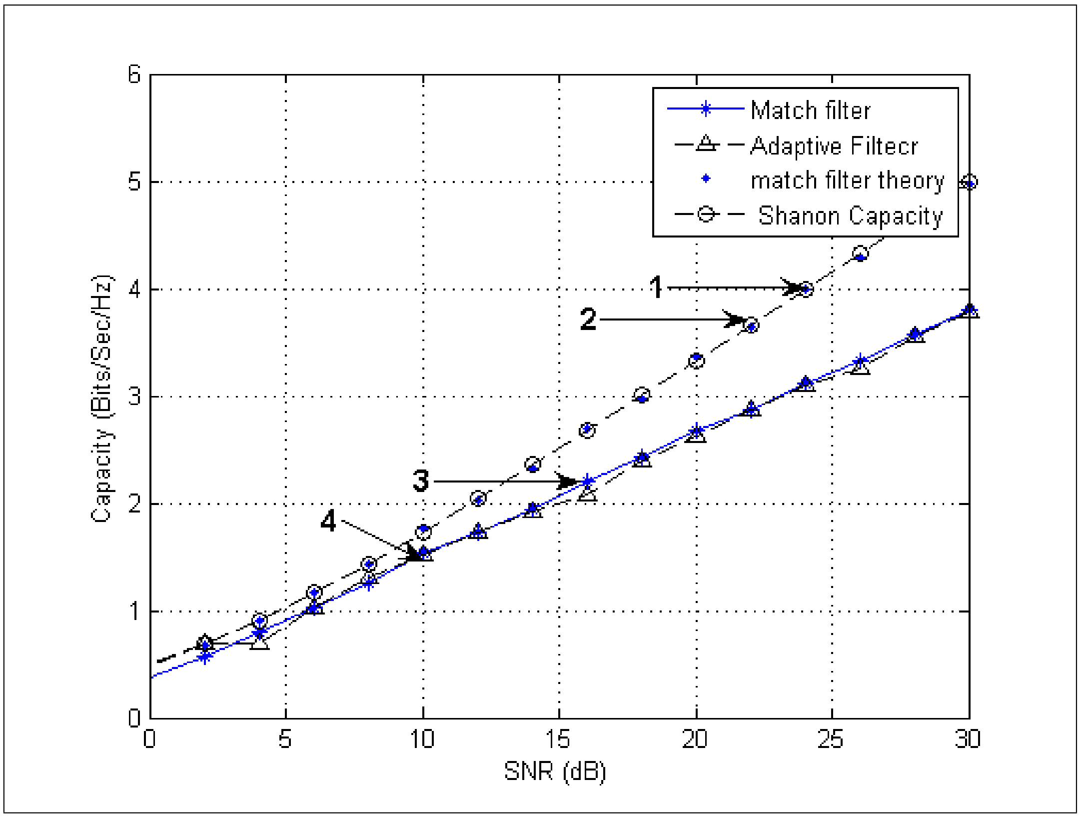

Figure 5.1: Information Capacity comparison

1. MF Theory (5.22)
2. Shannon Capacity Theory (5.6).
3. MF simulated (5.34)
4. Adaptive simulated (5.23, 5.30)

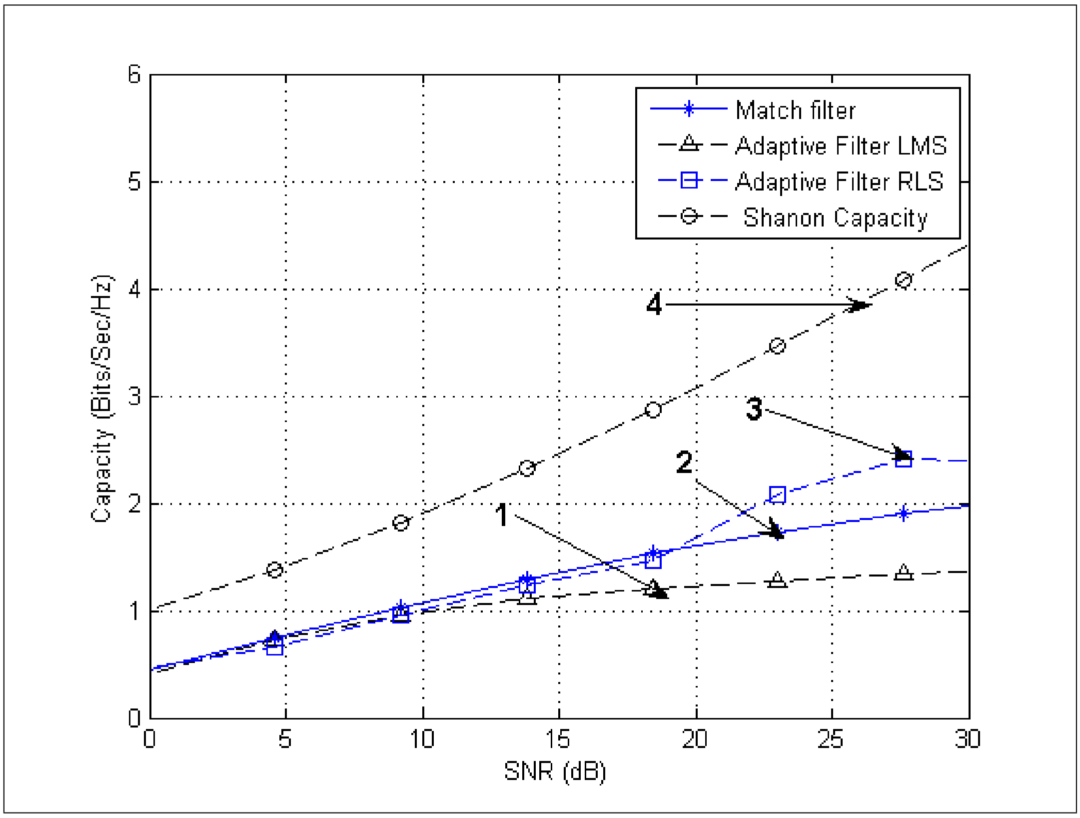

Figure 5.2: Information Capacity comparison

1. Adaptive filter LMS
2. MF simulated (5.22)
3. Adaptive simulated RLS (5.23, 5.30)
4. Shannon Capacity theory (5.6)

Figure 5.1 shows the theoretical capacity results of Shannon and the match filter overlapping. The simulated result for the BPSK bench mark of the matched filter and adaptive filter in a Gaussian channel indicates that the performance of the adaptive algorithm for the AWGN channel is equal to that of the MF of the same channel. The adaptive filter works better for that channel by employing the Least mean square (LMS) algorithm.

Figure 5.2 shows that the theoretical capacity results of Shannon and the match filter overlaps, BPSK modulation was used in both MF and the adaptive filter in a flat fading Raleigh channel, using least mean square (LMS) algorithm and the result obtained is poor due to the Raleigh channel. Introducing the RLS to the system, improves the performance as compared to the match filter which is used as a good reference to measure the performance of adaptive filter's algorithms, see Figure 5.3. As we have stated earlier, MIMO systems consist of transmit and receive antennas, it is considered a network with transmission paths connecting each input to output.

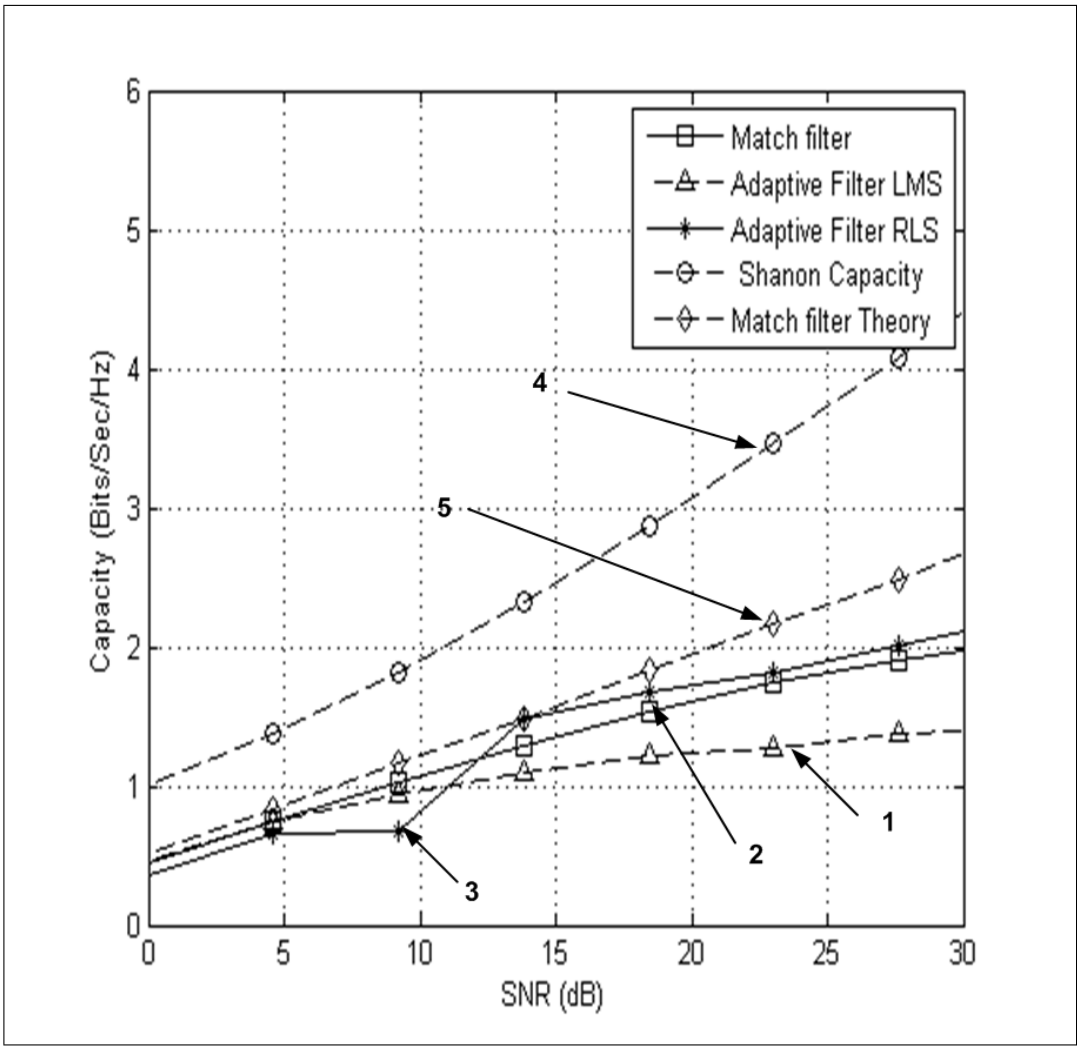

Figure 5.3: Information Capacity comparison

1. MF simulated (5.22)
2. Adaptive filter LMS
3. Adaptive simulated RLS (5.23, 5.30)
4. Shannon Capacity theory (5.6)
5. Matched Filter theory (5.22)

5.5 sumary

A mathematical analysis and simulation results to estimate the quality of digital communication systems was achieved. However, more fundamental measure is the maximum information rate at which the communication is possible with vanishingly small error called information channel capacity. Due to uncertainty, as proved by shannon, an adaptive system is employed to eliminate excess error. The capacity of a channel with intersymbol interference (ISI) and minimum mean square error (MMSE) receiver, with error due to small capacity lose, was achieved by adaptive system in exchange for easy implementation.

Chapter 6

Adaptive Information Capacity of Mobile Communication Systems with MMSE DFE and OFDM Receivers

6.1 Introduction

The information channel capacity is a fundamental measure of estimating the quality of a digital communication channel with vanishingly small probability of bit error, showing that the capacity of a stationary channel with inter-symbol interference (ISI) is achievable by both the single carrier modulation with ideal MMSE-DFE receiver and multi-carrier modulation over narrow sub-channels with OFDM receivers.

The input-output mutual information is an indicator of how much coded information can be pumped through a channel reliably given a certain input signaling, whereas the MMSE measures how accurately each individual input sample can be recovered using the channel output. Interestingly, the strong relevance of mutual information to estimation and filtering is by providing a non-coding operational characteristic for mutual information [32] [82]. The input-output mutual information can be expressed as a time-integral of the causal MMSE. This also points to a simple proof of the result that Gaussian inputs achieve capacity by observing that the linear estimation upper bound for MMSE is achieved for Gaussian inputs [83].

IEEE 802.11 wireless Local Area Network standards employ OFDM, which offers high spectral efficiency and superior tolerance to multipath fading. In OFDM, the computationally efficient Fast Fourier Transform [10] is used to transmit data in parallel over a large number of orthogonal subcarrier which is maintained in a frequency selective fading channel [11].

This work introduces a new technique AMUD in cellular mobile communications has been considered by many authors [4][60]as a promising way of increasing the information capacity of cellular mobile communication systems to improve the performance of the equalizer, feedback error elimination by forward error correction and in designing the equalizer with a minimum mean square error (MMSE) criterion. The time domain DFE allows the elimination of inter-symbol interference (ISI) based on previous decisions and thus improves performance over linear equalization. It will explicitly assume the feed-forward equalization in the frequency domain, which enables a low complexity solution.

6.1.1 System Model

The signal in additive Gaussian noise may be expressed as

$$y_t = \sum_{i=-M}^{M} a(i)h(t - iT) + N(t) \tag{6.1}$$

where a(i) is the ith symbol, ht is the channel response , T is the inverse symbol rate and $N(t) = \sigma w(t)$, where $w(t)$ is normalized white Gaussian noise.

The discrete time received sample vector $\mathbf{y}(t)$ of equation (6.1) at time n, over a running window of length (2p+1), can be expressed in a matrix form:

$$\mathbf{y}(n) = \mathbf{H}\mathbf{a}(n) + \mathbf{n}(n) \tag{6.2}$$

where $\mathbf{H}$ is Toeplitz matrix obtained from the channel impulse response in order to present convolution as matrix multiplication. The vector a(n) contains the transmitted symbols during that window period, $\mathbf{n}(n)$ is AWGN with covariance $E\{\mathbf{n}(n)\mathbf{n}^H\} = \sigma^2 I$.

6.1.2 Decision Feedback Equalization(DFE)

The decision feedback equalization [7] consists of two filters, a feedforward and feedback filter. The diagram below shows both the feedforward and feedback taps spaced at symbol interval T. The feedforward is identical to a linear transversal equalizer while the feedback has its input sequence of decision on previously detected symbol.

The feedforward and feedback filters have an infinite duration impulse response, which shows that the optimum feedforward filter in a zero forcing DFE is the whitened match filter. The feedbacks are simply related to the filter coefficient. We can apply MSE criteria to optimize the coefficient of the filters.

$$I_k = \sum_{j=k1}^{0} c_j v_{k-j} + \sum_{j=1}^{k2} c_j I_k - j \tag{6.3}$$

where I_k is the estimate of the k_{th} information symbol c_j tap coefficient of filters $[I_k, ..., I_k - k2]$ are the detected symbols. In feedforward, the equalizer is assumed

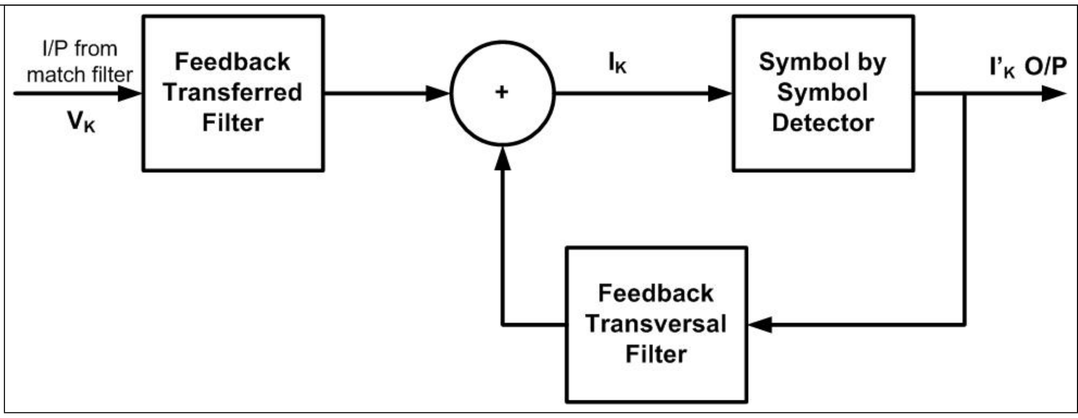

Figure 6.1: Decision Feedback Equalization Model

1. I_k= Symbol estimate
2. V_k=Input from match filter
3. I'_k=Output

to have $[k1+1]$ taps and k2 is the feedback. DFE is classed non linear because of previously detected symbols $\hat{I}_k$. Considering MSE criterion:

$$j(k1, k2) = E|I_k - \hat{I}_k|^2 \tag{6.4}$$

this will form a set of linear equations

$$\sum_{j=-k1}^{0} \psi_{lj} c_j = f^*_{-1}, \ l = -k1, ..., -1, 0 \tag{6.5}$$

where

$$\psi_{lj} = \sum_{m=0}^{-1} fm^* fm + l - j + N_0 \delta_{lj}, \ L_{ij} = -k1, ..., -1, 0 \tag{6.6}$$

The coefficients of the feedback filters from the equalizers are given by the intersymbol interference from the previously detected symbols.

$$c_k = \sum_{j=k1}^{0} c_j f_k - j, \ k = 1, 2...k2 \tag{6.7}$$

6.2 MMSE DFE

The discrete-time Gaussian channel is considered with inter-symbol interference (ISI). Under the assumption of perfect feedback, an information-theoretic derivation of the minimum mean-squared error (MMSE) decision-feedback equalizer (DFE) is presented. Whereas previous works have used information theory to analyze the zero-forcing and MMSE DFE structures, this work derives the MMSE DFE directly by means of information-lossless projections applied to the average mutual information of the Gaussian ISI channel. Specifically, the perfect-feedback MMSE DFE works by performing an information-lossless conversion of the ISI channel, which must be viewed in a sequence-wise manner, into a sequence of input-output pairs that must be viewed symbol-wise. With ideal interleaving, the latter can also be viewed as a memoryless Gaussian channel. This equivalence resolves the paradoxical result that perfect post-cursor ISI cancelation is in general an information-increasing operation. We find that it is not perfect cancelation that increases the mutual information, but rather the mathematically inconsistent assumption that the perfect-feedback MMSE DFE can be viewed as a sequence-wise channel with memory. In consideration of the model above, the time inter symbol interference channel where the output of the channel at the k^{th} time instance is given as in equation (6.1)

$$y_k = \sum_{j=-\infty}^{\infty} a_j x_k + n_k \tag{6.8}$$

Input sequence x_k and noise sequence n_k are both complex-valued, zero-mean wide-sense stationary (WSS) processes that are statistically independent of each other. Moreover, the noise sequence is assumed to be circularly symmetric and Gaussian. The sequence a_k is assumed to be in l_2, i.e, $\sum_k^{\infty} = |a_k|^2 \ < \infty$, so the output y_k is also WSS. The naturally context of quadrature amplitude modulation (QAM) signaling over a time-dispersive Gaussian channel when the received signal is processed by a matched filter and sampled at the symbol rate [84][85]. In facilitation z-transform is introduced to present a convolution operation. Thus for any sequence h_k, stochastic or deterministic, we write that:

$$h_z = \sum_{k=-\infty}^{\infty} h_k z^{-k} \tag{6.9}$$

This will allow ISI in (6.8) to be expressed as:

$$y_z = a(z)x(z) + n(z) \tag{6.10}$$

x(z), n(z), and y(z) do not exist as true z-transforms, but since x_k, n_k, and y_k are WSS processes, their auto and cross correlation possess z transforms. For example, if we let $R_{xy}(k) = E[x_1 + ky_1^*]$, then the cross spectrum of x(z) and y(z) is given by:

$$S_{xy}(z) = \sum_{k=-\infty}^{\infty} R_{xy}(k) z^{-k} \tag{6.11}$$

in that sense we can deduce that:

$$S_y(z) = a(z)S_x(z)a^*(\frac{1}{z^*}) + S_n(z) \tag{6.12}$$

$$S_{yx}(z) = a(z)S_x(z) \tag{6.13}$$

where $x(z)$ and $n(z)$ are independent. we use $a^*(\frac{1}{z^*})$ to represent $\sum_{k=-\infty}^{\infty} a_k^* z^k$. The average mutual information of the ISI channel, which we denote by (I(x(z);y(z))), is given by [86][87][88].

$$I(x(z); y(z)) = lim_{\longrightarrow\infty} \frac{1}{N} I(x_1^N; y_1^N) \tag{6.14}$$

Using the notation $I(x_1^N; y_1^N) = I(x_1, x_2, ...x_N; y_1, y_2, ...y_N)$ with the function I(.;.) denoting mutual information. If we are given that $E[|x_k|^2] = p$, then it is well known that the particular input process x_k that maximizes the average mutual information is a Gaussian process [86]. The spectrum $S_x(z)$ that maximizes the average mutual information is a function of both the channel a(z) and the noise spectrum $S_n(z)$, and it is determined by means of the so-called water filling procedure. Thus, we will assume hereafter that x_k is a Gaussian process. This being the case, it is known that:

$$I(x(z); y(z)) = \int_{-\pi}^{\pi} log \frac{S_y(e^{j\theta})}{S_n(e^{j\theta})} \frac{d\theta}{2\pi} \tag{6.15}$$

in nats per two dimensions, since the symbols are complex valued. In the sections that follow. The properties are incorporated in Section 6.4 while deriving the MMSE DFE directly from I(x(z); y(z)). This approach is in contrast to previous works that have started with various DFE structures and then analyzed them in an information-theoretic context [89],[90],[91],[92].

The MMSE DFE receiver essentially converts the ISI channel into a sequence of input-output pairs that must be viewed symbol wise; with ideal interleaving, this can be viewed as a memoryless Gaussian channel. This conversion is achieved by means of information-lossless projections that yield a set of sufficient statistics. Additionally, we are able to resolve the paradoxical idea that perfect feedback in an MMSE DFE receiver structure can actually lead to a fictitious increase in mutual information. This idea is reported and discussed in [89],[91],[92]. For perfect post-cursor ISI cancelation to be information increasing, the effective channel yielded by the MMSE DFE receiver must be viewed as a sequence-wise channel with memory, something our derivation shows is mathematically inconsistent. This resolution allows us to state a new converse to the coding theorem for the perfect-feedback MMSE DFE receiver system.

6.2.1 Mutual information between Gaussian processes

The mutual information between Gaussian random variables and some of the results to review are well known, but others are not [85]. let Lemma 1: Let $X = x_k k \epsilon \varrho$, $Y = y_k k \epsilon \rho$, $Z = z_k k \epsilon \beta$, and $(X; Y; Z)$ each be a set of jointly Gaussian zero-mean random variables with the sets ϱ, ρ, and β being arbitrary. Then the conditional mutual information.

$$I(X; Y/Z) = I((\mathbf{E} - \mathbf{\Pi}_z)(X); (\mathbf{E} - \mathbf{\Pi}_z)(Y)) \tag{6.16}$$

where E is the identity operator and $\mathbf{\Pi}$ denotes the operator that orthogonally projects on to Z, this Lemma is shown in [93]. Since the operator (E-$\mathbf{\Pi}_z$) yields that part of the argument which is orthogonal to Z, we see that the conditional mutual information has been expressed as the mutual information between the parts of X and Y that are orthogonal to Z. Lemma 2: With the same hypotheses as Lemma 1, let $\mathbf{\Pi}_Y$ be the orthogonal-projection operator onto Y. Then we have that

$$I(X; Y) = I(X; \mathbf{\Pi}_Y(X)) \tag{6.17}$$

Previously two lemmas in this chapter follow naturally from the more fundamental result for Gaussian variables that the mutual information between X and Y is a function of only the angles between their associated Hilbert spaces [93]. For example, in Lemma 2 the non-zero angles between X and Y are the same as those between

X and $\mathbf{\Pi}_Y(X)$ so that the mutual information is unaltered. In Lemma 1, those parts of X and Y that lie in Z contribute nothing to the mutual information. The inner product of the Hilbert space is expectation, so for zero-mean Gaussian random variables x and y is

$$\mathbf{\Pi}_y(X) = E[x/y] = \frac{E[xy^*]}{E[|y|^2]}y \tag{6.18}$$

The following lemma is a variation of the well known Shannon capacity $log(1+SNR)$ result for the mutual information between two zero-mean Gaussian random variables, i.e the capacity of a memoryless discrete-time Gaussian channel; it evaluates the signal-plus-noise power divided by the noise power:

Lemma 3: Given zero-mean jointly Gaussian random variables x and y:

$$I(x;y) = log(\frac{E[|y|^2]}{E[|y - E[\frac{y}{x}]|^2]}) \tag{6.19}$$

Lemma 4: Suppose that at least one of the zero-mean WSS processes x_k and y_k is regular (ie., non-predictable). That is, $\int_{-\pi}^{\pi} |log(S_x(e^{j\theta}))|d\theta \ < \infty$ or $\int_{-\pi}^{\pi} |log(S_y(e^{j\theta}))|d\theta \ < \infty$ then for all k we have:

$$I(x(z); y(z)) = I(x_k; y_{-\infty}^{\infty}/x_{-\infty}^{k-1}) \tag{6.20}$$

6.2.2 Linear Prediction Theory Results

Given the regular (Lemma 4), zero-mean WSS process x_k. The innovations process for x_k in [85] is given by:

$$(ix)_k = x_k - E[x_k \ x_{-\infty}^{k-1}] \tag{6.21}$$

From linear prediction theory for scalar processes, we know that:

$$x_k = \sum_{j=0}^{\infty} (\emptyset_x)_j (i_x)k - j \tag{6.22}$$

where $\emptyset_x(Z) = \sum_{k=0}^{\infty} (\emptyset_x)kZ^{-k}$ is causal, harmonic (i. e., $\emptyset_x 0 = 1$), and minimum-phase. This means that $(\emptyset_x(z))^{-1}$, which we shall write as $\emptyset_x^{-1}(z)$ is also causal and harmonic. Moreover, we have that:

$$S_x(Z) = g_x \emptyset_x(Z) \emptyset_x^*(1/Z^*) \tag{6.23}$$

where $g_x = E[|(i_x)|^2]$ is the geometric mean of the spectrum $S_x(e^{j\theta})$. That is:

$$g_x = exp\left(\int_{-\pi}^{\pi} log(S_x(e^{j\theta}))\frac{d\theta}{2\pi}\right) \tag{6.24}$$

This allows us to formally write that $X(Z) = \O_x(z)i_x(z)$, and if we consider the formal Z-transform of the sequence $x_k = E[x_k^{k-1}{}_{-\infty}]$, we get that $\hat{x}(z) = x(z) - i_x(z) = (1 - \O_x^{-1}x(z))$. These results are summarized in the following lemma. Lemma 5: Given a regular, zero-mean WSS process x_k, define the processes $\hat{x}$ and $(i_x)_k$ by $\hat{x}_k = E[x_k/x_{-\infty}^{k-1}]$ and $(i_x)_k = x_k - \hat{x}_k$. Then:

$$x_z = \O_x(z)i_x(z) \tag{6.25}$$

$$i_x(z) = \O_x^{-1}(z)X(z) \tag{6.26}$$

$$\hat{x}(z) = (1 - \O_x^{-1}(Z))X(Z) \tag{6.27}$$

The polynomial $\O_x(z)$ is causal, harmonic, and minimum phase; the spectral factorization of $S_x(z)/g_x$ is $\O^*(1/Z^*)\O(z)$, where g_x given by equation (6.24). Having established the necessary background we proceed in the next section for the derivation of the MMSE DFE receiver structure.

6.3 Information Theoretic Derivation of MMSE DFE

Deriving MMSE DFE, we begin by proving the average mutual-information result previously stated in equation (6.15). The approach given in [93] has properties that suggest that MMSE DFE, is a canonical equalization structure for systems that combine equalization with coded modulation. For the Gaussian ISI channel in equation (6.10) with a regular, zero-mean WSS Gaussian input, we consider $I(x(z); y(z))$. We know from Lemma 4 that:

$$I(x(z); y(z)) = I(x_k; y_{-\infty}^{\infty}/x_{-\infty}^{k-1}) \tag{6.28}$$

for all k. Using the chain rule of mutual information, expressing $I(x_k; y_{-\infty}^{\infty}/x_{-\infty}^{k-1})$, in two different ways:

$$I(x_k; y_{-\infty}^{\infty}/x_{-\infty}^{k-1}) = I(x_k; y_{-\infty}^{\infty}) + I(x_k; x_{-\infty}^{k-1}/y_{-\infty}^{\infty}) \tag{6.29}$$

$$I(x_k; y_{-\infty}^{\infty}/x_{-\infty}^{k-1}) = I(x_k; x_{-\infty}^{k-1}) + I(x_k; y_{-\infty}^{\infty}/x_{-\infty}^{k-1}) \tag{6.30}$$

then, in combining equations (6.29) and (6.30) with equation (6.28) allows us to see that:

$$I(x_k; y_{-\infty}^{\infty}/x_{-\infty}^{k-1}) = I(x_k; y_{-\infty}^{\infty}) + I(x_k; x_{-\infty}^{k-1}/y_{-\infty}^{\infty}) - I(x_k; x_{-\infty}^{k-1}) \tag{6.31}$$

When applying Lemma 2 to the first term and Lemma 1 to the second term we get:

$$I(x(z); y(z)) = I(x_k; E[x_k/y_{-\infty}^{\infty}]) + I(x_k - E[x_k/y_{-\infty}^{\infty}]); (x_j - E[x_j/y_{-\infty}^{\infty}]_{j=-\infty}^{k-1}) - I(x_k; x_{-\infty}^{k-1}) \tag{6.32}$$

To define the sequences $\tilde{x}_k$ and e_k by $\tilde{x}_k = E[x_k/y_{-\infty}^{\infty}]$ and $e_k = x_k - \tilde{x}_k$. Making use of the hat-notation for the one-step predictor as in Lemma 5, ie., $\tilde{x}_k = E[x_k/x_{-\infty}^{k-1}]$ and $\hat{e}_k = E[e_k/e_{-\infty}^{k-1}]$, we find that:

$$I(x(z); y(z)) = I(x_k; \tilde{x}_k) + I(e_k; e_{-\infty}^{k-1}) - I(x_k; x_{-\infty}^{k-1}) \tag{6.33}$$

$$I(x(z); y(z)) = I(x_k; \tilde{x}_k) + I(e_k; \hat{e}_k) - I(x_k; \hat{x}_k \tag{6.34}$$

and, the average mutual information of the Gaussian ISI channel has been expressed in terms of three pairs of scalar-valued Gaussian variables [85]. Before considering these pairs in more detail, we apply Lemmas 3 and 5 to (6.34) to get that:

$$\begin{aligned} I(x(z); y(z)) &= log\left(\frac{E[|x_k|^2]}{E[|x_k - \tilde{x}_k|^2]}\right) - log\left(\frac{E[|x_k|^2]}{E[|x_k - \hat{x}_k|^2]}\right) + log\left(\frac{E[|x_k|]}{E[|e_k - \hat{e}_k|^2]}\right) \\ &= log\left(\frac{E[|x_k|^2]E[|(ix)_k|^2 E[|e^k|^2]}{E[|e_k|^2]E[|x_k|^2]E[|(i_e)_k|^2]}\right) \\ &= log\left(\frac{g_x}{g_e}\right) \end{aligned} \tag{6.35}$$

we can explicitly calculate Se(z) to be:

$$Se(z) = S_x(z) - S_{xy}(z)S_y^{-1}(z)S_{yx}(z) \tag{6.36}$$

$$Se(z) = \frac{S_x(z)S_n(z)}{S_y(z)} \tag{6.37}$$

so that $g_e = g_x g_n/g_y$. Finally then, the result given in equation (6.15) is derived since $I(x(z); y(z)) = log(g_y/g_n)$. We now look more closely at the three mutual-information terms that compose the righthand side of equation (6.34). The first term is $I(x_k; \tilde{x}_k)$. Since $\tilde{x}(z)$ is the orthogonal projection of $x(z)$ onto $y(z)$, it can be expressed as $\tilde{x}(z) = S_{xy}(z)S_y^{-1}(z)y(z)$. Incorporating equation (6.12) and equation (6.13), it was observed that:

$$\tilde{x}(z) = c(z)(a(z)x(z) + n(z)) \tag{6.38}$$

where

$$c(z) = \frac{S_x(z)a^*(1/z^*)}{a(z)S_x(z)a^*(1/z^*) + S_n(z)} \tag{6.39}$$

we must be very careful, however, in our interpretation of this representation. Without further clarification, the channel in equation (6.45) represents $I(x(z); \tilde{x}(z))$, not $I(x_k; \tilde{x}_k)$. These are two very distinct channels. The first is a sequence-wise interpretation of the channel, while the second is a symbol-wise interpretation of the channel. Clearly, only this second interpretation is relevant to our discussion. The second term in equation (6.34) is $I(e_k; \hat{e}_k)$. By Lemma 5, this is representable as:

$$\hat{e}(z) = (1 - \text{Ø}_e^{-1})e(z) \tag{6.40}$$

where $\text{Ø}_e^{-1}(z)$ is the causal, harmonic, minimum-phase whitening filter for $Se(z)/ge$, and of course $e(z) = x(z) - \tilde{x}(z)$. Again, we are interested in only the k_{th} input and the k_{th} output. And similarly, the third channel $I(x_k; \hat{x}_k)$ comes from the following:

$$\hat{x}(z) = (1 - \text{Ø}_e^{-1})(z)x(z) \tag{6.41}$$

The inputs and outputs of the channels in equations (6.38), (6.40), and (6.41) are inter-related in such a manner that allows them to be combined to form a channel that is equivalent as far as mutual information is concerned. The first and second channels are combined as shown in parts (a) and (b) of the Figure 6.2. Since we are adding the outputs of the two channels, we must still verify that the mutual information of the overall channel is equal to the sum of the mutual information of the two component channels. Lemma 6: When the channels $I(x_k; \tilde{x}_k)$ and $I(e_k; \hat{e}_k)$ are combined as shown in Figure 1, we have that:

$$I(x_k\hat{e}_k + \tilde{x}_k) = I(x_k; \tilde{x}_k) + I(e_k; \hat{e}_k) \tag{6.42}$$

This lemma can be proven directly. For example, see [91][92] where the left hand side is shown to equal $I(x(z); y(z))$ when x_k is white. The result can also be shown to follow from a much more general statement concerning certain relationships of orthogonal projection channels. The latter approach sidesteps the algebraic details associated with the direct proof. It also allows one to easily generalize the result to other Gaussian channels such as the multivariate ISI channel [94], the finite-dimensional ISI channel, and the synchronous Gaussian multiple-access channel [95].

It should be pointed out that the channel shown in part (b) of Figure 1 is sometimes given as the perfect-feedback MMSE DFE structure for the Gaussian ISI channel. We see, however, that unless x_k is a white process $I(x_k; \hat{x}_k) = 0$, this structure does not model the Gaussian ISI channel accurately. (6.29) shows that it models the channel $I(x_k; y_{-\infty}^{\infty}, x_{-\infty}^{k-1})$ instead of the ISI channel of interest, $I(x_k; y_{-\infty}^{\infty}/x_{-\infty}^{k-1})$. To incorporate the third channel $I(x_k; \hat{x}_k)$, we can express $x(z)(1 - \varnothing_e^{-1}(z)$ as $x(z)(1 - \varnothing_e^{-1})(z) + x(z)(\varnothing_e^{-1})(z) + \varnothing_e^{-1})(z)$. When this representation is incorporated into part (b) of Figure 1, the result is part(c) of the same figure. Note that the last parallel branch of this figure is simply the third channel of interest. Thus, the subtraction of the third mutual-information term in equation (6.34) suggests the removal of this parallel branch. We know that:

$$\varnothing_x^{-1}(z) - \varnothing_e^{-1}(z) = \varnothing_x^{-1}(z) \left(1 - \frac{\varnothing_y(z)}{\varnothing_n(z)}\right). \qquad (6.43)$$

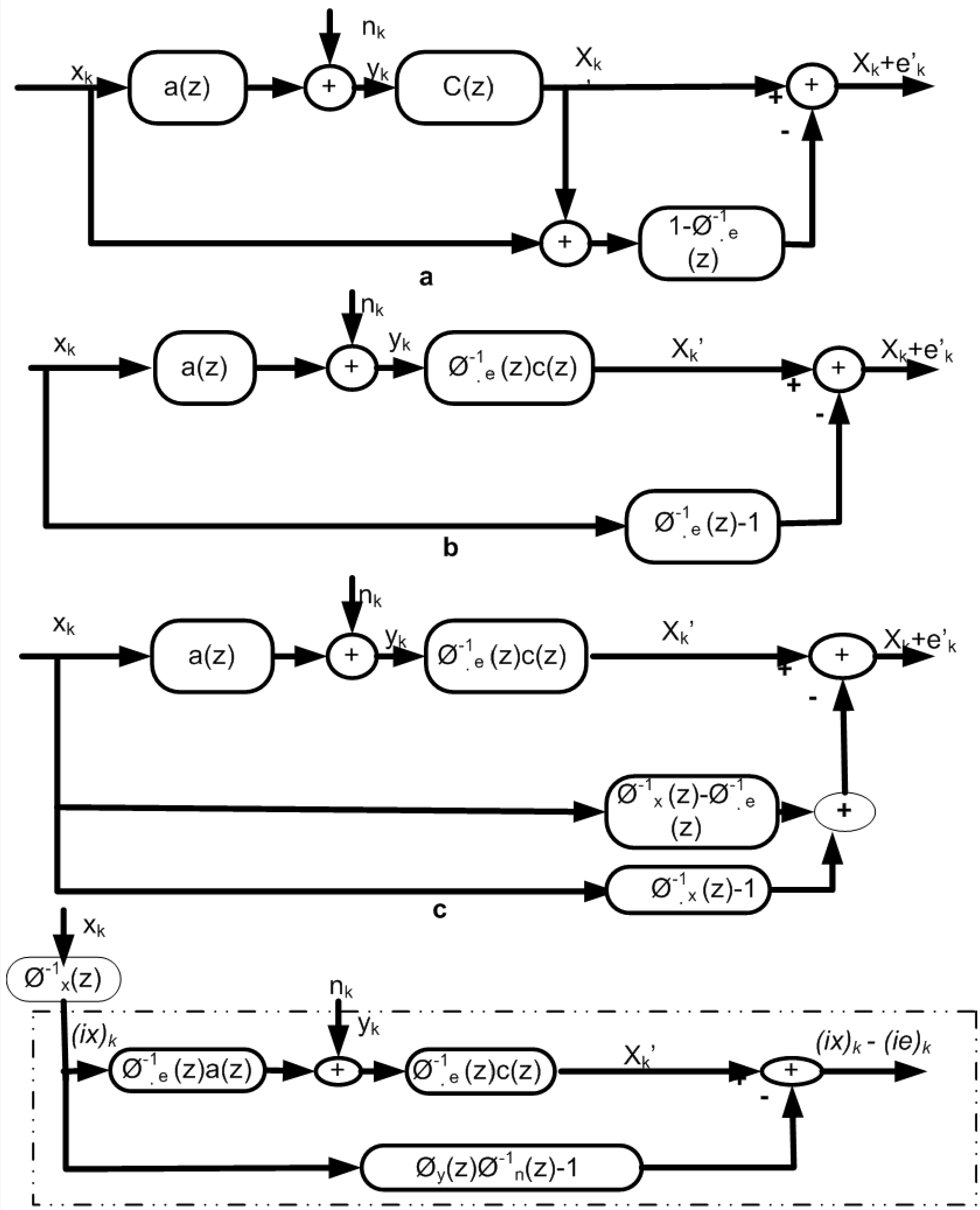

Figure 6.2: MMSE DFE Structure

1. X_k= Input process

2. n_k= noise spectrum

3. $X_k + e'_k$= Output

The combination of (6.34) correspond to the model pictured in figure b. It is easily seen that $\hat{e}_k + \tilde{x}_k - x_k + (i_x)_k = (i_x)_k - (i_e)_k$ and it is not hard to show that $I((I_x)_k; (i_x)_k - (i_e)_k) = I(x(z; y(z)))$. In addition, we can show that $I(x_k); (i_x)_k - (i_e)_k < I((I_x)_k; (i_x)_k - (i_e)_k)$ whenever x_k is not white. Hence, figure b only makes sense if we consider $(i_x)_k$ to be the input. Note that the symbol-wise interpretation of this channel is equivalent to the memoryless channel that is yielded by perfect interleaving. This, then, is the canonical MMSE DFE model, and it is the model that is typically assumed in the literature. Thus, we have shown that from the viewpoint of mutual information, there is no loss in generality in assuming that the receiver of the Gaussian ISI channel is the perfect-feedback MMSE DFE. Of course, perfect feedback means that the post-cursor ISI is completely removed by the receiver [85].

This equivalence was derived by means of information-lossless orthogonal projections that convert the ISI channel, which is naturally viewed in a sequence-wise manner, to a channel that must be viewed symbol-wise. That is, the perfect-feedback MMSE DFE structure has built into it the fact that at time instance k, only those past symbols, ie., $x_{-\infty}^{k-1}$, are available at the receiver. A sequence-wise interpretation violates this by inherently assuming knowledge of future symbols, ie., x_{k+1}^{∞} as well.

The Figures below shows BER comparisons:

- MMSE equalizer and Zero forcing.
- MMSE DFE with MMSE and BPSK.

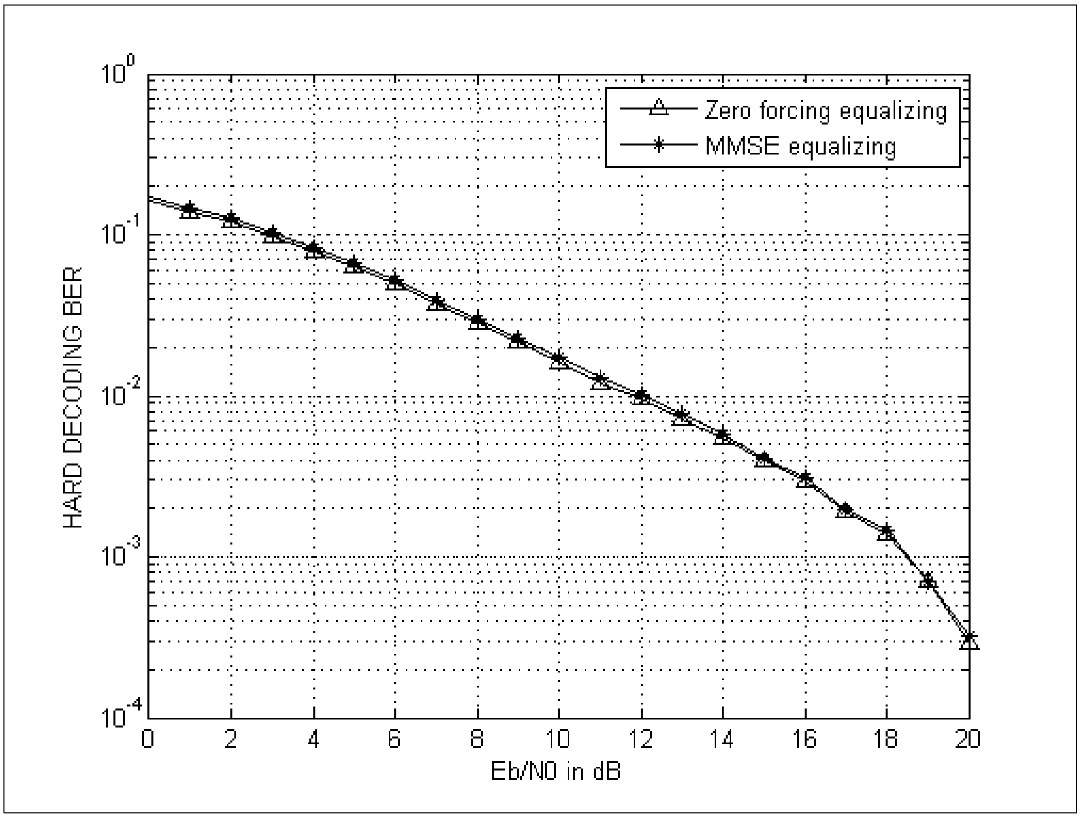

Figure 6.3: BER Comparison

1. MMSE Equalizer
2. Zero Forcing Equalizer

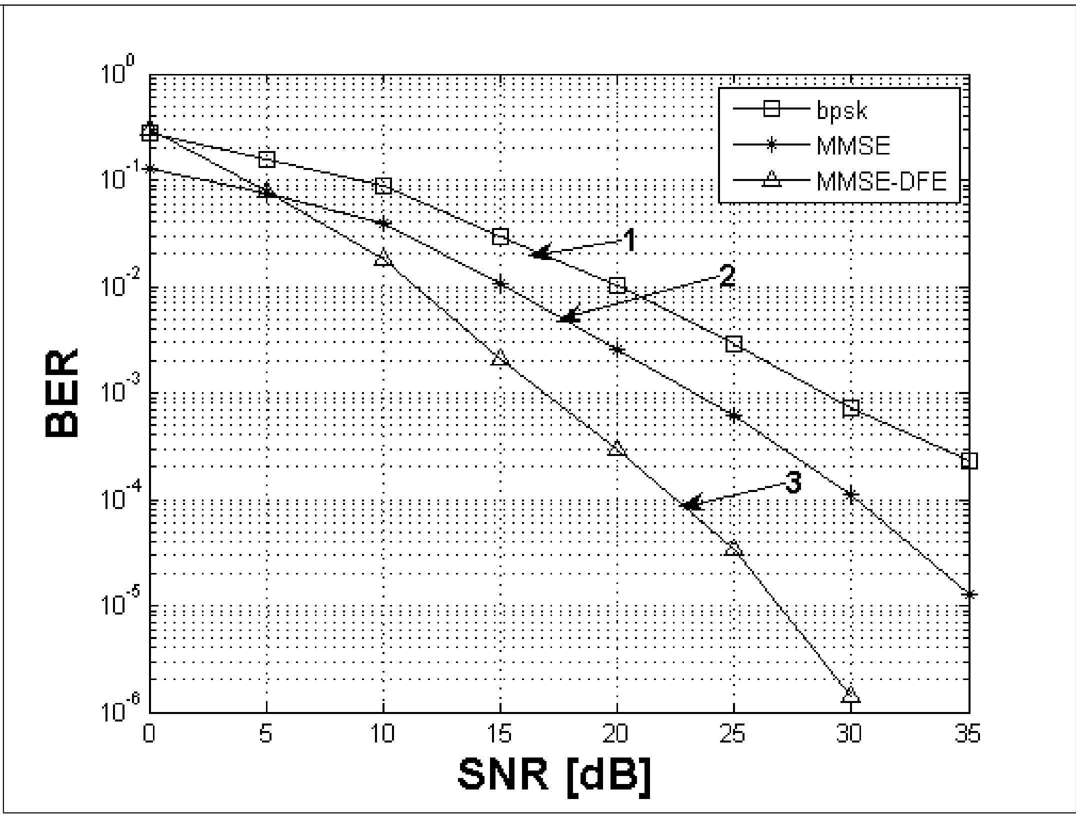

Figure 6.4: BER Comparison

1. BPSK
2. MMSE
3. MMSE DFE

The BER comparison in Figure 6.3 shows that zero forcing and MMSE overlap each other, indicating that their performance is pretty close to each other while in Figure 6.4. The figure below shows that MMSE DFE has a 6dB SNR gain at BER of 10^{-4} to MMSE and BPSK.

6.3.1 MMSE Derivation conclusion

We have seen fundamentally how the MMSE DFE under the assumption of perfect feedback, allows one to achieve the capacity of the Gaussian-noise channel with inter-symbol interference. The MMSE DFE effectively makes use of information-lossless projections to convert the ISI channel into a memoryless Gaussian channel. This method of derivation can be applied to other channels (finite-dimensional ISI, multivariate ISI, and synchronous multiple-access) to yield the feedback equalizers given in [94][96] as well as the multiuser decision feedback receiver given in [95].

6.3.2 Adaptive MMSE Receivers

Recalling back from the previous chapter, the linear MMSE equalizer is considered as a special case of the Decision Feedback Equalization (DFE) when all decision feedback coefficients are equal to zero. The output of the MMSE filter at the n_{th} symbol interval is

$$\mathrm{b}(n) = \sum_{m=-P}^{P} f(m) y_k(nT - mT) \tag{6.44}$$

where f(m) are the adaptive filter coefficients, T is the symbol interval. The total number of adaptive equalizer coefficients is $(2p+1)$. The symbol estimate $\hat{a}(n)$ is obtained as:

$$\hat{a}(n) = b(n) - \mathbf{d^H}(n)\mathbf{a}_D(n) \tag{6.45}$$

where $\mathbf{d}(n)$ is a vector of decision aided coefficient sequences, defined as,

$$\mathbf{d}(n) = [d_1, d_2, ..., d_k]^T. \tag{6.46}$$

The elements of $\mathbf{d}(n)$ represent the weighting coefficients which multiply the respective known symbols. The vector $\mathbf{a}_D(n)$ contains symbols known to the receiver with unknown symbols set to zero. It is defined as:

$$\mathbf{a}_D(n) = [a(n+1), a(n+2), ..., a(n+K)]^T \tag{6.47}$$

The coefficients of $\mathbf{d}(n)$ and $\mathbf{f}(n)$ are obtained adaptively during a training period. After the training period, the coefficients $\mathbf{d}(n)$ and $\mathbf{f}(n)$ can be kept during data detection. Alternatively, in a decision directed mode, these coefficients can be updated by tentative decisions[20][8].

6.3.3 LMS Adaptive Algorithm

As stated in 5.2.3, the following steps to be implemented and considered for improved performance correspond to the LMS algorithm as stated in [4]:

$$\mathbf{f}(n+1) = \mathbf{f}(n) + \alpha_1 e^*(n)\mathbf{y}(n) \tag{6.48}$$

$$\mathbf{d}(n+1) = \mathbf{d}(n) - \alpha_2 e^*(n)\mathbf{a}_D(n) \tag{6.49}$$

for n $= 0, 1, 2, ...,$ where f(n) is the linear filter coefficient sequence and d(n) is the decision aided coefficient sequence, both at the n^{-th} symbol iteration, and (e^*) denotes conjugation, α_1 and α_2 being step sizes. Similarly, the Recursive Least Square (RLS) algorithm can also be used to provide faster convergence. The coefficients are updated once every symbol interval [4][60].

6.3.4 Training of the Adaptive MMSE Receiver

In any adaptive system, training is very essential and thus it is very necessary to send training signal to acertain the behaviour of the channel, the receiver structure consists of an adaptive symbol spaced MMSE FIR filter and the adaptive decision feedback (DFE) symbol spaced FIR filter. The linear MMSE equalizer is considered as a special case of the DFE when all decision feedback coefficients are equal to zero. In order to simplify derivations, the symbol powers are normalized to 1, $\mathrm{E}\mathbf{a}(n)\mathbf{a}^H(n) = I$. The vector is expressed as:

$$\mathbf{a}(n) = \mathbf{a}_D(n) + \mathbf{a}_U(n) \tag{6.50}$$

where $\mathrm{a}_D(n)$ contains known symbols and $\mathrm{a}_U(n)$ contains unknown symbols. The channel matrix H is split into two parts during training period $\mathrm{H} = \mathrm{H}_D + \mathrm{H}_U$, where H_D consists of channel responses corresponding to symbols in $\mathrm{a}_D(n)$ and H_U correspond to symbol in $\mathrm{a}_U(n)$. The filter coefficients are obtained by minimizing the MSE, $\mathrm{E}[|e^n|^2]$, where $e(n) = a(n) - \hat{a}(n)$, $\hat{a}(n) = \mathrm{f}^H(n)\mathrm{y}(n) - \mathrm{d}^H(n)\mathrm{a}_D$. There is a range of adaptive algorithms offering simple adaptive solutions [8] to obtain the optimal coefficients d and f.

6.3.5 Arbitrary Gaussian Noise and Water Pouring Analogy

If a white thermal noise is passed through a filter whose transfer function is $\mathbf{Y}(f)(n)$, the resulting noise has a power spectrum $\mathbf{N}(f) = \mathbf{K}|\mathbf{Y}(f)^2|$ and is known as Gaussian noise. We can calculate the capacity of a channel perturbed by any Gaussian noise from the white-noise result. Suppose our total transmitter power is P and it is distributed among the various frequencies according to P(f). Then:

$$\int_0^w P(f)df = P. \tag{6.51}$$

We can divide the band into a large number of small bands, with $\mathbf{N}(f)$ approximately constant in each. The total capacity for a given distribution $\mathbf{P}(f)$ will then be given by:

$$C_1 = \int_0^w log\left(1 + \frac{P(f)}{N(f)}\right) df, \tag{6.52}$$

since, for each elementary band, the white-noise result applies. The maximum rate of transmission will be found by maximizing C_1 subject to condition (1). This requires that we maximize:

$$C_1 = \int_0^w \left[log\left(1 + \frac{P(f)}{N(f)}\right) + \lambda P(f)\right] df. \tag{6.53}$$

The condition for this is, by the calculus of variations, or merely from the convex nature of the curve $log(1+x)$ is:

$$\frac{1}{N(f)+P(f)} + \lambda = 0 \tag{6.54}$$

or $N(f)+P(f)$ must be constant. The constant is adjusted to make the total signal power equal to P. For frequencies where the noise power is low, the signal power should be high, and vice versa, as we would expect. The power of the water level line above the curve $N(f)$ is an indication of the water level above the vessel of shape $N(f)$ with the water volume P. If P is too small, we cannot make $P(f)+N(f)$ constant across the whole bandwidth W, since this would require negative power at some frequencies.

In simple words, there is just not enough power "water" to cover the whole vessel with an uneven bottom described by curve $N(f)$. It is easily shown, however, that in this case the best $P(f)$ is obtained by making $P(f)+N(f)$ constant whenever possible, and making $P(f)$ zero at other frequencies. With low values of P, some of the frequencies will not be used at all. If the water filling analogy has the spectrum $N(f)$, keeping the total noise power constant and always adjusting the spectrum $P(f)$ to give the maximum transmission, we can determine the worst spectrum for noise. This turns out to be the white-noise case. Although this only shows it to be the worst among the Gaussian noises, it can be shown that the white Gaussian noise is the worst among all possible noises with the given power N in the band.

6.3.6 Simple Generalization

The water filling analogy has been discussed in the case where $N(f)$ was variable across certain bandwidth (W). The things that are more likely to arise in practical situations is the case where the channel transfer function $H(f)$, is uneven across the bandwidth (W). At the same time the Gaussian noise is represented by the receiver thermal AWGN with uniform spectral density across the bandwidth (W) equal to N_0. An inverse filter with transfer function $1/H(f)$ would equalize the signal (elliminating ISI) and make the noise spectrum $N(f) = N_0/H(f)$. The water filling analogy can be readily applied again to the system with the noise spectral density $N(f) = N_0/H(f)$.

6.4 Multicarrier Transmission

Multicarrier transmission has been proposed for high data communication since the 1960's [47]. The advantages of this technique are that the frequency selectivity of the channel gets smoother in individual subchannels and the intersymbol interference (ISI) becomes more practical even for very high data rates. Obvious examples are discrete multitone (DMT) transmission for high bit rate digital subscriber lines (HDSL) [97] and orthogonal frequency division multiplexing (OFDM) for digital TV broadcasting [98][99].

The equation (6.53) is the mathematical reason behind the multicarrier modulation. The entire channel bandwidth is divided into many narrow subchannels. Data transmission takes place in parallel. The symbol duration is significantly increased and ISI in subchannels eliminated. It could be concluded that with appropriate channel coding techniques and after some time delay caused by the coding/decoding process, channel capacity is achievable on every of the individual subchannels. If the channel bandwidth is W and the channel is divided into K channels of bandwidth $\triangle W$, then the capacity of the channel with index $k, k = 1, 2, ..., K$ is:

$$C_k = \triangle W log \left(1 + \frac{P(k\triangle W)}{N(k\triangle W)}\right), \tag{6.55}$$

where $P(k\triangle W)$and $N(K\triangle W)$ are signal and noise densities at frequency $f_k = k\triangle W$ respectively. The total capacity is:

$$C_k = \sum_{k=1}^{k} \triangle W log \left(1 + \frac{P(k\triangle W)}{N(k\triangle W)}\right), \tag{6.56}$$

or if the number of subchannel K goes to infinity, then the capacity of multicarrier modulation (MCM) becomes

$$C_{MCM} = \int_0^w log \left(1 + \frac{P(f)}{N(f)}\right) df, \tag{6.57}$$

The receiver signal spectral density $P(f) = S_a S_h(f)$ depends on the transmitted signal spectral density S_a and the channel transfer function amplitude characteristic $S_h(f)$. $P(f)$ can be controlled by S_a if the channel amplitude characteristics S_h is known, making sure that the water filling rule is satisfied. Achieving the capacity requires knowledge of the channel. Then with the appropriate information loading per subchannel, the total channel capacity can be achieved. Subchannels have different channel capacities due to different signal to noise ratios per subchannel and can carry, without error, different amounts of information. Various implementation issues related to MCM arises, such as

- Excessive delay due to very narrow bandwidth of subchannels.
- Inter-sub-channel interference (it is difficult to produce a large number of narrow band subchannels with high selectivity filters preventing cochannel interference).

- Difficulty in adaptive information loading per subchannel due to lack of information at the transmitter about the channel. This problem is particularly difficult in the case of a mobile channel since the channel is to a various degree time variable.

Those issue are beyond the scope of this analysis.

6.4.1 The MMSE Decision feedback Receiver

The receiver structure consists of an adaptive symbol spaced MMSE FIR filter and the adaptive decision feedback (DFE) symbol spaced FIR filter. The linear MMSE equalizer is considered as a special case of the DFE when all decision feedback coefficients are equal to zero. The output of the MMSE filter at the n_{th} symbol interval are as shown:

$$\mathbf{b}(n) = \sum_{m=-P}^{P} f(m)yk(nT - mT) \tag{6.58}$$

where $\{f(m)\}$ are the adaptive filter coefficients, T is the symbol time interval. The total number of adaptive equalizer coefficients is (2p+1). The symbol estimate â(n) is obtained as:

$$\hat{a}(n) = b(n) - \mathbf{d}^H(n)\mathbf{a}_D(n) \tag{6.59}$$

where $\mathbf{d}(n)$ is a vector of decision aided coefficient sequences, defined as:

$$\mathbf{d}(n) = [d_1, d_2, ..., d_k]^T \tag{6.60}$$

.

The elements of $\mathbf{d}(n)$ represents the weighting coefficients which multiply the respective known symbols. The vector $\mathbf{a}_D(n)$ contains symbols known to the receiver with unknown symbols set to zero. It is defined as:

$$\mathbf{a}_D(n) = [a(n+1), a(n+2), ..., a(n+K)]^T \tag{6.61}$$

The symbol powers are normalized to 1, $E\{\mathbf{a}(n)\mathbf{a}^H(n)\} = 1$.

6.5 Multicarrier Modulation(MCM) and MMSE-DFE Capacity Comparison

From the equation (5.17) of chapter 5, shows the result for the DFE MMSE in time discrete domain. The equation could be used to calculate the information capacity achievable by a DFE receiver and it could be shown that the ideal MSE-DFE is the information capacity achievable (canonical) device [80]. For the sake of comparison with multicarier modulation, where the frequency representation is used, it is more appropriate to use the expression for DFE MMSE in frequency domain [80][81][79].

$$log \frac{1}{\varepsilon_{MMSE-DFE}} = \int_0^W log \left[\frac{S_a(f)}{N_0} |S_{hh}(f)|^2 + 1 \right] df \tag{6.62}$$

where $S_a(f)$ is the average symbol power spectral density, ($S_a(f) = 1$) in our case. In general, $S_a(f) = 1$ does not have to be a constant. However, if the symbol sequence is uncorrelated, then ($S_a(f) = 1$) is a constant, and without loss of generality it can be assumed to be 1. AWGN spectral density is denoted by N_0 and $S_h(f)$ is the fourier transform of the channel response h, autocorrelation function.

$$C_{MMSE-DFE} = \int_0^W log \left(1 + \frac{S_h(f)^2}{N_0} \right) df \tag{6.63}$$

By comparing (6.57) for the capacity of multicarrier modulation C_{MCM}

$$C_{MCM} = \int_0^W log \left(1 + \frac{S_h(f)^2}{N_f} \right) df \tag{6.64}$$

and (6.63) for capacity of MMSE-DFE ($C_{MMSE-DFE}$), we can see that they are in essence identical. The signal spectral density $P(f)$ in the equation (6.63) is $|S_h(f)|^2$ and the noise spectral density is assumed to be uniform N_0. But what really matters is the signal to noise ratio $|S_h(f)|^2/N_0$ which could be variable across the bandwidth. Then we can write

$$C_{MCM} = C_{MMSE-DFE} = \int_0^W log(1 + SNR(f))df \tag{6.65}$$

.

6.6 Simulation and Result

Figures below demonstrates the performance of wiener solution(optimum combining), classical adaptive filters by LMS, the presented adaptive MMSE by LMS and adaptive MMSE by RLS algorithm in Gaussian channel. The performance results of wiener solution is bench mark as it maximize the output signal to noise ratio. With the RLS algorithm the best adaptive performance were obtained which indicates that the simulation of the RLS algorithm, convergence is according to signal to noise ratio, as it overlaps the performance result of Wiener's solution.

The performance presented by the scheme is very close to Wiener solution of signal combining with a lower computational complexity then RLS. The proposed scheme in flat fading Raleigh wireless communication channels is clear that the proposed scheme achieves performance exactly to Wiener solution.

The Shannon capacity formula with average power constraint is expressed in this chapter. Our developed tool analyzes the performances of MMSE estimation and adaptive filter in two channel environment. Equation (6.65) is the well known shannon capacity formula with the average power constraint [33]. The developed tool analyzes the performances of MMSE estimation, adaptive filter and MCM in a two channel environment. Figure 6.5 shows the information capacity of MMSE DFE and the upper bound of Shannon Capacity. In this curve, QPSK signal is transmitted through Raleigh frequency selective channel of impulse response C=[0.5 1.1 1.5 -1]. MMSE DFE was used to detect symbols, it shows a better performance indicating the implementational issues as the curve stabilizes.

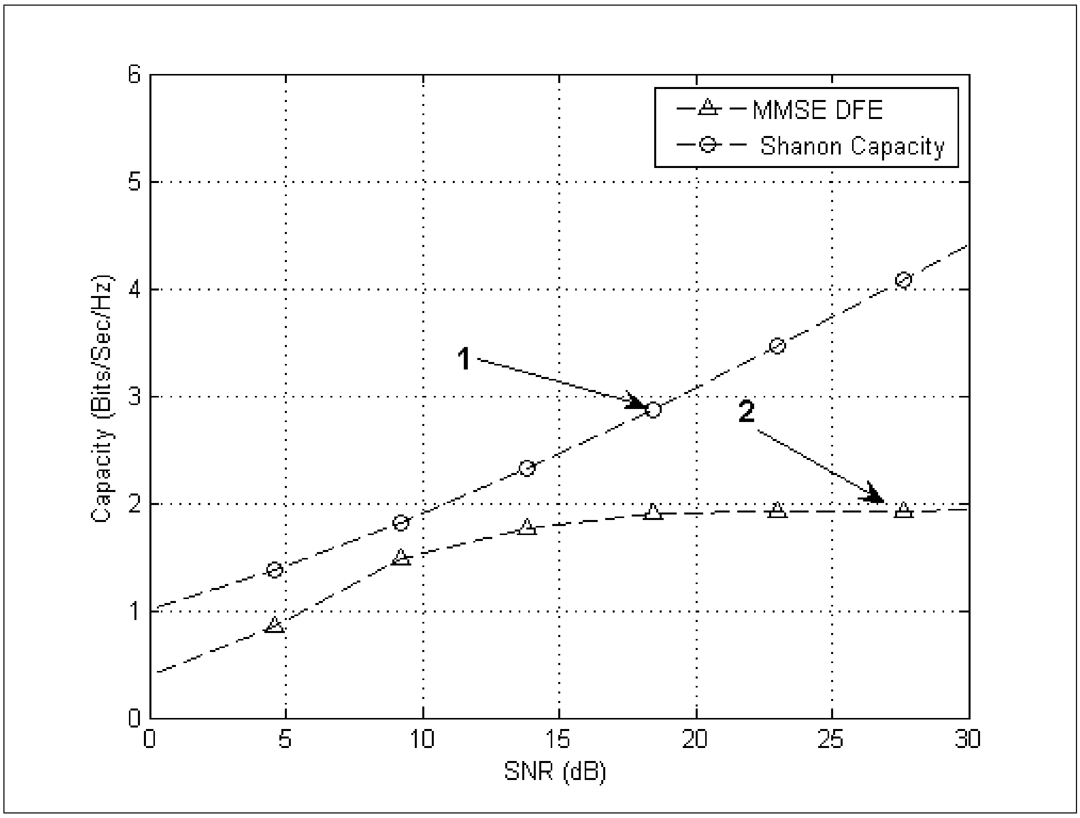

Figure 6.5: Information Capacity Comparison

1. Shannon Capacity Theory

2. MMSE DFE

The theoretical capacity results of Shannon and the match filter overlapping was shown in Figure 6.6. The simulated result for BPSK bench mark of match filter and adaptive filter in a Gaussian channel indicates that the performance of the adaptive algorithm for the AWGN channel is equal to that of the MF and MMSE of the same channel. The adaptive filter works better for the AWGN channel by employing the Least mean square (LMS) algorithm. The simulated result with BPSK modulation for match filter and adaptive filter in a flat fading Raleigh channel, compared with the Gaussian channel, least mean square (LMS) algorithm performance in this system is poor in a Raleigh channel, but introducing the RLS algorithm, the system performs better than the match filter which is a good reference for measuring the performance of the adaptive filter's algorithms as shown in Figure 6.6

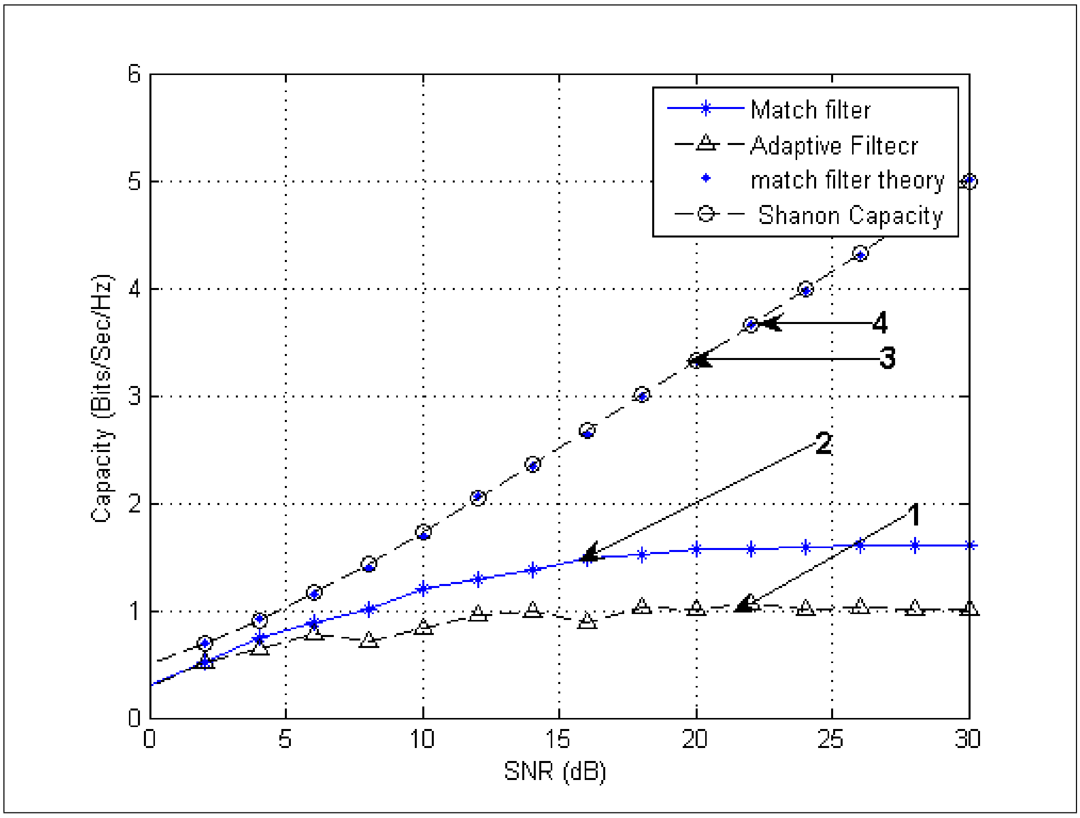

Figure 6.6: Information Capacity Comparison

1. Adaptive simulated
2. Match Filter
3. Match Filter Theory
4. Shannon Capacity Theory

In conclusion, It has been shown that the channel capacity of the multicarrier modulation format is equivalent to the channel capacity when the MMSE-DFE receiver is used. For DFE, it is important to emphasise the link between the channel achieving DFE structure and the MMSE criterion for the DFE coefficient estimation algorithm. For example, the zero forcing DFE is not a capacity achieving device. Implementation issues regarding MCM and MMSE-DFE are neglected. However, it should be emphasized that the implementation issues are exactly the issues that make one or the other technique more attractive for actual implementation. As far as the channel information capacity achieving criterion is concerned, both techniques are equivalent and could be implemented as adaptive multiuser detectors.

6.7 summary

It has been shown that the channel capacity of the multicarrier modulation format is equivalent to the channel capacity when the MMSE-DFE receiver is used. For DFE, it is important to emphasis the link between the channel achieving DFE structure and the MMSE criterion for DFE coefficient estimation algorithm. For example zero forcing DFE is not capacity achieving device.

Implementation issues regarding MCM and MMSE-DFE are neglected. However, it should be emphasized that the implementation issues are exactly the issues that make one or the other technique more attractive for actual implementation. As far as the channel information capacity achieving criterion is concerned both techniques are equivalent and could be implemented as adaptive multiuser detectors.

Chapter 7

Comparisons of Adaptive MMSE Multiuser Receivers for MIMO OFDM Wireless Channel

7.1 AMUD MIMO OFDM comparisons

Comparative analysis were made considering two different techniques and the results obtained were published in [100] and [101].

- AMUD MIMO OFDM over Turbo-Equalization for Sc Wireless Channel.
- Adaptive vector Precoding for Multiuser MIMO OFDM.

7.2 AMUD MIMO OFDM over Turbo-Equalization for Sc Wireless Channel

7.2.1 Introduction

IEEE 802.11 wireless Local Area Network standards employ OFDM, which offers high spectral efficiency and superior tolerance to multi-path fading [29]. In OFDM, computationally-efficient Fast Fourier Transform [10] is used to transmit data in parallel over a large number of orthogonal subcarriers which are maintained even in frequency selective fading [11][12][13]. Throughput and capacity can be improved when multiple antennas are applied at the transmitter and receiver sides, especially in a rich scattering environment [15][16] as well as frequency-selective fading channels.

The conventional approaches implements an equalizer to remove ISI or use maximum A - Posteriori (MAP) or maximum likelihood (ML) detection while a joint detection technique of AMUD MIMO OFDM and joint equalization decoding (Turbo equalizer) to totally eliminate ISI. A recent approach that significantly reduces the complexity of joint equalization and decoding is the so called "turbo equalization" algorithm, where MAP/ML detection and decoding are performed iteratively on the same set of received data. It has recently been shown that passing of soft information, the use of interleaving, and the controlled feedback of soft information are essential requirements to achieve performance gains with an iterative system [102][103].

The iterative principle has been extended to encompass single carrier equalization techniques while the multicarrier equalization technique employs joint channel estimation as stated in [104]. This allows single carrier systems to combine the operations of equalization and channel coding to operate in a wideband channel with performance that could not previously be achieved with traditional equalization and forward error correcting (FEC) techniques [105]. Iterative equalization techniques have been shown to give excellent error rate performance for both fixed and fast fading channels [106].

AMUD MIMO OFDM is for demodulation of digitally modulated signals with multiple access interferences (MAI). Conventionally individual channel estimation as stated by [1] was improved by joint estimation as stated in [104]. This scheme was designed for total elimination of MAI in the system. In a single user environment, every match filter maximum likelihood receiver plays the role of Adaptive MMSE maximum likelihood receiver [4][20]. In the implementation, AMUD MIMO OFDM, provides robustness and mobility in a time variable frequency selective multipath fading channel; it improves the bit error rate performance and therefore enhances channel capacity of a multi-cellular environment. MIMO OFDM mitigates multiple access interference and increases capacity [59][22].

In [20] A MMSE MUD techniques were used effectively to achieve the performance of a maximum likelihood estimator but on a linear complexity. The contribution of part of this chapter has been elaborated in chapter 4 as follows:

- Enhanced joint channel estimation and signal detection makes the new technique effectively mobile and thus one can easily get network wherever one goes because of continuous handover (due to training).

- Bpsk modulation schemes achieve better BER in both memory 2 and 4 respectively for the iterative scheme.

- Memory 4 performance at BER 10^{-5} has approximately a dB gain difference when compared to memory 2 performance.

- The sum rate capacity result in the new technique is very close to MIMO theoretical upper bound.

7.3 System Structure

Figure 7.1, shows the system model for an AMUD MIMO OFDM, with Nt and Nr transmit and receive antennas with k subcarriers in one OFDM block. At time t, a data block $b'[n,k] : k = 0,1,...,n$ transformed into different signals $x1[n,k] : k = 0,...,k-1$ and i =1, 2, ..., n, and i is the numbers of sub channels of the OFDM system. Signals transmitted are modulated by $x1[n,k]$. The FFT received at each receive antenna is the superposition of the transmitted signals. The receive signal at j_{th} receive antenna is:

$$y_j[n,k] = \sum_{i=1}^{N_t} H_{i,j}[n,k]x_i[n,k] + n_j[n,k] \tag{7.1}$$

Where $H_{i,j}[n,k]$ is the frequency response between antennas i and j, $n_j[n,k]$ is the additive Gaussian noise with zero mean and unit variance σ_n^2 .

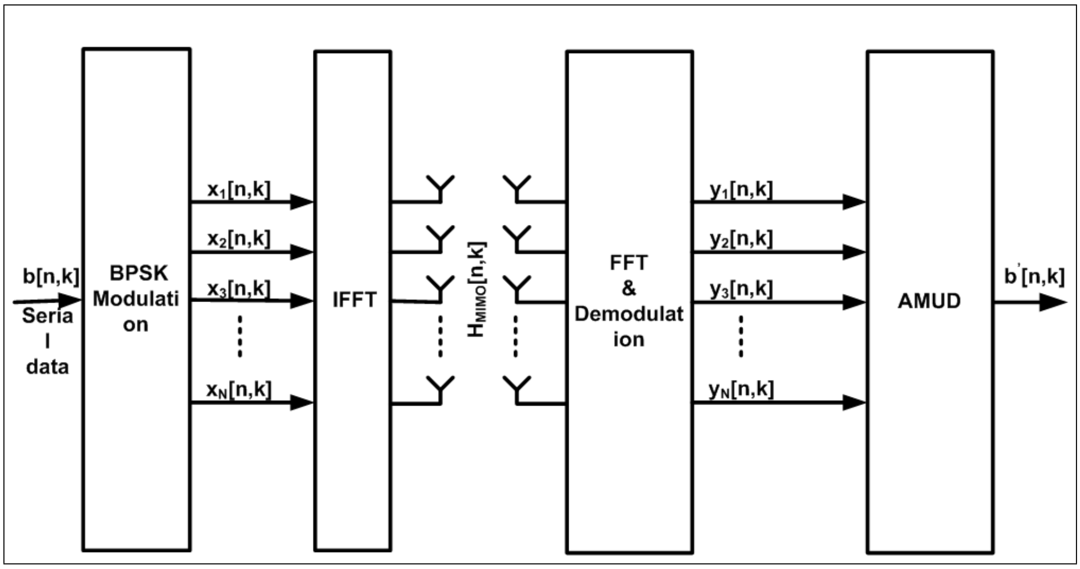

Figure 7.1: System Model for AMUD MIMO OFDM

1. $b[n, k]$ = Serial input data
2. $X_N[n, k]$ = OFDM transmit symbols
3. y_k = Received signal
4. H_{MIMO} = MIMO channel
5. $b'[n, k]$ = Output

7.3.1 Principal of Turbo Equalization

The iterative equalization receiver structure in figure 7.2 used in this study shows that both the equalizer and the decoder employs the optimal symbol by symbol Maximum A-Posteriori (MAP) soft input soft output (SISO) algorithm [107]. Soft input symbols are fed into the decoder from a sampled receive filter stream r(t) and bit-wise hard decisions are produced as the final output. It is possible to equalize and decode in an iterative manner that is similar to turbo decoding.

The equalizer provides soft outputs, i.e., reliable information on the coded bits for the channel decoder. The soft information on the bit c_k is usually given as a log-likelihood ratio (LLR) or L-value as:

$$\lambda^E(c_k) = log\frac{P(c_k) = +1|r)}{P(c_k) = -1|r)} \tag{7.2}$$

which is the ratio between the conditional bit probabilities in the logarithmic domain. These L-values are deinterleaved and given to the channel decoder, which uses them to recover the information bits u'.

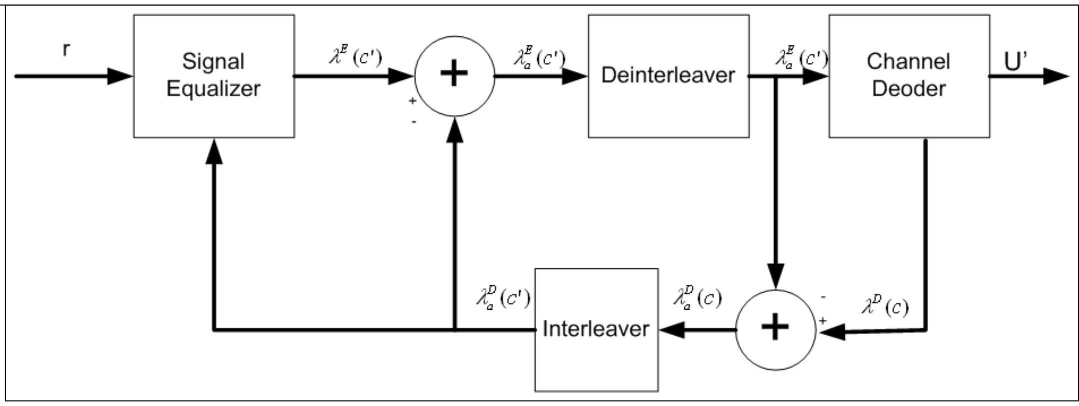

Figure 7.2: Iterative structure

1. r = Received filter stream
2. $\lambda^E(c')$ = LLR (L value)
3. U' = Output
4. $\lambda_a^E(c_k)$ = Equalization output

At the first iteration there is no feedback information from the channel decoder available, so the equalizer calculates the L-values $\lambda^E(c')$ which are based on the received samples r from the channel. The L-values are deinterleaved to break consecutive bits far apart and thus giving the channel decoder independent input values. The interleaving is an essential part in the iterative receiver scheme, since the extra information on an individual data bit is due to the different neighboring bits in the detection and decoding processes feedback branch to the equalizer. Therefore we need to use the more complex SISO decoder instead of the conventional hard output decoder. The equalizer is able to produce the L-values $\lambda^E(c')$ based on the received samples from the channel, so that information is not repeated in the feedback. Hence, the feedback only contains the extra information that is obtained from the surrounding bits in the channel decoding. The input L-values and the obtained extra information are called intrinsic and extrinsic information, respectively. The extrinsic information from the channel decoder stated in [102][103] is given as:

$$\lambda_a^D c_k = \lambda^D(c) - \lambda_a^E c_k \tag{7.3}$$

where $\lambda_a^E c_k$ denotes the extrinsic information from the equalizer. The turbo equalization technique is based on the utilization of this extrinsic information at the next iteration round [102]. So it is passed through the interleaver to the equalizer as a priori information on the bit reliabilities. By exploiting this side information in the detection, more reliable decisions are achieved. Also in the equalizer output the extrinsic information $\lambda_a^E c_k$ is extracted from the output as follows:

$$\lambda_a^E c_k = \lambda^E(c) - \lambda_a^D c_k \tag{7.4}$$

This equalizer information is again used in the SISO decoder to produce new soft outputs and furthermore, the new extrinsic information according to equation (7.3). As soon as this feedback information becomes available, the new iteration can be started. The number of iterations may depend on the processing power available or the achieved performance improvement. At the final stage, there is no need for the SISO decoder, since only hard decisions $\hat{u}$ on the information bits are needed. The Turbo equalization receiver is able to improve the performance, but at the cost of higher complexity.

7.3.2 Adaptive MMSE Receiver for MIMO OFDM

In an adaptive filter the parameters are continuously changing due to the received training sequence from the transmitter which informs the receiver to adjust the parameter of the filters to match the desired signal. In the single user environment every match filter Maximum Likelihood (ML) plays the role of an Adaptive MMSE ML receiver [4][20].

An adaptive turbo receiver structure used in this thesis shows that the bank of matched filters in the adaptive linear MMSE filters trains the filter coefficients and retrieves the signatures. Training is employed using the least mean square (LMS) approach to adaptively update the linear coefficient, an MMSE convergence of the filter coefficients provides estimates of the received signatures.

An adaptive MMSE filter minimizes the error by an adaptive algorithm, the steepest descent algorithm is used to minimize the mean square error (MSE). For simplicity, a fractionally spaced adaptive linear transversal filter for Adaptive MMSE detection is used, which is insensitive to the time differences in the signal arrival times of different users, thus the receiver timing recovery is extremely simplified [4][65]. Consider the received signals, symbols $y_1[n,k]$, $y_2[n,k]$ and $y_3[n,k]$ and let their general form for any node and any path in the network is $y_N[n,k] = r_n[m]$. Where n is the specific number assigned to the signals at nodes. $\mathbf{y_1}[n,k]$, $\mathbf{y_2}[n,k]$ and $\mathbf{y_3}[n,k]$ the received digital signal output symbol block from the adaptive filters is $b'[n,k]$.

Recalling the principle of the proposed technique in chapter 3 from equation (3.14) to equation (3.26). The same principle of the adaptive multiuser system will be applied to the Turbo equalizer in this chapter to provide a better performance compared to the conventional.

The equation explains that the updated weight vector is computed from the current weight vector by adding the input vector scaled by the complex conjugate value of the error by μ which controls the size of correction. The iteration of the equation produces the value of the Mean Square Error at which the vector tends to its optimal value a_{opt}. Minimum error value cannot be reached by a finite number of iterations though it is approachable. To achieve proper adaptation, the weight vector must be updated at a rate fast enough to track the channel variations. The method of steepest descent can be viewed as a feedback model which may become unstable. The stability of the steepest descent algorithm depends on the step size parameter μ and the auto correlation matrix $\mathbf{R}$. The eigenvalues of $\mathbf{R}$ are all real and positive, the condition for convergence and stability of the steepest descent algorithm depends on the step size parameter μ.

7.3.3 Capacity Equation

System capacity will be significantly improved by MIMO channels [1]. In OFDM [10][11][19], the entire channel is divided into many narrow parallel sub channels. The capacity formula for the proposed scheme is stated in [20], based on the assumption the channel matrix consists of independent and identically distributed iid Rayleigh fading coefficients and Figure 7.5 is the sum rate capacity of the scheme analyzed in this chapter. The capacity formula for adaptive multiuser detection by

Rapajic is as stated in [20] as:

$$C = log\left(\frac{1}{\sigma_e^2}\right) \tag{7.5}$$

where σ_e^2 is the noise variance of the signal at the receiver.

7.3.4 Performance Comparison and Simulations

The achievable bit error rate of the following three cases were compared by Monte Carlo simulation: OFDM SISO, MIMO OFDM and AMUD MIMO OFDM systems. Perfect channel state information was assumed, BPSK Modulation and a flat fading channel model were employed in the simulation. The configurations considered for this simulation are an OFDM system with 64 subcarriers, 16 symbol time periods and 4 symbol period for antenna configuration $N_t = N_r = 2$ and 8.

Figure 7.3 and 7.4 Shows the SNR in dB versus the BER of the SISO OFDM, 2 X 2 MIMO and AMUD OFDM. The simulation results show that at an average Bit Error Rate of 10^5 , AMUD OFDM MIMO performs better than other schemes and provides a 2dB SNR gain to the conventional MIMO OFDM scheme.

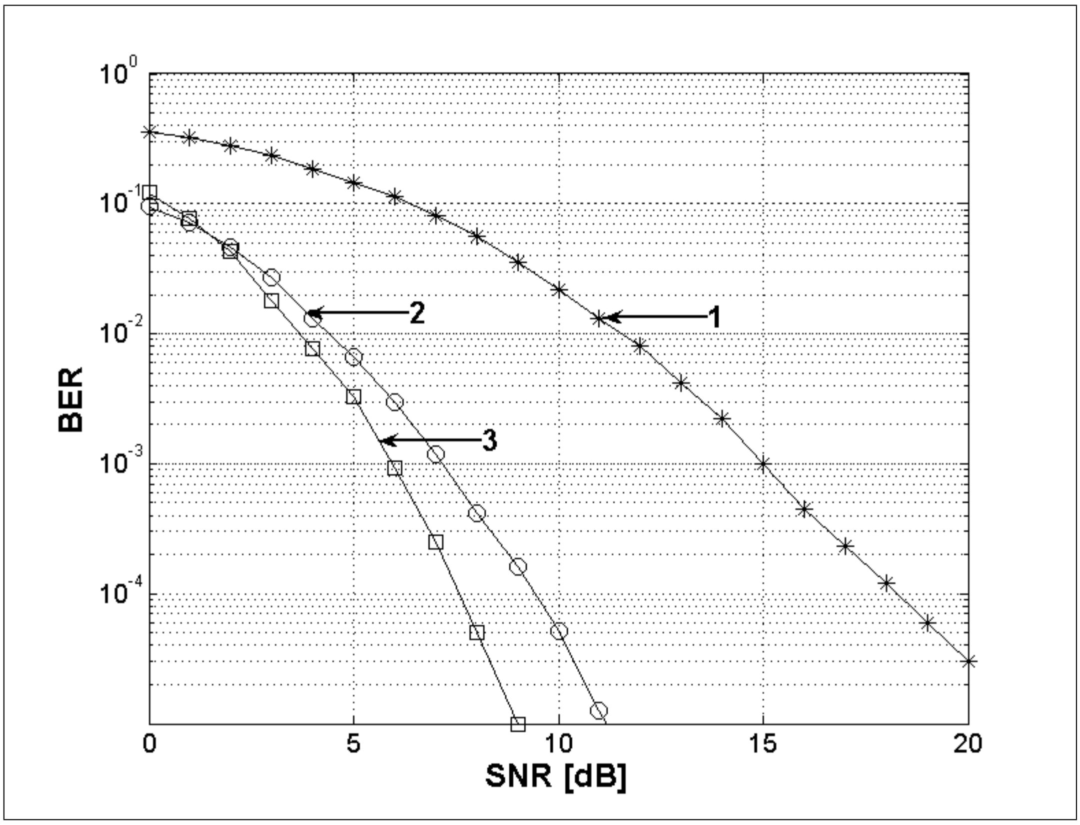

Figure 7.3: The schemes 2×2 Bit error rate comparison

1. OFDM SISO
2. OFDM MIMO
3. AMUD OFDM MIMO

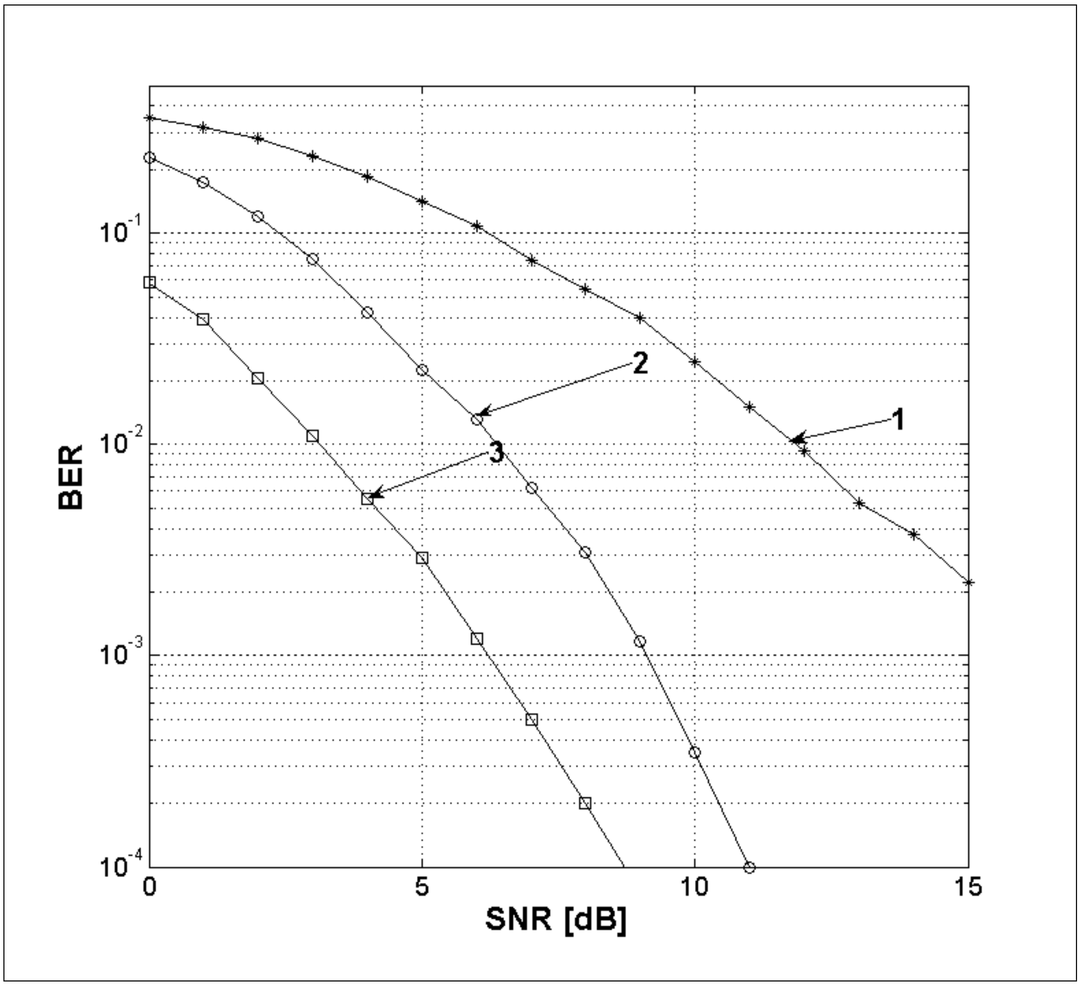

Figure 7.4: The schemes 8×8 Bit error rate comparison

1. OFDM SISO
2. OFDM MIMO
3. AMUD OFDM MIMO

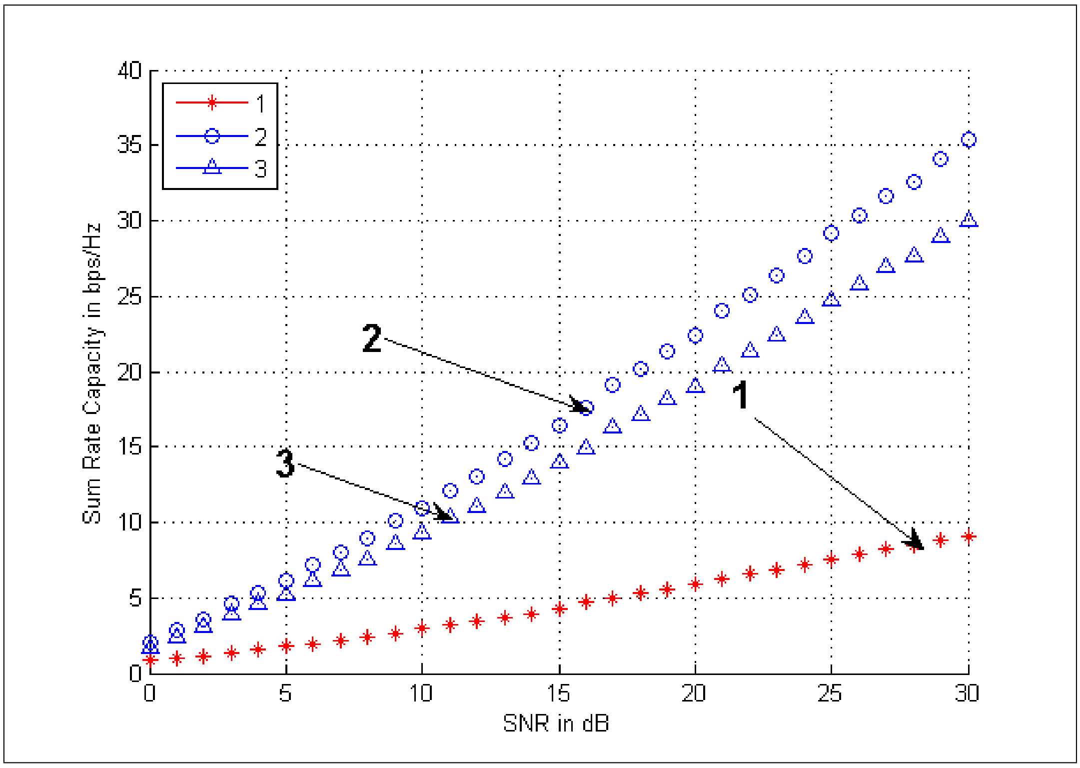

Figure 7.5: Capacity comparisons (in bits/sec/Hz) (4×4)

1. OFDM SISO - Sum rate capacity
2. OFDM MIMO - Sum rate capacity
3. AMUD OFDM MIMO - Sum rate capacity

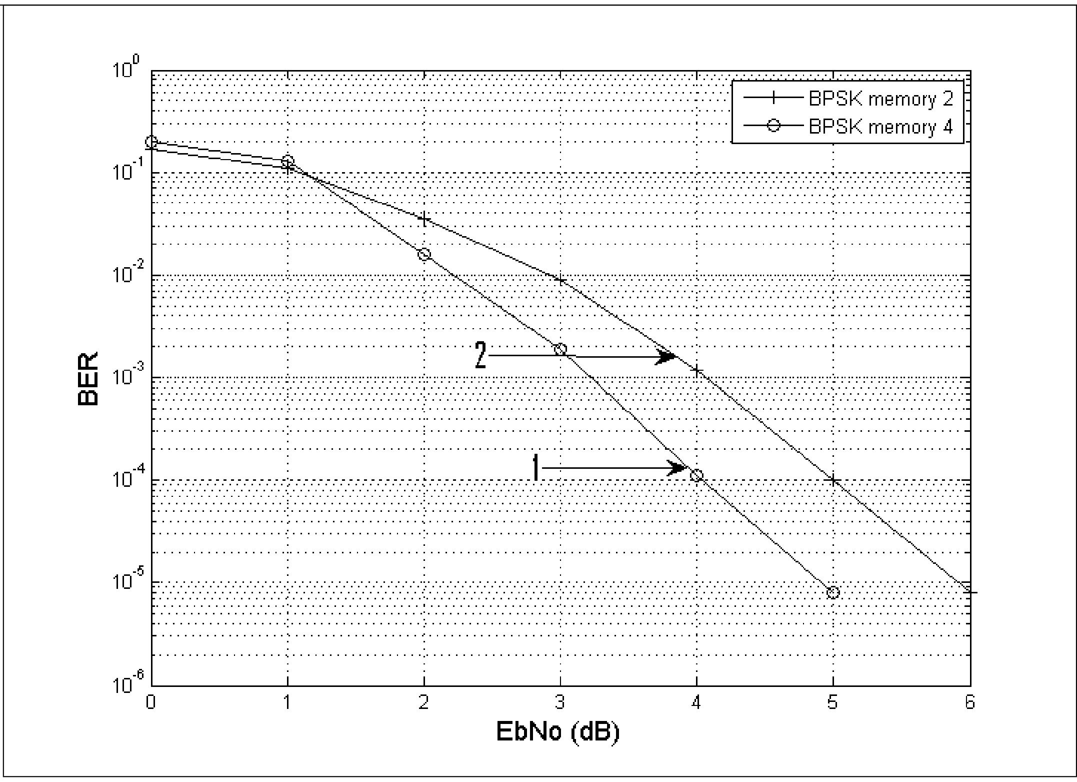

Figure 7.6: The schemes memory2 and 4 Bit error rate comparison

1. BPSK Memory 4
2. BPSK Memory 2

Figure 7.5, is the sum rate capacity comparison in bits/seccond/Hz of the OFDM SISO, MIMO OFDM and AMUD MIMO OFDM technique in an Adaptive Multiuser Detection for MIMO OFDM over Tubo Equalization for single Carrier Transmission Wireless, which is very close to MIMO capacity upper bound.

For channel coding we used a half rate recursive systematic convolutional code with memory mc = 2, constraint length L = 4, generator polynomial G = [7 5], block length = 4096. The simulation result in Figure 7.6 shows that the principles of iterative decision linear equalization have been extended to interleaved space time block code over the AMUD MIMO OFDM for broadband wireless channel. ISI resolution relies on jointly MMSE criteria and operates on multi-dimensional modulation symbols, whose individual components can be detected in accordance with another criteria. When the optimum MAP criteria is chosen, substantial performance gains over conventional space time turbo transmission scenarios were achieved.

7.4 Adaptive vector Precoding for Multiuser MIMO OFDM

In a multiuser communication scenario, diversity can be exploited through making appropriate choices among users with independently faded channels [108]. In the literature, multiuser scheduling has been considered in the context of channel allocation for a space division multiple access/time division multiple access network as stated in [109], but mainly with the downlink and the assumptions that users are equipped with only one antenna or transmit only one data stream.

In this chapter, spatially compatible users are grouped together in the same time or frequency slot, which is usually measured by channel correlation among users. This approach raises two potential concerns. First, a globally optimal allocation requires a thorough search of all possible choices, and suboptimal or heuristic alternatives induce complexity versus performance tradeoffs. Second, the physical layer details are largely neglected; either the compatibility metric depends solely on the channel and is independent of the underlying transceiver structures; or a conservative view is taken that treats multiuser interference (MUI) as background noise.

The combination of multiple input multiple-output (MIMO) signal processing with orthogonal frequency division multiplexing (OFDM) is regarded as a highly promising solution to achieving data rates for next generation wireless communication systems operating in frequency selective fading environments. To realize the extension of the MIMO with OFDM, a number of changes are required in the base-band signal processing. An overview of the changes includes, time and frequency synchronization, channel estimation, synchronization tracking, and signal detection.

Moreover, when channel state information (CSI) is available at the transmitter, linear precoding can be used to further improve system performance by tailoring the transmission to the instantaneous channel conditions [110] while retaining the benefits of all-linear processing. CSI at the transmitter is mandatory in the multiuser downlink, where a base station attempts to communicate simultaneously with multiple users.

The term precoding, uses the same idea as frequency equalization, except that the fading is inverted at the transmitter instead of the receiver. The technique requires the transmitter to have knowledge of the sub-channel flat fading gains, which must be obtained through estimation. Note that precoding requires knowledge of the channel state information (CSI) at the transmitter. When the receiver has multiple antennas, the transmit beamforming cannot simultaneously maximize the signal level at all of the receive antenna signal and thus precoding is used. There are two main problems with precoding in the wireless setting. First, precoding is channel inversion, and channel inversion is not power efficient in fading channels. Implicitly, an infinite amount of power is needed for channel inversion on a Rayleigh fading channel. Thus precoding is mostly applied in wireline multi-carrier systems like high bit rate digital subscriber lines [111].

In this thesis an adaptive vector precoding scheme for multi-user MIMO OFDM system adopts a time scheduling approach to service the users. The key contributions in this chapter are:

1. To evaluate the multi-user channel capacity and Bit-error rate performance.
2. Developing a joint-transmitter receiver design for implementing water-filling for multi-user MIMO OFDM systems.

7.4.1 System Model

The MIMO OFDM transmitter consists of OFDM transmitters among which the incoming bits are multiplexed, and then, each branch in parallel performs encoding, and inverse fast Fourier transformation (IFFT) and before the final transmission signal is up converted to radio frequency (RF) and transmitted. For reliable detection, it is typically necessary that the receiver knows the wireless communication channel and keeps track of phase and amplitude drifts. To enable estimation of the wireless communication channel, the transmitter occasionally sends known training symbols. In WLANs, a preamble, which includes channel training sequences, is added to every packet. Moreover, to track the phase drift, pilot symbols are inserted into every MIMO OFDM data symbol on a predefined subcarrier.

The system transmits N_T signal and N_R receives antennas at $N_S \leq min(N_T, N_R)$ symbol streams. The input-output relation is

$$\mathbf{y} = \mathbf{HF} + \mathbf{v} \tag{7.6}$$

Where y is the received signal vector, H the channel matrix, F is the precoder matrix (the data symbol vector) and v the noise vector, the elements of the noise vector v are independent and identically distributed and complex Gaussian distributed with zero mean and variance 1. The elements of the data symbol vectors are from an alphabet A with zero mean and variance 1. The elements of the channel matrix H are iid. and complex Gaussian distributed with zero mean and variance P, and every element is distributed according to the Jakes model [112]. In order to reduce the feedback [113], the precoder F is limited to be unitary, H. Thus, the signal-to-noise ratio (SNR) per transmit antenna is given by P.

The singular value decomposition (SVD) of the channel H $= U \sum V^H$, for several performance criteria in [113], the optimal precoder F consists of the first N_S columns of the right unitary matrix v calculated by the SVD of the channel matrix, thus $F = \mathrm{v}'$. Even through a closed form, expression of the BER optimal precoder is still unknown, it has been shown in [114] that, depending on the system parameters, the optimal precoder is either v$'$ or vM', where M is a unitary matrix with constant modulus entries, e.g., the Hadamard or the DFT matrix. We assume

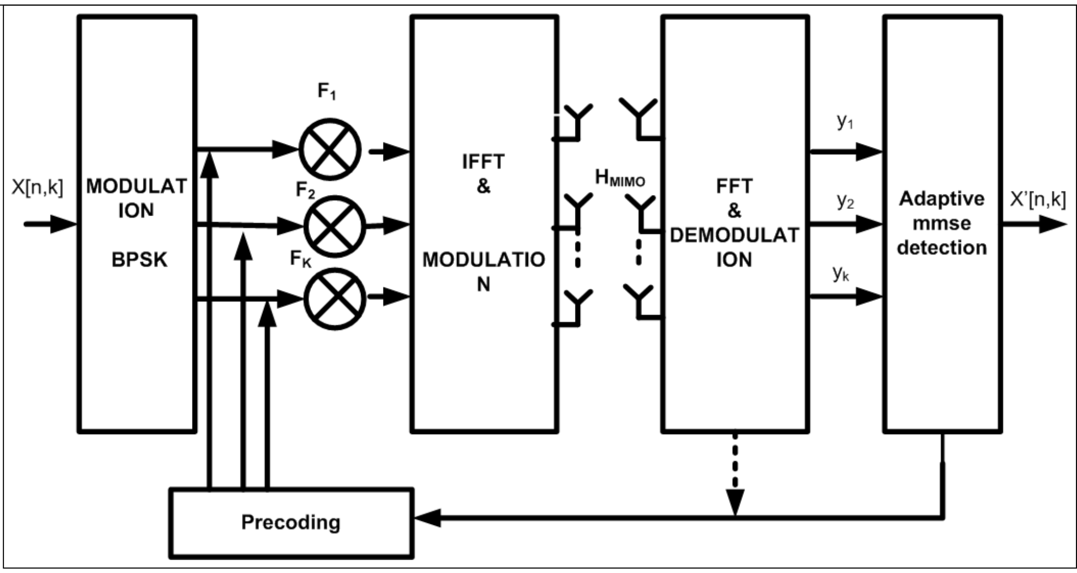

Figure 7.7: System Model

1. $b[n,k]$ = serial input data
2. F_k = Optimal precoder
3. y_k = Received signal
4. H_{MIMO} = MIMO channel
5. $b'[n,k]$ = Output

that the data is transmitted in frames, and that the receiver can perfectly estimate the channel at the start of each frame. The optimal precoder for this channel is calculated, quantized, and sent to the transmitter over the delay and error-free feedback link. We distinguish between a dedicated and a non-dedicated feedback channel. The dedicated channel is only used for transmitting the feedback to the transmitter. The non-dedicated channel is also used to transmit data. In the latter case, the transmitter has to distinguish between when the codeword ends and when the data starts [111]. The receiver first must estimate and correct for the frequency offset and the symbol timing, e.g., by using the training symbols in the preamble. Subsequently, the CP is removed, and the point fast Fourier transformation (FFT) is performed per receiver branch. Since the MIMO algorithms that are proposed in this chapter are multi carrier algorithms, MIMO detection has to be done per OFDM subcarrier [21][3]. Therefore, the received signals of the subcarrier are routed to the

R_{th} MIMO detector to recover the data signals transmitted on that subcarrier. Next, the symbols per transmit stream are combined, and finally detection is performed for the parallel streams and the resulting data are combined to obtain the signal

7.4.2 Precoding scheme

At the transmitter, the precoding technique uses the estimated channel information calculated at the mobile station to improve the performance. After operating the weighted vector that can remove the channel interference factor at the transmitter in advance, the signal will be transmitted. So, received signals are only detected as operating the weighted vector simply without the complex detection techniques at the receiver.

7.4.3 SVD technique

Once we know the influence of the channel, it is possible to eliminate it using the Singular Value Decomposition (SVD) technique. Since SVD multiplies an orthogonal matrix to the transceiver, unlike ZF and MMSE, it does not have to consider the transmit power. Figure 8.2 shows the basic structure of SVD, where V is a weighted vector made by feedback information and U is a vector used to recover the original signal [115][1].

7.4.4 Analysis of the Adaptive Precoder

Precoding is a generalization of beamforming to support multi-layer transmission in multi-antenna wireless communications, the purpose of precoding is to distinguish between spatial properties of signal and noise. The term beamformer is derived from the fact that early antennas were designed to form pencil beams so as to receive a source signal radiating from a specific direction and attenuate the signals originating from other directions that were of interest. In a single-layer beamforming, the same signal is emitted from each of the transmit antennas with appropriate weighting such that the signal power is maximized at the receiver output. When the receiver has multiple antennas, single-layer beamforming cannot simultaneously maximize the

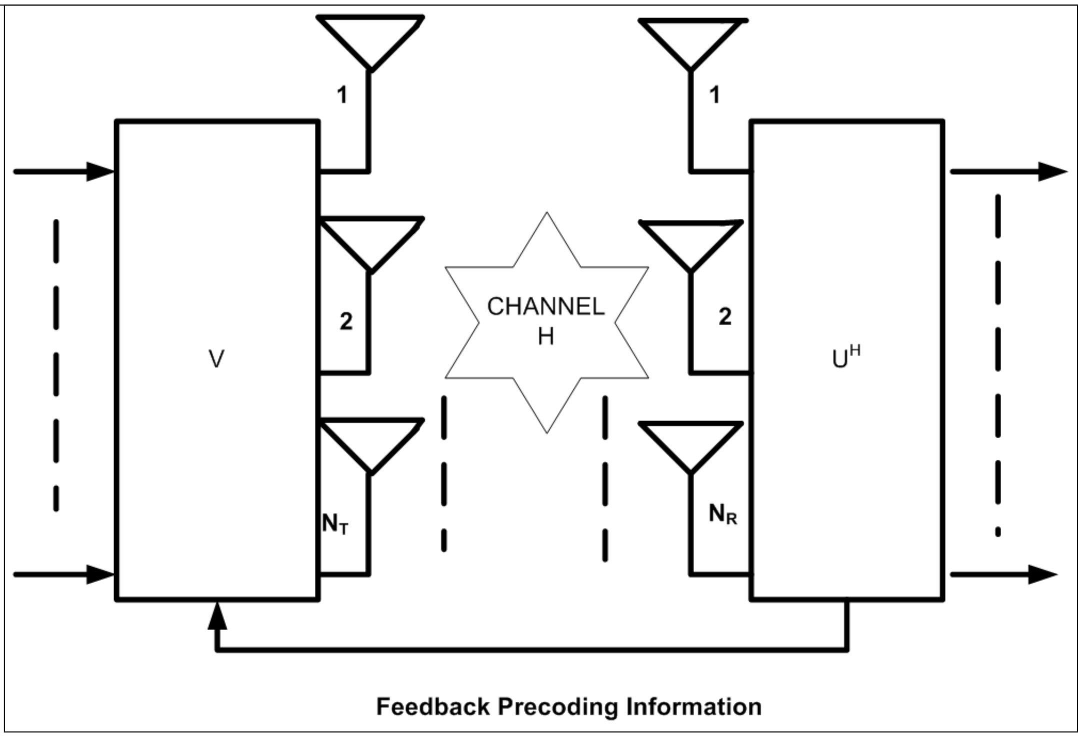

Figure 7.8: Structure of SVD

1. V = Weighted Vector
2. U^H = Recovery Vector
3. H = MIMO channel

signal level at all of the receive antennas. Thus, in order to maximize the throughput in multiple receive antenna systems, multi-layer beamforming is required.

This proposed scheme for precoding will adopt a joint effort at both the transmitter and receiver. This will use a zero forcing like approach in order to mitigate multiuser interference. Let H_j be the j^{th} user subchannel and F_i be the user i transmit vector.

The fundamental idea of zero forcing solution [112][116] is that interference is removed by forcing $H_j \cdot F_i = 0$ for i not equal to j, which means that all the other users besides the user of interest will be forced to have a zero contribution by adopting this scheme, resulting in a constraint that the total number of transmit antennas must always be greater than number of receiver antennas, as indicated in [117].

Let the combined impulse response of the precoding weight vectors along with the channel impulse response be represented as: the transmitter matrix j for user j will not interfere with the signal at the output of the receivers for other users if it lies in the null space of the above given channel vector. Let $U_j \Sigma V_j{}^H$ represent the singular value decomposition of the channel under consideration where U and V represent the left and right singular vectors respectively and Σ represents the matrix of the singular values of the decomposed channel. Let the received vector be represented by Y, the channel matrix by H, the transmitted vector by $\tilde{F}$ and $\mathbf{v}$ represent the additive white gaussian noise and $(.)^H$ represents the hermitian transpose.

As indicated in Figure 8.1, the classical method utilizing the channel decomposition approach can be described as follows. The received signal can be represented as $[\mathrm{Y} = \mathrm{H}F + \mathrm{v}]$. The singular value decomposition of the channel $[\mathrm{Y} = \mathrm{U}\Sigma\mathrm{V}^H\mathrm{F} + \mathrm{v}]$, by utilizing the matrix of right singular vectors V of the channel, pre-processing of the signal is achieved and matrix of transmit vectors is formed
Let $F = V\tilde{F}$ $[Y = U\Sigma V^H V\tilde{X} + \mathbf{v}] = U\Sigma\tilde{F} + \mathrm{v}]$ the received signal is partially whitened and post processing at the receiver end is achieved by utilizing the matrix of left singular vectors U, $[U^H Y = U^H U\Sigma\tilde{F} + U^H\mathrm{v}]$. Thus the received signal after post- processing can be represented as: $[\tilde{Y} = \Sigma^{-1}\Sigma\tilde{F} + \Sigma^{-1}U^H\mathrm{v}]$ $[\tilde{Y} = \tilde{F} + v]$. Extending the same concept to multi-user MIMO case:

$$H_j\tilde{V}_j^{(0)} = [U_j^{(1)}, U_j^{(0)}]^H\Sigma[V_j^{(0)}V_j^{(1)}] \tag{7.7}$$

The transmitted signal F is subject to additive white Gaussian noise (AWGN) n, and multipath propagation AWGN channel H. The MU-MIMO system consists of N_T transmitting and N_R receiving antennas. The channel matrix H is a $(N_R \times N_T)$ complex matrix, the received vector y is a N_R dimensional complex BPSK signal vector, the transmitted signal x is a N_T dimensional vector and n is the N_T dimensional noise vector. A BPSK modulation scheme is used in order to eliminate modulation gain and simply show the performance advantage of MU-MIMO. More advanced modulation schemes are expected to offer extra gain in data rates but at the same time an increased complexity.

7.4.5 Multiuser Precoding

Multi user MIMO OFDM systems provide high capacity with the benefits of space division multiple access. The channel state information at the access point (AP) is very important since it allows joint processing of all the users signal which result in a significant performance improvement and increased data rates [1]. If the channel state information is available at the AP, it can be used to efficiently eliminate or suppress multi-user interference (MUI) by beamforming. The precoding also allows us to perform most of the complex processing at the AP which results in a simplification of user terminals. Linear precoding techniques have an advantage in terms of computational complexity [118].

The basic idea behind this solution is to utilize the right singular vectors of the channel matrix in order to form the precoding matrix.

Thus an optimal precoding matrix can be formed such that all the MUI becomes zero by choosing a precoding matrix F_i that lies in the null space of the other users channel matrices. Thereby, a MU MIMO downlink channel is decomposed into multiple parallel independent single user MIMO channels [117]. Thus we can define the zero MUI constraint forces F_i to lie in the null space of H_i. The singular value decomposition (SVD) of H_i whose rank is L_i. Thus the proposed system chooses the last right singular vectors $N_T - L_i$ where N_T is number of transmit antennas.

Caire in [112], proposed a successive precoding algorithm in order to define a simplified solution of the power control problem. By allowing a certain amount of interference, this algorithm reduces the capacity loss due to the subspace nulling. In short, first calculate the maximum capacity that an individual user can achieve. The basic ideology behind this solution is to utilize the right singular vectors of the channel matrix in order to form the precoding matrix:

$$F = [F_1 F_2 F_3 .... F_K] \subseteq C^{N_T \times N_R} \tag{7.8}$$

Thus an optimal precoding matrix can be formed such that all MUI are zero by choosing a precoding matrix F_i that lies in the null space of the other users channel matrices. Thereby, a MU MIMO downlink channel is decomposed into multiple parallel independent single user MIMO channels [109][119].

$$\tilde{H}_i = [H_1^T....H_{i-1}^T H_{i+1}^T....H_K^T]^T \tag{7.9}$$

where K indicates the number of users, the zero MUI constraint forces F_i to lie in the null space of H_i. The singular value decomposition (SVD) of H_i whose rank is L_i, in the proposed system chooses the last right singular vectors $N_T - L_i$ where N_T is number of transmitter antennas:

$$H_i \tilde{V}_i^{(0)} = U_i \Sigma [V_i^{(1)} V_i^{(0)}]^H \tag{7.10}$$

The equation above $V_i^{(0)}$ indicates the null space of the right singular matrix V.

7.4.6 Adaptive Precoding

Precoding is generalized beamforming to support multi-layer transmission in MIMO radio systems. Conventional beamforming considers linear single-layer precoding so that the same signal is emitted from each of the transmit antennas with appropriate auto updated weighting such that the signal power is maximized adaptively at the receiver output. When the receiver has multiple antennas, the single-layer beamforming cannot simultaneously maximize the signal level at all of the receive antennas and so precoding is used for multi-layer beamforming in order to maximize the throughput performance of a multiple receive antenna system. In precoding, the multiple streams of the signals are emitted, from the transmit antennas with independent and appropriate weighting per each antenna such that the link throughput is maximized at the receiver output.

7.4.7 Adaptive MMSE Receivers

In chapter 6.5, The linear MMSE equalizer is considered as a special case of the Decision Feedback Equalization (DFE) when all decision feedback coefficients are equal to zero. The output of MMSE filter at the nth symbol interval is:

$$\mathrm{b}(n) = \sum_{m=-P}^{P} f(m) y_k(nT - mT) \tag{7.11}$$

where f(m) are the adaptive filter's coefficients, T is the symbol interval. The total number of adaptive equalizer coefficients is $(2p+1)$. The symbol estimate $\hat{a}(n)$ is obtained as:

$$\hat{a}(n) = b(n) - \mathbf{d}^{\mathbf{H}}(n)\mathbf{a}_D(n) \tag{7.12}$$

where $\mathbf{d}(n)$ is a vector of decision aided coefficient sequences, defined as:

$$\mathbf{d}(n) = [d_1, d_2, ..., d_k]^T. \tag{7.13}$$

The elements of $\mathbf{d}(n)$ represent the weighting coefficients which multiply the respective known symbols. The vector $\mathbf{a}_D(n)$ contains symbols known to the receiver with unknown symbols set to zero. It is defined as:

$$\mathbf{a}_D(n) = [a(n+1), a(n+2), ..., a(n+K)]^T \tag{7.14}$$

The coefficients of $\mathbf{d}(n)$ and $\mathbf{f}(n)$ are obtained adaptively during a training period. After the training period, the coefficients $\mathbf{d}(n)$ and $\mathbf{f}(n)$ can be kept during data detection. Alternatively, in a decision directed mode, these coefficients can be updated by tentative decisions [4].

7.4.8 LMS Adaptive Algorithm

In chapter 6.6, the following steps correspond to the LMS algorithm stated in [4] as:

$$\mathbf{f}(n+1) = \mathbf{f}(n) + \alpha_1 e^*(n)\mathbf{y}(n) \tag{7.15}$$

$$\mathbf{d}(n+1) = \mathbf{d}(n) - \alpha_2 e^*(n)\mathbf{a}_D(n) \tag{7.16}$$

for n $= 0, 1, 2, ...$, where f(n) is the linear filter coefficient sequence and d(n) is the decision aided coefficient sequence, both at the $n(-th)$ symbol iteration, and $(e)^*$ denotes conjugation, α_1 and α_2 being step sizes. Similarly, the Recursive Least Square (RLS) algorithm can also be used to provide faster convergence. The coefficients are updated once every symbol interval [60][4].

7.4.9 Training of the Adaptive MMSE Receiver

Recalling chapter 6.61, to simplify derivations, the symbol powers are normalized to 1, $\mathrm{E}\mathbf{a}(n)\mathbf{a}^H(n) = I$. The vector is expressed as:

$$\mathbf{a}(n) = \mathbf{a}_D(n) + \mathbf{a}_U(n) \tag{7.17}$$

where $\mathrm{a}_D(n)$ contains known symbols and $\mathrm{a}_U(n)$ contains unknown symbols. Accordingly, the channel matrix H is split into two parts $\mathrm{H} = \mathrm{H}_D + \mathrm{H}_U$, where H_D consists of channel responses corresponding to symbols in $\mathrm{a}_D(n)$ and H_U correspond to symbols in $\mathrm{a}_U(n)$. The filter coefficients are obtained by minimizing the MSE, $\mathrm{E}[|e^n|^2]$, where $e(n) = a(n) - \hat{a}(n)$, $\hat{a}(n) = \mathrm{f}^H(n)\mathrm{y}(n) - \mathrm{d}^H(n)\mathrm{a}_D$. There is a range of adaptive algorithms offering simple adaptive solutions [8] to obtain the optimal coefficients d and f.

7.4.10 Performance analysis

The capacity of multi-user MIMO downlinks is intimately connected with a result as indicated in [120] called "writing on dirty paper", which can be briefly summarized as follows, let X represent a transmitted signal, W and Z are additive white noise terms, so that the received signal $Y = X + W + Z$. It is shown in [120] that if W is known deterministically to the transmitter, then the capacity of the communication channel is same as a channel with only the second interference term: $Y = X + Z$ regardless of whether or not the receiver knows W and independent of the statistics of W. When the users are known at the transmitter, space division multiple access can be employed to increase capacity [121]. In particular, the capacity of the channel for user j is indicated in [122] as:

$$C_j = max_{X_j} \log_2 |I + (\sigma_n^2 I + H_j \tilde{X}_j \tilde{X}_j{}^* H_j^*)^{-1} H_j X_j X_j^* H_j^*| \tag{7.18}$$

The capacity is thus the function of not only what modulation matrix is chosen for the particular user of interest, but also those chosen for all other co-channel users as well. Viewing the problem entirely form the perspective of receiver j, capacity is maximized when, $H_j \tilde{X}_j = 0$ or in other words, when the transmit matrix $\tilde{X}_j$ for all other then j lies in the null space of H_j. If this is done, then the capacity of user j is equal to the waterfilling capacity of the channel matrix H_j [123], note that $N_T \geq N_R$ is a necessary condition for achieving a requirement not imposed in the blind transmitter case.

For the purpose of simulations, the comparison was made between the proposed vector precoding scheme and the zero forcing approach. The systems considered for the simulation were full rank systems. As seen from the simulations results the proposed adaptive vector precoding scheme outperforms the zero forcing precoding method even at significantly lower values of SNR. The reason for this could be due to the fact that traditional zero forcing approach needs to be inverted at the receiver and under such circumstances, the spectral nulls are introduced in the process of reception. In the vector precoding approach the channel does not need to be inverted under the assumption that the transmitter has complete channel state information. The adaptive vector precoding approach exploits the orthogonal nature of the right singular matrix.

In the case of a multi-user MIMO OFDM system the proposed method adopts a time division multiple access scheme in which each user is serviced at a time. In this way the decentralization of users is achieved. The proposed system is compared with different configurations in MIMO adopting a zero forcing like approach. The problem with the sum rate capacity maximization in a multi-user channel, is that such an approach may result in one or two "strong" users large enough to taking a dominant share of the available power, potentially leaving weak users with little or no throughput [120][118].

At higher SNRs, the relatively small gap between channels with and without channel information at the transmitter is sufficiently small. However, this assumes that the channel is full rank, but when the channel is rank deficient, the gaps are larger, and complete or even only the partial channel information, available can be advantageous. Multi-user capacity could have a different meaning. It is possible to consider the capacity of one particular user in the context of a system, or to consider the sum capacity of all users in the system. Under a single power constraint, it is possible to achieve a variety of different combinations of rates for different users by

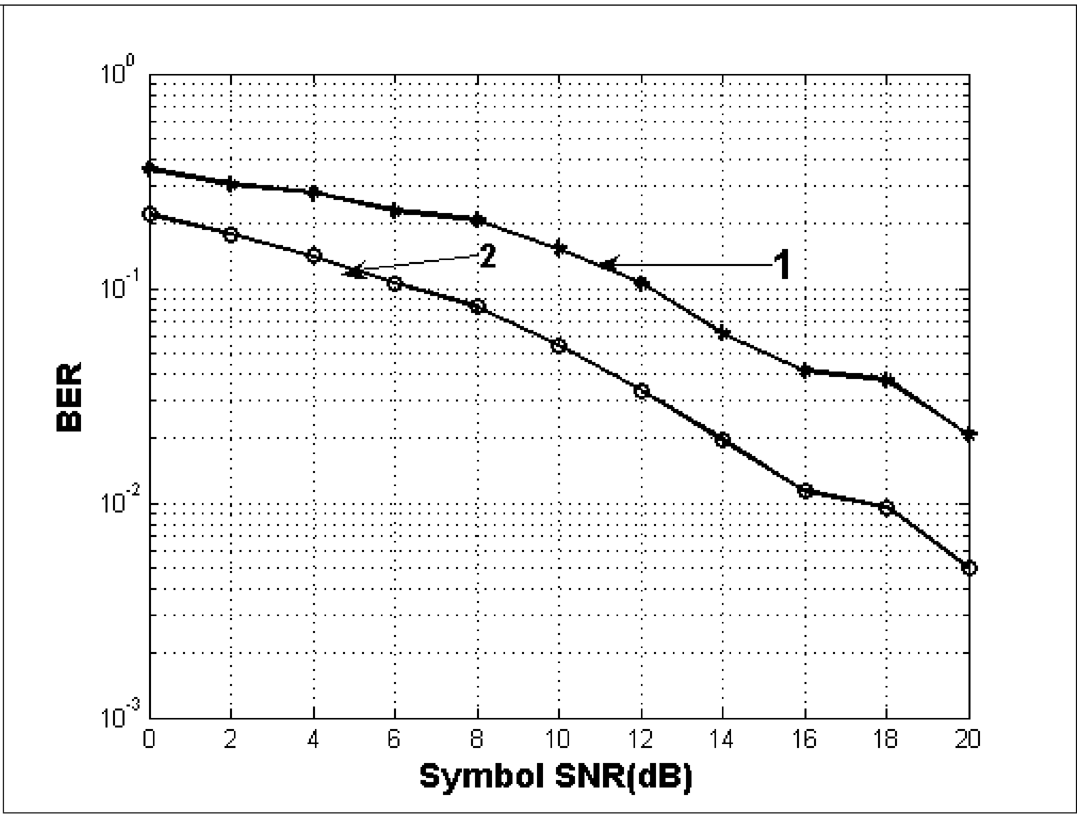

Figure 7.9: Bit error rate

1. Zero forcing
2. Vector Precoding

allocating resources differently to different users.

7.4.11 Performance results

Figure 8.3 indicates the BER of a simple MU-MIMO OFDM system with BPSK modulation over a channel, by adopting zero-forcing precoding in this chapter, the geometric mean decomposition methods is presented with comparison in the adaptive vector precoding. Figure 8.4 shows the capacity of a MIMO system, presented with a comparison of the vector precoding capacity for the blind transmitter, transmitter with CSI and the multiuser MIMO case with the proposed approach.

The joint transmitter and receiver scheme for implementing the multi-user downlink vector precoding scheme was demonstrated in this project. The simulation results indicate a capacity improvement as well as the improvement in the bit error rate performance compared with the zero forcing approach. In the vector precoding approach the channel doesnt need to be inverted under the assumption that the transmitter has complete channel state information. Results show that designing the precoders based on the standard pseudo-inverse is optimal under the assumption of a total power constraint. However, the pseudo-inverse is no longer sufficient and vector precoding provides better performance.

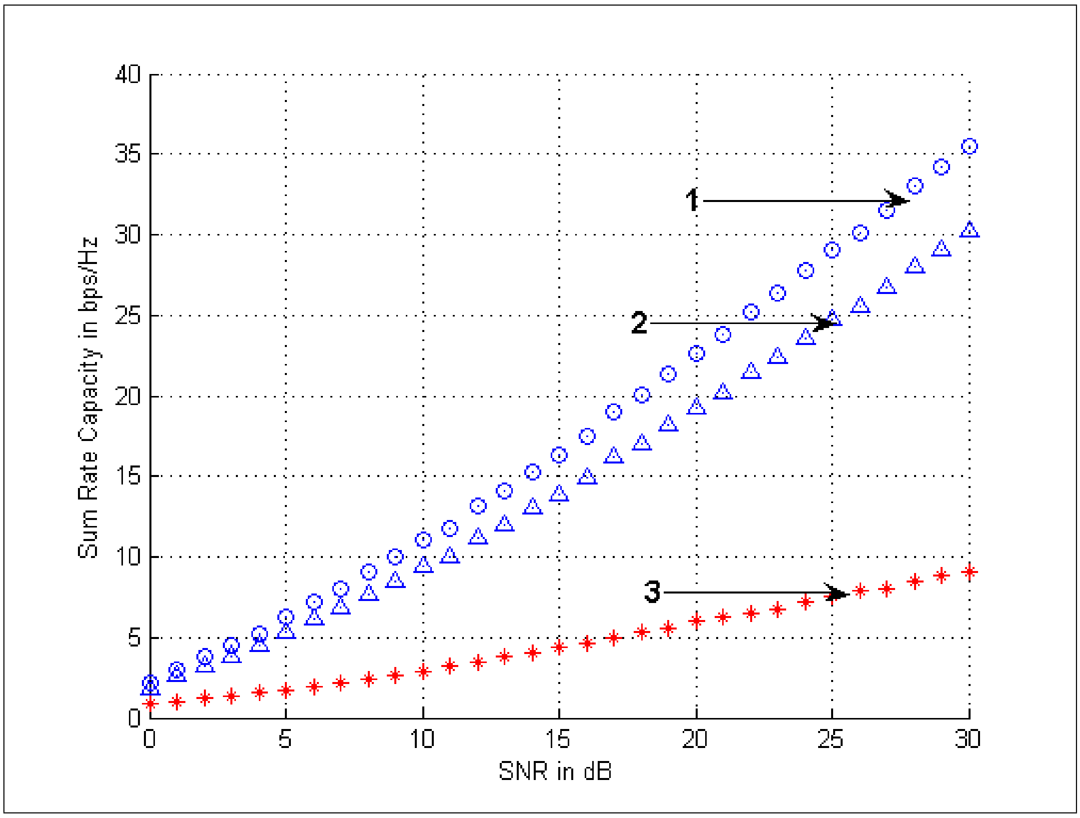

Figure 7.10: Egordic Capacity

1. Shannon Capacity Theory
2. MIMO OFDM Pre coding
3. SISO

7.5 Summary

There are two comparisons made with the newly proposed technique firstly; The turbo equalization algorithm is effective in achieving reasonably iteration gain when signal power of unknown interference is as large as those of the known users. The AMUD MIMO OFDM performs as well as MAP equalizer such that the memory4 has 1dB gain to memory2 signifying the higher the memory the better the SNR, AMUD MIMO OFDM equally shows the higher the number of the antennas the better the SNR gain.

Secondly Adaptive vector Precoding for Multiuser MIMO OFDM was demonstrated, the joint transmitter-receiver design for multi-user precoding, the BER performance and simulation results suggest an improvement in BER performance of the system as compared to transmitter side precoding alone. This can be mainly attributed to the fact that the proposed solution avoids channel inversion usually required in the precoding process. The capacity results also indicate a better mitigation of MUI in case of the MIMO OFDM system. More advanced linear precoding schemes should be addressed. For example, it is well known that in low SNR conditions under channel uncertainty, regularizing the pseudo inverse can considerably improve the performance. It is interesting to examine this property in the context of generalized inverses. ZF decoding using pseudo-inverse (the decorrelator) is probably the most common decoding algorithm. The results suggest that adaptive vector precoding outperform ZF under uncertainty conditions.

Chapter 8

Conclusion

The combination of MIMO and OFDM has emerged as a promising solution for future high rate wireless communication systems. The discourse commenced with a historical review of the 50-years of OFDM literature. More specifically, the milestones in the history of OFDM were presented in the literature, where the key events and contributions across several decades were summarized. Furthermore, an overview of the advances in MIMO techniques was provided, followed by the introduction of combined MIMO OFDM systems, where some of the associated contributions found in the literature were outlined and acknowledged.

The state of the art review of MIMO OFDM further discussed the specific limitations of existing techniques designed for multiuser MIMO OFDM systems. More specifically, this research investigates the joint detection techniques and the channel estimation approaches in comparison to individual estimation approach by Emre Telatar in his famous paper of 1999 which become a bench mark. This new technique provides higher data rate performance, higher mobility and higher carrier frequencies for easy and reliable multiuser transmission in wireless systems.

It was pointed out explicitly that in the open literature there was a paucity of information on multiuser MIMO OFDM detectors, which are capable of supporting a higher number of users than the number of receive antennas. Recall that in such a rank-deficient scenario a particular challenge is imposed by the insufficient degree of freedom due to having a singular channel matrix. These challenging difficulties were overcomed with the advent of the AMUD techniques, resulting in attractive and efficient solutions to the above-mentioned problems. This was the main contribution of this thesis that AMUD MIMO OFDM achieves enhance channel estimation resulting in a continuous hand-over and thus one can get network wherever you are. This thesis analyzed a novel implementation of a distributed MIMO OFDM wireless communication system as demonstrated. AMUD MIMO OFDM is a reliable mobile communication system with potential to operate sufficiently in cooperative wireless communications.

The second second contribution of this thesis is on the information channel capacity of single carrier system with MMSE DFE and Multicarrier systems with OFDM receivers, showing that: (a) the adaptive MMSE Multiuser Receivers in MIMO OFDM wireless system provides higher data rate performance, higher mobility and higher carrier frequencies for easy and reliable multiuser transmission in wireless systems, and (b)the information capacity comparisons of mobile communication systems with MMSE DFE and OFDM receivers apart from different implementations, are essentially identical when it comes to the criterion of achievable channel information capacity.

Lastly, few comparisons were demonstrated with the proposed technique, the "Adaptive Vector Precoding for MIMO OFDM", this involves developing a joint-transmitter receiver design for implementing water-filling for multi-user MIMO OFDM systems for evaluation of the multi-user channel capacity and bit-error rate performance. Moreover "Adaptive MMSE Multiuser Detection for MIMO OFDM over Turbo-equalization for single-Carrier transmission wireless Channel" were equally demonstrated in the thesis, showing that the enhanced joint channel estimation and signal detection makes the new technique effectively mobile and thus one can easily get network wherever one goes because of continuous handover (due to training).

Chapter 9

Future Recommendations

AMUD MIMO OFDM is an active research, a key challenge in the technique is to effectively control three qualities at once: transmit power, transmit rate and coding rate. It will be interesting to extend the analysis by considering both rate and coding adoption based on the channel condition.

Adaptive transmission has recently been identified as a key technology for exploiting potential system diversity and improving power-spectral efficiency in wireless communication systems. An adaptive resource-allocation approach, which jointly adapts subcarrier allocation, power distribution, and bit distribution according to instantaneous channel conditions, for multiuser multiple-input multiple-output/orthogonal frequency-division multiplexing systems. The resultant scheme was able to:

- Optimize the power efficiency.
- Guarantee each user's quality of service requirements, including bit-error rate and data rate.
- Ensure fairness to all the active users.
- To be applied to systems with various types of multiuser-detection schemes at the receiver.

It is also demonstrated that the MIMO system is able to multiplex several users without sacrificing antenna diversity by using the proposed algorithm.

Efficient resource management is a major issue in the operation of wireless communication systems given the limited resource availability. In contrast to most existing resource allocation techniques that assume perfect channel state information at the transmitter (CSIT), a novel adaptive resource management algorithm is proposed to optimize the spectral efficiency of a multiuser multi-input multi-output (MIMO)/orthogonal frequency division multiplexing (OFDM) system where only partial channel state information is available. A distinctive feature of the proposed method is that the allocation strategy is directly related to the users' spatial correlation and the quality of channel feedback information. It is expected that the results will show that the proposed scheme achieves significant throughput improvement compared to non-adaptive systems.

This thesis have demonstrated promising advantages of AMUD MIMO OFDM over conventional MIMO OFDM and SISO OFDM. However due to intrinsic ISI of the AMUD MIMO OFDM function, the conventional pilot aided channel estimation scheme used in MIMO OFDM are not directly applicable to AMUD MIMO OFDM.Promising techniques based on preambles have appeared in literatures. Still the following questions are not yet answered: What is the best chanel estimation scheme for the proposed scheme? What is its complexity compared to channel estimation in AMUD MIMO OFDM? What is the effect of timing synchronization error on AMUD MIMO OFDM.

Typically, the parameters of the OFDM transmission, e.g. frame length and CP length, are designed based on the characteristics of the radio environment, such as average or worst case delay and Doppler spreads. Cooperative AMUD MIMO OFDM processing may potentially induce increased delay spreads due to the fact that the distributed antenna heads can be placed far apart. An interesting future topic would be to evaluate the impact of the distributed antenna system on the design of OFDM parameters.

Adaptive MIMO-OFDM brings along an interesting observation, namely, that MIMO-OFDM exploits two dimensions: the time/frequency dimension and the spatial dimension. This raises a fundamental question for research in future wireless communication systems. What is the next dimension to exploit? Or do we, by this concept, reach the limit and can we only achieve higher data rates by exploiting these two dimensions more and more efficiently?

BPSK is the most elementary modulation scheme, which was used mainly in the thesis simulations. The results are purely dependent on the systems' potential. Nevertheless, channel capacity performance will be significantly increased by a more sophisticated modulation scheme. On the other hand, Symbol Error Probability will be increased too while the complexity of the system is increased. In a similar manner to the degree of freedom (DOF), by increasing the modulation level of the data signals, a saturation point will be reached, where further increment to the modulation level will not provide significant channel capacity gain. A changeover to a higher level modulation scheme needs further investigation to identify the Symbol Error Probability and complexity prices for increased channel capacity.

AMUD MIMO OFDM systems suffer from spatial correlation. Spatial correlation between the antenna elements of a MIMO node causes loss in the DOF and a loss in the DOF results to limited channel capacity gain. Conventional MIMO OFDM systems need to be carefully designed and built in order to avoid spatial correlation. However, in the case of AMUD MIMO OFDM systems, spatial correlation problem can be tackled by an avoidance technique. Through training, apart from the MMSE information, each user will receive spatial correlation information. If a device is providing MMSE good enough to contribute to the AMUD MIMO OFDM formation but is spatially correlated, it will be discarded from the system.

The loss due to the adaptive nature of the receivers' implementing the LMS algorithm, provided that the algorithm had enough time to converge to its steady state, is given as shown in the section 5.3 of equation (5.47). It should be noted that an occasion may arise where the LMS algorithm has not converged to its steady state. This needs future studies and analysis. Moreover, various implementation issues relating to MCM arise, and need to be addressed they are as follows:

- Excessive delay due to very narrow bandwidth of subchannels.
- Inter-sub-channel interference. (it is difficult to produce a large number of narrow band subchannels with high selectivity filters preventing cochannel interference).
- Difficulty in adaptive information loading per subchannel due to lack of information at the transmitter about the channel. This problem is particularly difficult in the case of the mobile channel since the channel is to a various degree time variable.

Conclusively if all the recommended problems mentioned are taking into consideration in the future, a more reliable, robust and higher data communication system will be achieved.

Bibliography

[1] E. Telatar, “Capacity of multi antenna gausian channels,” Technical Memorandum, Bell Laboratories, Lucent Technologies, Published in European Transactions on Telecommunications, vol. 10, no. 6, pp. 585–595, Nov/Dec 1999.

[2] L. Hanzo, M. Mnster, B. J. Choi, and T. Keller, ”OFDM and MC-CDMA for broadband multi-user communications”. NJ: IEEE Press/Wiley, 1995, p. 252.

[3] T. C. W. Schenk and A. V. Zelst, “Implementation of a MIMO OFDM based wireless LAN system,” IEEE Transactions on signal processing, vol. 52, no. 2, pp. 483–494, Feb 2004.

[4] P. B. Rapajic and B. S. Vucetic, “Adaptive receiver structures for asynchronous CDMA systems,” IEEE J. on Selected Areas in Commun., vol. 12, no. 4, pp. 685–697, May 1994.

[5] S. Verdu, ”Multiuser Detection”. The pitt Building, Trumpington st. Cambridge, CB2 1RP UK: Cambridge University Press, 2003, p. 451.

[6] U. Madhow and M. L. Honig, “MMSE interference suppression for direct-sequence spread-spectrum CDMA,” IEEE Trans. Commun., vol. 42, no. 12, pp. 3178–3188, Dec. 1994.

[7] J. Proakis and M.Salehi, ”Communication System Engineering”, 1st ed. Upper Saddle River, NJ, USA: Prentice Hall, 1994, p. 889.

[8] S. Haykin, ”Adaptive Filter Theory”, 4th ed. Englewood Cliffs,New Jersey: Prentice Hall, 1986.

[9] R. V. Nee and R. Prasa, "OFDM for wireless multimedia communications mobile communications", 1st ed. Boston.London: Artech House Publishers, 2000.

[10] L. C. Jr., "Analysis and simulation of digital mobile channel using orthogonal frequency division multiple acess," IEEE Trans. on commun., vol. 33, no. 7, pp. 665–675, July 1985.

[11] A. V. Zelt, A. V. Nee, and R. G. A. Awater, "Space division multiplexing for OFDM systems," Proc. of IEEE VTC-Spring., vol. 2, no. 7, pp. 1070–1074, May 2000.

[12] M. D. Batariere, J. F. Kepler, T. P. Krauss, S. Mukthavaram, J. W. Porter, and F. W. Vook, "An experimental OFDM system for broadband mobile communications," IEEE Trans. Veh. Technol. conf., vol. 4, no. 14, pp. 1947–1951, August 2001.

[13] Y. Li and N. R. Sollenberger, "Adaptive antenna arrays for OFDM systems with co-channel interference," IEEE Trans. on Commun., vol. 47, pp. 217–229, Feb. 1999.

[14] G. Foschini, "Layered space-time architecture for wireless communication in a fading environment when using multi-element antennas," Bell Labs Technical Journal, vol. 1, no. 2, pp. 41–59, 1996.

[15] G. J. Foschini and M. J. Gans, "On limits of wireless communications in a fading environment when using multiple antennas," IEEE wireless Pers. on Commun., vol. 6, no. 3, pp. 311–335, March 1998.

[16] G. G. Raleigh and J. M. Cioffi, "Spatio-temporal coding for wireless communication," IEEE Trans. on Commun., vol. 46, no. 1, pp. 357–366, March 1998.

[17] V. Tarokh, N. Seshadri, and A. R. Calderbank, "Space-time codes for high data rate wireless communication: Performance criterion and code construction,"

IEEE Transactions on Information theory, vol. 44, no. 2, pp. 744–756, March 1998.

[18] J. H. Winters, “On the capacity of radio communication systems with diversity in a rayleigh fading environment,” IEEE J. on Selected Areas in Commun., vol. 5, no. 5, pp. 871–878, June 1987.

[19] Y. Li, J. Chuang, and N. R. Sollenberger, “Transmit diversity for OFDM systems and its impact on high-rate data wireless networks,” IEEE Journal on Selected Areas Commun., vol. 17, no. 7, pp. 1233–1243, 1999.

[20] P. B. Rapajic and D. K. Borah, “Adaptive MMSE maximum likelihood CDMA multiuser detection,” IEEE J. on Selected Areas in Commun., vol. 17, no. 12, pp. 2110–2122, Dec 1999.

[21] Talwar, S. Tellado, J. Erceg, A. V. Paulraj, and H. Sampath, “A fourth-generation MIMO-OFDM broadband wireless system: Design, performance, and field trial results,” IEEE Communication Magazine, vol. 40, no. 9, pp. 143–149, Feb. 2002.

[22] G. L. Stüber, J. Barry, S. W. McLaughlin, Y. G. Li, M. Ingram, and T. G.Pratt, “Broadband MIMO-OFDM wireless communications,” IEEE Trans. Commun., vol. 92, no. 2, pp. 271–294, Feb. 2004.

[23] T. J. Willink, “MIMO OFDM for broadband fixed wireless access,” IEEE Proceedings Communications, vol. 152, no. 1, pp. 75–81, Oct. 2004.

[24] C. Yin, X. Zhao, and X. Hou, “A simulation study on channel estimation for MIMO-OFDM based beyond 3G mobile systems,” The Journal of China universities of Posts and Telecommunication, vol. 12, no. 3, pp. 7–11, March 2005.

[25] A. Pascual-Iserte, A. I. Prez-Neira, and M. A. Lagunas, “On power allocation strategies for maximum signal to noise and interference ratio in an OFDM-MIMO system,” IEEE Transactions On Wireless Communications, vol. 3, no. 3, pp. 808–820, May 2004.

[26] Y. Li, J. H. Winters, and N. R. Sollenberger, “MIMO-OFDM for wireless communications: Signal detection with enhanced channel estimation,” IEEE Transactions on Communications, vol. 50, no. 9, pp. 1471–1477, Sept. 2002.

[27] C. Y. Wong, R. S. Cheng, K. B. Letaief, and R. D. Murch, “Multiuser OFDM with adaptive subcarrier, bit and power allocation,” IEEE Journal on Selected Areas in Communications, vol. 17, no. 10, pp. 1747–1758, Oct. 1999.

[28] P. Xia, S. Zhou, and G. B. Giannakis, “Adaptive MIMO-OFDM based on partial channel state information,” IEEE Transactions on signal Processing, vol. 52, no. 1, Jan. 2004.

[29] IEEE, “Standard for local area networks wireless access systems,” IEEE 802.11, Trans. Veh. Technol., August 2003.

[30] Y. Li, L. Cimini, and N.R.Sollenberger, “Robust channel estimation for ofdm systems with rapid dispersive fading channels,” IEEE Transactions on Communications, vol. 46, no. 7, pp. 902–915, July 1998.

[31] I. Barhumi, G. Leus, and M. Moonen, “Optimal training design for mimo ofdm systems in mobile wireless channels,” IEEE Transactions on Signal Processing, vol. 51, no. 6, pp. 1615–1624, June 2003.

[32] E. Telatar and D. N. C. Tse, “Capacity and mutual information of wideband multipath fading channels,” IEEE Trans. on Information Theory, vol. 46, no. 4, pp. 1384–1400, July 2000.

[33] C. Shannon, “A mathematical theory of communication,” Bell Syst. Tech., vol. 27, no. 1, pp. 379–423, 623–656, Oct. 1948.

[34] A. Kaye and D. George, “Transmission of multiplexed PAM signals over multiple channel and diversity systems,” IEEE Transactions on Communication Technology, vol. 18, no. 5, pp. 520–526, Oct. 1970.

[35] W. V. Etten, "An optimum linear receiver for multiple channel digital transmission systems," IEEE Trans. Commun., vol. 23, no. 8, pp. 828–834, Aug. 1975.

[36] W. Lee, "Effects on correlation between two mobile radio base-station antennas," IEEE Transactions on Communications, vol. 21, no. 11, pp. 1214–1224, Nov. 1973.

[37] D. S. Shiu, G. J. Foschini, M. J. Gans, and J. M. Kahn, "Fading correlation and its effect on the capacity of multielement antenna systems," IEEE Transactions on Communications, vol. 3, no. 48, pp. 502–513, Mar. 2000.

[38] P. Kyritsi and D. C. Cox, "Modal analysis of MIMO capacity in a hallway," IEEE Globecom 2001, vol. 1, pp. 567–571, Nov. 2001.

[39] A. Paulraj, R. Nabar, and D. Gore, "Introduction to space-time wireless communications". Edinburgh building cambridge: Cambridge University Press, 2003, p. 308.

[40] D. Gesbert, M. Shafi, P. J. D. shan Shiu Smith, and A. Naguib, "From theory to practice: an overview of MIMO space-time coded wireless systems," IEEE Journal on Selected Areas in Communications, vol. 21, no. 3, pp. 281–302, Apr. 2003.

[41] L. Musavian, M. Dohler, M. R. Nakai, and A. Aghvami, "Transmitter design in partial coherent multiple antenna systems," IEEE Conference on Communication, vol. 4, pp. 2261–2265, May 2005.

[42] S. Vishwanath, S. A. Jafar, and A. Goldsmith, "Adaptive resource allocation in composite fading environments," IEEE Global Telecommunications Conference, vol. 2, pp. 1312–1316, Dec. 2001.

[43] A. Paulraj, R. Nabar, and D. Gore, "Introduction to space-time wireless communications". The Edinburgh building, cambridge: Cambridge University Press, 2003, p. 252.

[44] G. Munz, S. Pfletschinger, and J. Speidel, “An efficient waterfilling algorithm for multiple access OFDM,” IEEE Global Telecommunications Conference, vol. 1, no. 10, pp. 681–685,, 2002.

[45] J. M. Holtzman, “CDMA forward link waterfilling power control,” IEEE Proc. VTC 2000-Spring Tokyo. IEEE 51st 2000, vol. 3, no. 3, pp. 1663–1667, March 2000.

[46] R. S. Cheng and R. D. Murch, “Iterative bit power allocation for v-blast based OFDM MIMO system in frequency selective fading channel,” IEEE Wireless Communications and Networking Conference (WCNC2002), 2002.

[47] R. W. Chang, “Synthesis of band limited orthogonal signals for multichannel data transmision,” Bell Sys.Tech., vol. 55, no. 9, pp. 1775–1796, Dec. 1966.

[48] S. B. Weinstein and P. M. Ebert, “Data transmission by frequency division multiplexing using the discrete fourier transform,” IEEE Transactions on Communications, vol. 19, no. 5, pp. 628–634,, Oct. 1971.

[49] B. Hirosaki, “An analysis of automatic equalizers for orthogonally multiplexed QAM systems,” IEEE Transactions on Communications, vol. 28, no. 1, pp. 73–83, Jan. 1980.

[50] S. Verdu, “Minimum probability of error for synchronous gaussian multiple access channels,” IEEE Transactions on Information Theory, vol. 32, no. 1, pp. 85–96, Jan. 1986.

[51] IEEE, “Standard for local and metropolitan area networks part 16: Air interface for fixed broadband wireless access systems,” IEEE 802.16 archived (OPAC), 2001.

[52] D. Tse, “Optimal power allocation over parallel gaussian broadcast channels,” IEEE International Symposium on Information Theory, Ulm Germanys, June 1997.

[53] R. Knopp and P. A. Humblet, "Information capacity and power control in single-cell multiuser communications," IEEE International Conference on Communications, vol. 1, pp. 331–335, Mar. 1995.

[54] D. Kivanc, G. Li, and Liu, "Computationally efficient bandwidth allocation and power control for OFDMA," IEEE Transactions on Communications, vol. 2, no. 6, pp. 1150–1158, Nov. 2003.

[55] R. V. Nee, G. Awater, M. Morikura, H. Takanashi, M. Webster, and K. Halfor, "New high rate wireless LAN standards," IEEE Communications Magazine, vol. 37, no. 12, pp. 82–88, Dec. 1999.

[56] G. G. Raleigh and V. K. Jones, "Multivariate modulation and coding for wireless communication," IEEE Journal on Sel. Areas in Comm., vol. 17, no. 5, pp. 851–866, May 1999.

[57] A. V. Zelst, R. V. Nee, and G. Awater, "Maximum likelihood decoding in a space division multiplexing system," IEEE vtc, Tokyo Japan, May 2000.

[58] S. Nanda and J. K. R. Walton, "A high performance MIMO-OFDM wireless LAN," IEEE International Conference on Communications, vol. 43, no. 2, pp. 101–109, 2005.

[59] H. Sampath, T. S. Tellado, J. Erceg, and V. A. Paulraj, "A fourth generation MIMO-OFDM broadband wireless system: Design, performance, and field trial results," IEEE Commun. Mag., vol. 40, no. 9, pp. 143–149, Feb. 2002.

[60] S. U. H. Qureshi, "Adaptive equalization," Proceedings of the IEEE, vol. 73, no. 9, pp. 1349–1387, Sept 1985.

[61] S. Verdu, "Minimum probability of error for asynchronous gaussian multiple access channels," IEEE Transactions on Information Theory, vol. 32, no. 1, pp. 85–96,, Jan 1986.

[62] D. N. C. Tse and S. V. Hanly, “Linear multiuser receivers: Effective interference, effective bandwidth and user capacity,” IEEE Transactions on Information Theory, vol. 45, no. 2, pp. 641–657, Mar. 1999.

[63] R. Lupas and S. Verdu, “Linear multiuser detectors for synchronous code division multiple access channels,” IEEE Transactions on Information Theory, vol. 35, no. 1, pp. 123–136, Jan. 1989.

[64] A. Papoulis, ”Probability of random variables and stochastic processes”, 2nd ed. New York, NY:USA: McGraw-Hill Book Co., 1984, p. 576.

[65] S. A. Hana, M. El-Tanany, and S. A. Mahmoud, “Adaptive combiner for co-channel interference reduction in multiuser indoor radio systems,” IEEE Trans. Veh. Technol., vol. 4117126, no. 19-22, pp. 222–227, May 1991.

[66] Y. Li, “Simplified channel estimation for OFDM systems with multiple transmit antennas,” IEEE Trans. on Wireless Commun., vol. 1, no. 1, pp. 65–67, Jan. 2002.

[67] A.Wittenben, “A new bandwidth efficient transmit antenna modulation diversity scheme for linear digital modulation,” IEEE Int. on Communications, no. 1, pp. 1630–1634, May 1993.

[68] E. Lawrey, “Multiuser ofdm,” Proc. IEEE International symposium on Signal Processing and its Applications, vol. 2, no. 2, pp. 761–764, Aug. 1999.

[69] H. V. Poor and S. Verdu, “Single user detectors for multiuser channels,” IEEE Trans. Commun., vol. 36, no. 1, pp. 50–60, Jan. 1988.

[70] R. Kohno, H. Imai, M. Hatori, and S. Pasupathy, “Combination of an adaptive array antenna and a canceller of interference for direct sequence spread spectrum multiple access system,” IEEE J. Select. Areas Communications, vol. 8, no. 4, pp. 675–682, Apr. 1990.

[71] R. Kohno and N. Ishii, “Performance of joint spatial and temporal multiuser

detection using adaptive array antenna in both transmitter and receiver for DS/CDMA," in Proc. IEEE ISIT, p. 151, July 1997.

[72] L. C. Godara, "Application of antenna arrays to mobile communications, part i: Performance improvement, feasibility, and system considerations," Proc. of the IEEE, vol. 85, no. 7, p. 10311060, Jan. 1997.

[73] ——, "Application of antenna arrays to mobile communications, part ii: Beamforming and direction of arrival considerations," Proc. of the IEEE, vol. 85, no. 8, p. 10311060, Jul. 1997.

[74] J. H. Winters, J. Salz, and R. D. Gitlin, "The impact of antenna diversity on the capacity of wireless communication systems," IEEE Int. on Communications, vol. 42, no. 2, pp. 1740–1751, Feb 1994.

[75] B. Sklar, "Digital Communications Fundamentals and Applications". Prentice Hall International Editions, 2001, p. 1079.

[76] V. Raghavan and A. M. Sayeed, "Multi antenna capacity of sparse multipath channels," IEEE Trans. on Info.Theory, Aug. 2006.

[77] P. B. Rapajic, "Information capacity of a mobile communication channel with large number of receiving antennas," IEEE ITW, vol. 7204092, no. 4, pp. 104–109, Sept. 2001.

[78] J. Proakis, "Digital Communications", 4th ed. New York, NY: McGraw-Hill International Editions, 1998, p. 1002.

[79] J. M. Cioffi, G. P. Dudevoir, M. V. Eyubouglu, and G. D. F. Jr, "MMSE decission feedback equalizers and coding part 1: Equalization results and partii: Coding results," IEEE Trans. Commun., vol. 43, no. 10, pp. 2582–2604, Oct. 1995.

[80] J. Salz, "Synthesis of band limited orthogonal signals for multichannel data transmision," Bell Sys.Tech., vol. 52, no. 8, p. 32433263, Oct. 1973.

[81] C. A. Belfiore and J. H. P. Jr., “Decision feedback equalization,” IEEE Proceedings., vol. 67, no. 8, pp. 1143–1156, Aug. 1979.

[82] D. Guo, S. Shamai, and S. Verdu, “Mutual information and minimum mean square error in gaussian channels,” IEEE Trans. on Information Theory, vol. 51, no. 4, pp. 1261–1282, April 2005.

[83] T. E. Duncan, “On the calculation of mutual information,” SIAM Journal of Applied Mathematics, vol. 19, p. 3215220, July 1970.

[84] G. D. F. Jr, “Maximum likelihood sequence estimation of digital sequences in the presence of intersymbol interference,” IEEE Trans. Inform. Theory, vol. 18, no. 3, p. 363378, May 1972.

[85] T. Guess and M. K. Varanasi, “An information theoretic derivation of the MMSE decision feedback equalizer,” Thirty-Sixth Annual Allerton Conference on Communication, Control, and Computing, Sept. 1998.

[86] R. G. Gallager, ”Information theory and reliable communication”. New York: Wiley, 1968.

[87] W. Hirt and J. L. Massey, “Capacity of the discrete time gaussian channel with intersymbol interference,” IEEE Trans. Inform. Theory, vol. 34, no. 3, p. 380388, May 1988.

[88] S. Shamai, L. H. Ozarow, and A. D. Wyner, “Information rates for discrete time gaussian channel with intersymbol interference and stationary inputs,” IEEE Trans. Inform. Theory, vol. 37, pp. 1527–1539, Nov. 1991.

[89] J. R. Barry, E. Lee, and D. G. Messerschmitt, “Capacity penalty due to ideal zeroforcing decision fedback equalization,” IEEE Trans. Inform. Theory, vol. 1, pp. 422–427, May 1993.

[90] J. M. Cioffi, G. P. Dudevoir, M. V. Eyuboglu, and J. G. D. Forney, “MMSE decision feedback equalizers and coding part i: Equalization results,” IEEE Transactions Communication, vol. 43, no. May, p. 25822594, Oct. 1995.

[91] J. M. Cioffi, G. P. Dudevoir, M. V. Eyuboglu, and G. D. F. Jr., “MMSE decision feedback equalizers and coding part ii: Coding results,” IEEE Trans. Commun., vol. 43, no. 10, p. 25952604, Oct. 1995.

[92] S. Shamai and R. Laoria, “The intersymbol interference channel: Lower bounds on capacity and channel precoding loss,” IEEE Trans. Inform. Theory, vol. 42, no. 5, p. 13881404, Sept. 1996.

[93] Pinsker, ”Information and information stability of random variables and processes”. Holden-Day Inc., 1964, p. 256.

[94] J. Yang and S. Roy, “Joint transmitter receiver optimization for multi input multi output systems with decision feedbacks,” IEEE Trans. Inform. Theory, vol. 40, no. 5, p. 13341347, Sept. 1994.

[95] M. K. Varanasi and T. Guess, “Optimum decision feedback multiuser equalization with successive decoding achieves the total capacity of the gaussian multiple access channels,” in Proc. Thirty-First Asilomar Conf. Signals, Systems, and Computers, vol. 2, Nov. 1997.

[96] N. Al-Dhahir, J. M. Cioffi, and G. D. F. Jr., “A canonical finite length MMSE-DFE,” IEEE Trans. Inform. Theory, p. 598607, Oct. 1995.

[97] R. W. Chang and R. A.Gibbey, “A theoretical study of performance of an orthogonal multiplexing data transmission scheme,” IEEE Trans. Commun., vol. 16, no. 4, pp. 529–540, Aug. 1968.

[98] S. B. Weinstein and P. M. Ebert, “Data transmission by FDM using discrete fourier transform,” IEEE Trans. Commun., vol. 19, no. 5, pp. 628–634, Oct. 1971.

[99] A. Ruiz, J. M. Cioffi, and S. Kasturia, “Discrete multitone modulation with coset coding for the spectrally shapped channel,” IEEE Trans. Commun., vol. 40, no. 6, pp. 1012–1029, June 1992.

[100] T. Eneh, G. Oletu, K. Anang, P. Rapajic, and J. Eze, “Adaptive vector precoding for mimo-ofdm systems,” nternational conference ICT for Africa Covenant University Canaan Land Nigeria, March 2011.

[101] T. Eneh, G. Oletu, P. Rapajic, K. Anang, and B. Lawal, “Adaptive mmse multiuser detection for mimo ofdm over turbo-equalization for single-carrier transmission wireless channel,” IEEE IWCMC2011, July 2011.

[102] G. Bauch and V. Ram, “A comparison of soft-in/soft-out algorithms for turbo detection,” IEEE Proc. on the Int. Conf. On Tel., pp. 259–263, Jun. 1998.

[103] M. Tuchler, ”Iterative equalization using priors”. University of Illinois, Urbana-Champaign, IL, U.S.A: M.S. thesis, 2000.

[104] T. Eneh, P. Rapajic, and K. Anang, “Adaptive MMSE multiuser receivers in MIMO OFDM wireless communication,” IEEE Int. Conf. on Communication and Tech., Nov. 2010.

[105] C. Douillard, M.Jezeque1, C. Berrou, A. Picart, P. Didier, and A. Glavieux, “Iterative correction of intersymbol interference: Turbo-equalization,” European Transactions on Telecommunications, vol. 6, pp. 507–511, Sept. 1995.

[106] G. Bauch, H. Khorram, and J. Hagenauer, “Iterative equalisation and decoding in mobile communication systems,” Second European Personal Mobile Communications Conference, 1997.

[107] L. Bahl, J. Cocke, F. Jelinek, and J. Raviv, “Optimal decoding of linear codes for minimising symbol error rate,” IEEE Transactions on Information Theory, vol. IT-42, pp. 425–429, Mar. 1996.

[108] G. J. Foschini, “Layered space-time architecture for wireless communication in fading environments when using multielement antennas,” Bell Labs Techn. J, p. 4159, 1996.

[109] L. U. Choi and R. D. Murch, "A transmit preprocessing technique for multiuser MIMO systems using a decomposition approach," IEEE Transactions on Wireless Communications, vol. 3, no. 1, pp. 20–24, Jan. 2004.

[110] A. A. Scaglione, P. Stoica, S. Barbarossa, G. B. Giannakis, and H. Sampath, "Optimal designs for space-time linear precoders and decoders," IEEE Trans. on Signal Processing, vol. 50, no. 5, pp. 1061–1066, May 2002.

[111] Y. Nijsure, C. Litchfield, Y. Chen, and P. Rapajic, "Vector precoding scheme for multi-user MIMO systems," Vehicular Technology Conference Fall, vol. 52, no. 1090-3038, pp. 1–5, Jan. 2010.

[112] G. Caire and S. Shamai, "On the achievable throughput of a multiantenna gaussian broadcast channel," IEEE Trans. Inform. Theory, vol. 49, no. 7, pp. 1691–1706, Jul. 2003.

[113] H. Weingarten, Y. Steinberg, and S. Shamai, "The capacity region of the gaussian multiple-input multiple-output broadcast channel," IEEE Trans. Inform. Theory, vol. 52, no. 9, pp. 3936–3964, Sept. 2006.

[114] S. Vishwanath, N. Jindal, and A. Goldsmith, "Duality, achievable rates, and sum-rate capacity of gaussian MIMO broadcast‘channels," IEEE Trans. Inform. Theory, vol. 49, no. 10, pp. 2658–2668, Oct. 2003.

[115] S. M. Alamounti, "A simple transmit diversidty scheme for wireless communucarions," IEEE J. Select. Areas Commun., vol. 16, no. 8, pp. 1451–1458, Oct. 1998.

[116] H. Viswanathan, S. Venkatesan, and H. Huang, "Downlink capacity evaluation of cellular networks with known interference cancellation," IEEE Journal on Selected Areas in Communications, vol. 21, no. 5, pp. 802–811, June 2003.

[117] F. Liu, L. Jiang, and C. He, "MMSE vector precoding with precoding with joint transmitter and receiver design for MIMO systems," IEEE Transactions on Signal Processing, vol. 7, no. 2, pp. 2823–2833, June 2007.

[118] M. Tomlinson, "New automatic equaliser employing modulo arithmetic," Electronics Letters, pp. 138–139, March 1971.

[119] G. Caire and S. Shamai, "On the achievable throughput of a multi antenna gaussian broadcast channel," IEEE Transactions on Information Theory, vol. 49, no. 7, pp. 1691–1706, Jul. 2003.

[120] M. H. M. Costa, "Writing on dirty paper," IEEE Trans. Inform. Theory, vol. 29, no. 3, pp. 439–441, May 1983.

[121] H. Harashima and H. Miyakawa, "Matched transmission technique for channels with intersymbol interference," IEEE Trans. Comm, vol. 24, no. 4, pp. 774–780, Aug. 1972.

[122] Q. H. Spencer, A. L. Swindlehurst, and M. Haardt, "Zeroforcing methods for downlink spatial multiplexing in multiuser MIMO channels," IEEE Transactions on Signal Processing, vol. 52, no. 2, pp. 461–471, Feb. 2004.

[123] P. Viswanath and D. N. C. Tse, "Sum capacity of the vector gaussian broadcast channel and uplink downlink duality," IEEE Trans. Inform. Theory, vol. 49, no. 8, pp. 1912–1921, Aug. 2003.